This project has received funding from the European Union's Horizon 2020
research and innovation programme under grant agreement No 101006927.

VALID

Verification through Accelerated testing Leading to Improved wave energy Designs

Deliverable 1.3

Report on Uncertainties in Testing Methodologies:

a Guideline on Uncertainty Quantification in Hybrid Testing

Version 1.0

2023-06-30

Lead participant: RISE

Dissemination level: PU

This project has received funding from the European Union's Horizon 2020 research and innovation programme under grant agreement No 101006927.

VALID

DOCUMENT STATUS

Authors

Name	Organisation
Pär Johannesson	RISE
Fabio Santandrea	RISE
Martin Olofsson	RISE
Albin Bäckstrand	RISE
Joao Cruz	Yavin Four Consultants
Claes Eskilsson	AAU

Approval

Name	Organisation	Date
Natalie Williams Portal	RISE	2023-06-30

Document History

Version	Description	Reviewer	Date
0.1	First draft version	Y4C	2023-01-31
0.2	Draft version of with complete contents of Sections 1-4	TEC, Y4C	2023-03-08
0.9	Complete draft	TEC, Y4C, TUD, CPO, IDOM, WPN, JFC	2023-05-31
1.0	Final version	Project Officer	2023-06-30

Dissemination level

Short	Type	
PU	Public	X
PP	Restricted to other programme participants (including the Commission Services)	
RE	Restricted to a group specified by the consortium (including the Commission Services)	
CO	Confidential, only for members of the consortium (including the Commission Services)	

EU PROJECT NO: 101006927

Table of Contents

This project has received funding from the European Union's Horizon 2020 research and innovation programme under grant agreement No 101006927.

This project has received funding from the European Union's Horizon 2020
research and innovation programme under grant agreement No 101006927.

Tables

Figures

This project has received funding from the European Union's Horizon 2020
research and innovation programme under grant agreement No 101006927.

This project has received funding from the European Union's Horizon 2020
research and innovation programme under grant agreement No 101006927.

Executive Summary

The present report constitutes Deliverable 1.3 *"Uncertainty quantification for hybrid testing"*, developed within WP1 of VALID.

Part A presents guidance on uncertainty quantification in hybrid testing, comprising of both physical testing and numerical simulations. The presented methodology is based on the Variational Mode and Effect Analysis (VMEA) methodology along with methodologies from the Guide to the expression of Uncertainty in Measurement (GUM) and from uncertainty quantification in numerical simulations.

In Part B, the uncertainty analyses performed on the VALID User Cases are explained. A qualitative assessment was performed during a series of workshops where the insights of various stakeholders were gathered and categorized using the framework of basic VMEA. Individual sources of uncertainty were identified and ranked according to their expected impact as estimated by technical specialists in each of the test rigs targeted in the user cases. After this screening exercise, the uncertainties were quantified and aggregated using the framework of probabilistic VMEA.

Lastly, Part C consists of the nomenclature and references applied in this deliverable.

Project partner names

- RISE Research Institutes of Sweden AB
- Fundacion Tecnalia Research and Innovation
- Corpower Ocean AB
- RINA Consulting S.p.A.
- Biscay Marine Energy Platform SA
- IDOM Consulting, Engineering, Architecture, S.A.U.
- Aalborg University
- AVL List GMBH
- Wavepiston AS
- Delft University of Technology
- Aquatera Sustainability Ireland LTD
- Julia F. Chozas, Consulting Engineer
- Yavin Four Consultants, Unipessoal LDA
- Aquatera Atlantico
- Technical University of Denmark

This project has received funding from the European Union's Horizon 2020
research and innovation programme under grant agreement No 101006927.

Part A: Methodology for Uncertainty Quantification in Hybrid Testing

The aim of Part A is to present guidance on uncertainty quantification in hybrid testing, comprising of both physical testing and numerical simulations. The presented methodology is based on the VMEA methodology along with the ISO GUM recommendation "*Guide to the expression of Uncertainty in Measurement*" and methodologies from uncertainty quantification in numerical simulations.

This project has received funding from the European Union's Horizon 2020
research and innovation programme under grant agreement No 101006927.

1 Introduction

The design and development of Wave Energy Converters (WECs) entail making many decisions based on limited information about the properties of materials and components, as well as the environment where the final device will operate. In the present document, the term "uncertainty" will be intended as the condition of limited information on the actual value of variables that determine the capacity of WECs to perform their intended function. Uncertainty might affect intrinsic characteristics of the designed devices, such as material strength and surface roughness, or elements of the environment where they are supposed to operate, such as wave height and humidity.

Limitations to the information underpinning key decisions in the design process stem from a variety of reasons, which reflect the presence of some form of randomness, lack of knowledge, or combinations thereof. An example where uncertainty in the performance of the WECs originates from scarcity of information is represented by the effects of ageing and exposure to chemically aggressive environments on the components of WECs. Long-term degradation mechanisms may not be well understood at early design stages. Their importance might be revealed by unexpected failures when the system has reached a more mature configuration, and several decisions on materials and components selection have already been made.

The characterization of uncertainty in terms of randomness and incomplete knowledge is not unique to the development of WECs, but rather ubiquitous in engineering design. The relatively recent history of the WEC industry and the stochastic nature of the environmental factors to be considered in the sizing of the devices make uncertainty particularly prominent in designing these systems.

A typical approach to assess significant uncertainty in engineering design is to introduce sufficiently large safety factors and / or redundancy. The selection of safety factors and redundancy measures might be based on the experience accumulated in the field over many years, possibly combined with a test campaign at different structural levels (that is, material, component, subsystem, complete system) and environmental conditions, in order to identify the most critical failure modes and their likelihood. As WECs are a relatively recent technology with limited standardization, field experience, and a diversified range of potential technical solutions, the devices must be tested extensively to rigorously assess all uncertainty sources, which increases development costs and slows down their introduction to the market. Furthermore, without a specific characterization of the various sources of uncertainty, an exceedingly conservative approach is likely to prevail in the design of the devices, which further contributes to raising their overall cost with no gain in performance and reliability.

One of the purposes of testing is to reduce uncertainty in product development. Uncertainty affects physical measurements in any field of science and technology. More recently, the concept of virtual testing, i.e., the evaluation of product properties by means of numerical simulations, has become increasingly established across many industrial sectors, such as aerospace and automotive. As numerical simulations are only approximate representations of reality, uncertainty is also present in virtual testing, although the attention reserved for it is often limited in industrial practice.

Uncertainty plays a significant role to support decision-making in product development, as it provides a consistent and transparent approach to qualify different design options. The confidence in a certain technical solution can be corroborated in a way that is not solely dependent on the subjective judgement and experience of the designer. Furthermore, the techniques for uncertainty quantification in physical experiments, as well as numerical simulations, provide practical means to improve that confidence by reducing the uncertainty in the design variables that mostly contribute to the uncertainty in the overall performance.

The present document aims to introduce the WEC community to the basic concepts and methods of uncertainty analysis, offering practical guidance on how to apply them to hybrid

This project has received funding from the European Union's Horizon 2020 research and innovation programme under grant agreement No 101006927.

testing, which comprises both physical measurements and numerical simulations. The proposed methodology follows the VMEA approach that provides a unified computational framework for the evaluation of the total uncertainty (although the uncertainty from specific sources may be assessed via other methods). This view on the role of uncertainty quantification as tool to support the design and development of test procedures is supported by other similar approaches, see e.g., (Coleman and Steele, 2009) which provides useful information on applications to hybrid testing.

The problem formulation is addressed in Section 1.1, and the structure of the report is presented in Section 1.2.

1.1 Problem Formulation

Uncertainty affects every aspect of engineering design, not only those that relate to the performance of the final product. Every form of risk analysis conducted at different stages of a project requires some consideration of uncertainty sources which might affect budget and time planning. In this section, the scope of this Guide is defined and the types of problems, encompassing the life cycle of the products, for which it is expected to support the developers of WECs, are specified.

The present guide focuses on the analysis and quantification of uncertainty that characterize the outcomes of hybrid testing procedures, not uncertainties in the overall design process of WECs. Hybrid testing methodologies might target different key product characteristics of the WECs, and their development may parallel the level of maturity of the designed system itself, which will also be reflected in the uncertainty analysis. For example, the size and impact of uncertainty on the test results are presumably very different in proof-of-concept setups compared to fully developed and operating test benches.

The goal of the VALID project is to develop novel testing platforms, methods and knowledge that address the challenge of the costs associated with reliability testing of WECs in the marine environment. Assessment of the reliability and service life of WECs is particularly challenging because failure might take a long time to occur in the marine environment. Components and subsystems of WECs are usually designed to resist very harsh environmental conditions, which makes it difficult to observe failures under relatively short periods. Furthermore, most working examples of WECs are still at concept or prototype stage, with ample margins for design revisions and little field experience. WEC technologies usually undergo significant design changes between generations, from using standard components not designed for the same working conditions, towards building dedicated supply chains of specialized components. This adds to the complexity of reliability assessment at early stages. Hence, there is a need to speed up the test procedures in a controlled environment to detect design flaws and identify potential for improvement early in the design process.

As illustrated in VALID D1.1 and D1.2 (Bargiacchi et al., 2021; Ruiz-Minguela et al., 2021) a key element in the overall strategy pursued in the VALID project to address this need is to focus testing and analysis resources on those WEC components/subsystems whose failure would most severely compromise the intended function of the WECs (namely, power generation under a specified period of time and environment). The choice to focus the testing activities on critical components simplifies the assessment of system reliability at an early development stage, provided that the influence of the other components and subsystems can be adequately taken into account.

A central question in the VALID project is whether a proper mix of physical measurements and numerically simulated responses (i.e., hybrid testing) might be the key to fast and accurate reliability testing of WECs at the early development stage. Therefore, the focus is on the acceleration of component development through hybrid testing, rather than on reliability assessment of mature technologies.

The co-existence of physical and virtual test environments represents a specific challenge of hybrid testing to Uncertainty Quantification (UQ). Furthermore, the interest in accelerated testing and possible differences between the dimensions of tested components and those of their counterparts used in the marine environment poses additional challenges that are specific to the type of testing procedures targeted in the VALID project, which the VALID user cases exemplify.

1.2 Structure of Report

The content of this report is articulated in the following main building blocks, which address the specific purposes to present the methodology and to provide the reader with guidance to conduct uncertainty assessment in hybrid testing independently of the user cases developed in the VALID project:

Part A: Methodology for Uncertainty Quantification in Hybrid Testing

- Section 2: Background and motivation for uncertainty quantification in physical testing, numerical simulations, and reliability assessments.
- Section 3: Detailed description of the proposed methodology for UQ in Hybrid Testing, which is an adaptation of the VMEA methodology.
- Section 4: Presentation of and methods for UQ in physical measurements, with special emphasis on the ISO recommendation GUM , (ISO/TMBG, 2008).
- Section 5: Review of key concepts and methods for UQ in numerical simulations, with reference to appropriate standards and guidelines.
- Section 6: Guidance to evaluate the impact of the outcomes of UQ on decision-making and reliability assessments for design and development.

Part B: Applications to VALID User Cases

- Section 7: Applications of the proposed methodology to the User Case #1 - CorPower.
- Section 8: Applications of the proposed methodology to the User Case #2 - IDOM.
- Section 9: Applications of the proposed methodology to the User Case #3 - Wavepiston.

Note that Section 3 presents the methodology for UQ based on VMEA, whereas Sections 4 and 5 provide background and details on assessing uncertainties in the physical and numerical environments, respectively.

The reported examples in Part B, Sections 7-9, are based on the outcomes of a series of workshops where VALID project partners were invited to identify and discuss the role of different sources of uncertainty in each user case. The information provided by the developers of the testbeds considered in the user cases was quantified following the VMEA. The scope and goal of the workshops can be summarised as follows:

1. **First series (Basic VMEA)**: held during Spring of 2022, in approximately 3 sessions of 1 hour for each user case. The main goal was to discuss the relevant sources of uncertainty, indicating which should be prioritized in the follow-up quantitative analysis. Uncertainty sources in the physical as well as virtual parts of the test beds were considered. The input from the participants was codified according to the qualitative rating system defined in the basic VMEA methodology.
2. **Second series (Probabilistic VMEA)**: held during the Spring of 2023, following a similar format as that of the first series. The analysis focused on the elements that are thought to contribute the most to the overall uncertainty, according to the outcomes of the first series of workshops. Quantitative data on the uncertainty of measured and computed input

variables was collected, estimated and / or judged, and combined to evaluate the total uncertainty of the hybrid testing procedure using the probabilistic VMEA methodology.

It should be noted that the hybrid test rigs were under development during the work with the report, and therefore the estimated uncertainty reported in Sections 7-9 should be interpreted primarily as a preliminary uncertainty analysis, rather than the final estimate of the uncertainty in the results. In particular, the present report aims to demonstrate how such preliminary results may be refined as the designs of all the physical and virtual components of the test rigs evolve. The examples included in Sections 7-9 illustrate how uncertainty quantification can support the design of novel testing methods, by facilitating the early identification of key uncertainty factors affecting the accuracy and robustness of test results. A view on uncertainties in early development stages can help the rational allocation of resources in the process of the development of physical and virtual components of the hybrid rigs.

This project has received funding from the European Union's Horizon 2020 research and innovation programme under grant agreement No 101006927.

2 Background on Uncertainties and Reliability

This section provides an overview of and background for the components of the proposed methodology for UQ in hybrid testing. It also gives motivation for addressing uncertainties. Sections 2.1 and 2.2 present a discussion on uncertainties in physical measurements and in numerical simulations, respectively. The reliability and uncertainty methodology, VMEA, is presented in Section 2.3.

2.1 Uncertainty in Physical Measurements

It is an empirical fact in scientific experimentation, as well as in engineering practice and many circumstances of everyday life, that no physical quantity (e.g., length, time, electrical current) can be measured with complete certainty.

2.1.1 What is Measurement Uncertainty?

Repeated measurements under nominally identical conditions will produce somewhat different values, instead of identical ones. A task such as measuring the length of a table with a measuring tape offers an intuitive illustration of this point: depending on how firmly the tape is held, or even the ambient temperature or humidity of the skin, one might expect different readings for the length of the table.

The observation of the presence of multiple sources of uncertainty in this everyday example can be generalized to virtually any case where a measurement is performed. Uncertainty arises from all the elements that participate in the measurement process, which may be broadly categorized as:

- Test equipment.
- Test environment.
- Test method.
- Test objects.
- Operator.
- Unknown sources of variability.

Each item in the above list can be broken down into multiple factors relevant to the quantity and specific circumstances targeted by the measurement procedure, as graphically illustrated in Figure 1. The identification of individual sources of uncertainty is an important step in the methodology.

This project has received funding from the European Union's Horizon 2020 research and innovation programme under grant agreement No 101006927.

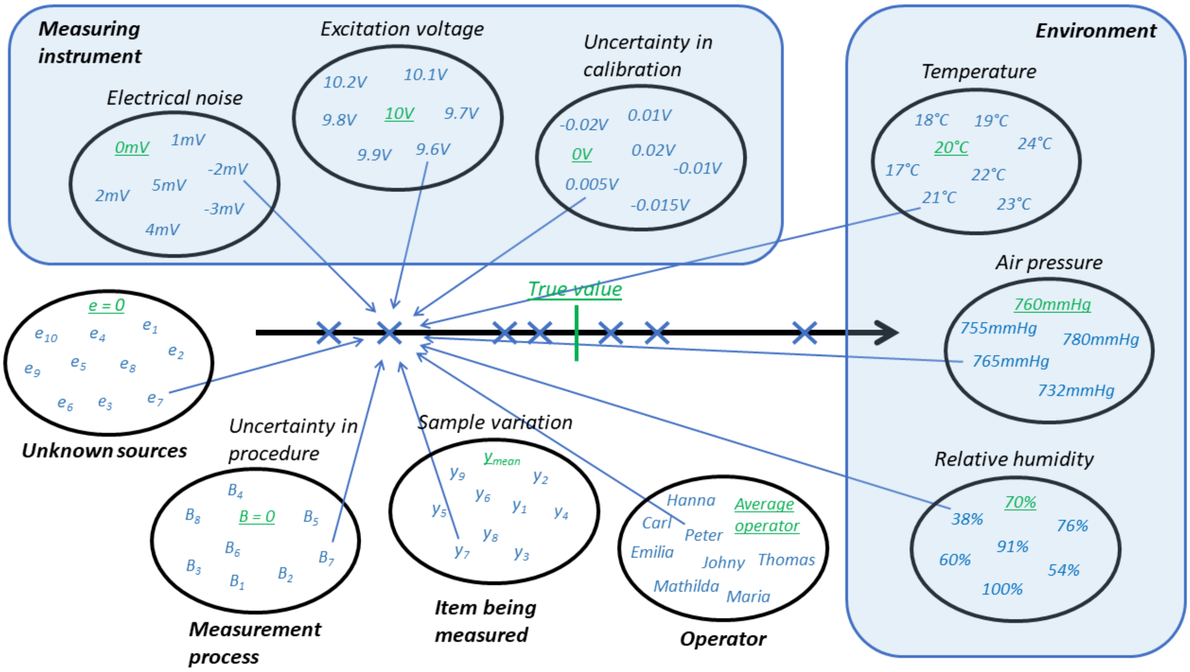

Figure 1: General map of possible sources of uncertainty that contribute to make the results of the measurement of a quantity different from its true value.

2.1.2 Why Consider Measurement Uncertainty?

In everyday measurements, uncertainty is rarely a concern because the error associated to a crude measurement or estimation is unlikely to result in any severe consequence. However, there are cases where measurement uncertainty plays a significant role even in ordinary situations, although the end customers may not be aware of it and adequate safeguard and control systems are in place to reduce the impact of measurement errors on them. For example, fuel dispensers undergo regular inspections by independent bodies to verify that the variation of released fuel does not exceed a maximum value stipulated by national law (0.5% in Sweden, for example).

Therefore, the importance of measurement uncertainty depends on the context of the intended application of the quantity being measured. Regarding measurements done at different stages of product development and manufacturing, for example, Syam discussed the following applications that motivate the quantification of uncertainty (Syam, 2021):

1. Measurement comparison.
2. Measurement traceability.
3. Pre-production phase.
4. Post-production phase.
5. Measurement/production process improvement.

Item 1 in the above list is encountered in many situations and has pervasive consequences beyond the purely technical level. A fair comparison of measurements is essential to establish mutual trust between business partners, for example buyers and suppliers of manufactured parts who need to agree on the dimensions of the traded products. Differences among measurements performed on the same object by independent parties might stem, for example, from the equipment, the operators, the measurement sites, or any combination thereof.

This project has received funding from the European Union's Horizon 2020
research and innovation programme under grant agreement No 101006927.

In general, the comparison between different measurement results is meaningful only if their uncertainty is taken into account in the assessment. As a practical example, the verification of the technical specification provided by a supplier for the electrical resistance of a component can be conceptualised. The manufacturer stated a nominal value of 20kΩ, but some independent evidence that such a value is correct is to be gathered. A third-party testing laboratory is then given the task to measure the resistance, and the result is compared to the value stated by the manufacturer. The resistance measured by the laboratory is 17kΩ. Two possible scenarios emerge, graphically represented in Figure 2:

1. (Left-hand-side of Figure 2) No measurement uncertainty is provided neither from the manufacturer nor the independent laboratory. The discrepancy between the resistance values measured by the two parties might reflect the existence of an actual difference between the two values, or it might be just the result of some effect that was not adequately controlled during the test (for example, temperature, or calibration of the measuring equipment). There is no reason to exclude that additional measurements would not result in different values. Therefore, in this scenario there is no rational way to assess which of the two measurements is closer to the true value of the resistance.
2. (Right-hand-side of Figure 2). The measured resistance values are provided with their estimated uncertainty. The range within which the true value is expected to fall turns out to be significantly larger for the measurement provided by the supplier than for the one done by the independent laboratory. Therefore, the magnitude of the uncertainty estimated in the two cases suggests that the value provided by the laboratory is more credible than the one presented by the supplier.

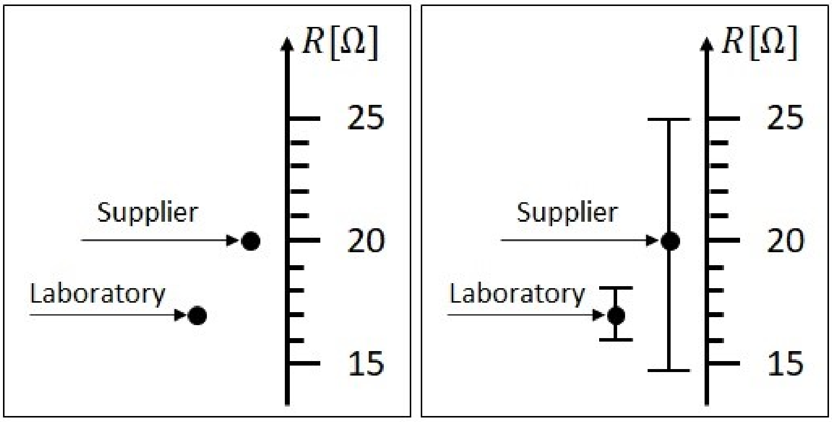

Figure 2: Illustrative example of the importance of uncertainty in comparison between measurements.

A number of comments and reflections can be made based this example:

1. Only one measurement point is shown in order to avoid cluttering the graphical representation. The displayed points might be the direct outcomes of measurements, or the result of some operation on the raw data, such as averaging. Regardless, the observations about the consequences of not taking into account measurement uncertainty are the same.
2. One pragmatic argument to accelerate the decision process, i.e., to establish if the resistance value provided by the supplier can be trusted, by avoiding the quantification of measurement uncertainty might be that, for the purpose of the intended application of the tested component, a discrepancy of 3kΩ is acceptable. Such argument is based on the implicit assumption that the value stated by the supplier is correct, or at least the closest to

This project has received funding from the European Union's Horizon 2020 research and innovation programme under grant agreement No 101006927.

the true value of the resistance. Without estimating the uncertainty in each measurement, that is just an assumption hardly distinguishable from a leap of faith.

3. The quantification of uncertainty to qualify measurement results to support decision-making requires that the assessment of uncertainty is carried out by similar procedures and with a level of thoroughness that adequately minimize the risk of underestimating or overestimating the uncertainty. Furthermore, the process to quantify the uncertainty should be transparent, that is it should be possible for external parties to reconstruct how the various sources of uncertainty have been assessed and combined into the final result. Considerable efforts have been spent over the years to address these issues by promoting standardized terminology and common practice for the assessment of measurement uncertainty. Notable examples of the results of these initiatives are International Vocabulary of Metrology (VIM) (ISO/TMBG, 2007) and GUM (ISO/TMBG, 2008), which are widely internationally accepted references with applications across many scientific and engineering fields.

2.1.3 Methods for Measurement System Analysis

For Measurement System Analysis (MSA) and uncertainty quantification in physical testing, it is common practice to use the ISO recommendation GUM (ISO/TMBG, 2008). Each of the identified uncertainty sources are quantified by its sensitivity coefficient, c_i, and its standard uncertainty, u_i, in terms of a standard deviation. The so-called combined standard uncertainty, u_y, of measurement y is then calculated as the root sum of squares as:

$$u_y = \sqrt{\sum_{i=1}^{n} u_{y,i}^2} = \sqrt{\sum_{i=1}^{n} c_i^2 \cdot u_i^2} \tag{1}$$

where $u_{y,i}$ is the resulting uncertainty from source i, and n is the total number of uncertainty sources.

The measurement uncertainty is often presented as an interval with a specific level of confidence. Typically, a 95% confidence level is used, giving an interval $Y = y \pm 2 \cdot u_y$, where y is the measured value of the quantity Y. Generally, the measurement uncertainty can be given as an interval $Y = y \pm U$, where U is called the expanded uncertainty calculated as $U = k \cdot u_y$, where k is the coverage factor corresponding to the chosen level of confidence. In the case of 95% confidence, the coverage factor is $k = 2$.

Established methods to analyse and quantify measurement uncertainty, as well as the rigorous definition of the degree of confidence associated with the computed uncertainty are presented in Section 4, following the ISO recommendation GUM (ISO/TMBG, 2008). Additional information on standard terminology in the field of uncertainty analysis can be found in VIM (ISO/TMBG, 2007).

2.2 Uncertainty in Numerical Simulations

As even the most sophisticated computational models used in engineering analysis are built upon assumptions, simplifications of the governing physical laws and uncertain parameters, their outcomes are expected to deviate, to some extent, from the reality that they are designed to simulate. Numerical simulations can be considered a form of virtual experiments, as they share with their physical counterparts the capacity to produce information about the behaviour of entities that obey the laws of physics under various circumstances.

2.2.1 What is Uncertainty in Numerical Simulations?

Unless some form of randomness is intentionally introduced in the computational models, numerical simulations are deterministic, and hence they return exactly the same output for a given input, which makes them fundamentally different from physical experiments as devices to generate information. The error in the results of virtual experiments is defined as their deviation from reference values used for validation (which are typically measured), rather than from a true value whose existence is convenient to assume but impossible to demonstrate. A consequence of this definition is that the error in a simulated quantity can be always determined, provided that measurement data suitable for model validation are available.

In cases where validation data are not available, such as when physical experiments of a given system are unfeasible, uncertainty quantification, possibly supplemented by sensitivity analysis, provides some indication of the error that can be expected for the simulated results. In these cases, the meaning of uncertainty for numerical simulations resembles more closely its counterpart in physical experiments. In contrast, the way to quantify uncertainty differs significantly between physical and virtual experiments because repeated runs of the simulations for the same set of input deterministic variables and parameters will produce identical results, which prevents the estimation of a suitable interval where the true value is expected with a given confidence level. The spread in measurement results observed in physical experiments has to be simulated by supplementing the computational model with adequate mathematical representations of the uncertainty that characterizes the actual design variables and parameters.

2.2.2 Why Consider Uncertainty in Numerical Simulations?

The role of numerical simulations in engineering analysis has steadily grown in the last decades, boosted by the larger availability of computational resources, in the form of more accessible and more powerful hardware, software tools, and user-oriented interfaces. Numerical models enable the simulation of the behaviour of engineered systems under conditions which would be more costly and / or unfeasible to reproduce in a laboratory environment.

As numerical simulations evolve towards a widespread technique or toolbox that are more accessible to designers and non-specialists in computational methods, the challenge to ensure their credibility becomes increasingly critical. The notion of 'simulation governance' has been introduced in the last decade as "*the managerial function concerned with assurance of reliability of information generated by numerical simulation*" (Oberkampf and Imbert, 2018; Szabó and Actis, 2012). Uncertainty quantification is a key element of Simulation Governance. The industrial perspective on uncertainty quantification in numerical simulations for the energy sector has been discussed in (Pasanisi and Dutfoy, 2012). For an example of the risk entailed by poor quality management of numerical simulations, see e.g. (Arnold, 2009).

While noting that the methods to represent and evaluate uncertainty in computational models are reviewed in more detail in Section 5, the main reasons to conduct uncertainty quantification in numerical simulations can be summarized as follows:

1. To assess the robustness of simulated predictions against uncertainty in design variables and parameters.
2. To identify the design variables and parameters that mostly contribute to the variability of simulation results, thus supporting a rational allocation of resources to reduce the impact of the sources of variability on the performance of the designed products.
3. To support the rational estimation of simulation error under conditions where validation data are not available.
4. To enable the implementation of robust design methodologies, which target the optimal utilization of materials without compromising safety requirements.
5. To enable the construction of confidence intervals or other rational measures of credibility for the validation of simulated results.

A notable example of point 5 in the context of the VALID project is given by the derivation of safety factors from the probabilistic analysis of uncertainty in design variables, which will be illustrated in more detail in the methodology presented in Section 3 and in Section 6 on design and reliability evaluations.

2.2.3 Methods for Uncertainty Quantification in Numerical Simulations

Numerical modelling and simulation are effective tools to mitigate risk and to reduce the time and cost of product design and development. In spite of the broad popularity of Computer Aided Engineering (CAE) in industrial practice, comparatively little effort is often devoted to the analysis and quantification of uncertainty that inevitably characterizes computational models. Uncertainty in input parameters, model structure, loads, and boundary conditions originate from the inherent variability of physical quantities, as well as from incompleteness of information about the object or system being modelled. The uncertainty in input is propagated through the numerical models, thus leading to a quantitative estimation of the spread in the output variables.

UQ associated with computational models is part of the Verification and Validation (V&V) process, which systematically addresses the comparison between model predictions and experimental data. V&V and UQ are necessary activities for the credibility assessment of the results of numerical simulations, particularly in the case of novel engineering fields where standardized requirements for design and testing are not available or in safety-critical applications where underestimation of risk and variability may lead to hazardous consequences or financial loss.

The majority of UQ methods found in industrial applications rely on probabilistic frameworks, wherein uncertain variables are modelled as probability distributions derived from experimental data and expert elicitation. Random number generators and sampling algorithms such as Monte Carlo and Latin Hypercube are often used to evaluate the probability distributions and explore the design space where the input variables and parameters are defined.

The literature on V&V and UQ is vast and diversified, spanning areas of fundamental mathematics and statistics, numerical methods, and applications in virtually any field of engineering. For a concise and pragmatic introduction to UQ for computational models, the guide authored by the Stochastics Working Group at NAFEMS (National Agency for Finite Element Methods and Standards) is a recommended starting point (NAFEMS, 2018). A comprehensive guide to the expression of uncertainty for computational models can be found in the "Handbook of Uncertainty Quantification" (Ghanem et al., 2017). For an overview of existing standards for V&V and UQ in modelling and simulation, the reader is directed to the review by Freitas (Freitas, 2020). Additionally, Section 5 gives a more comprehensive overview and review of relevant methods for UQ in numerical simulations.

2.3 Variation Mode and Effect Analysis Methodology

The structure of the methodology for UQ in hybrid testing is based on the VMEA methodology, which is a probabilistic reliability and robustness methodology that studies the uncertainty around a nominal design. An adaption of VMEA to marine energy applications can be found in (Johannesson et al., 2016). Based on all uncertainty sources, the methodology determines the total uncertainty which can be used to derive a statistically based safety factor. The statistical safety factor is constructed through a confidence interval, which is determined from an overall standard deviation of the defined target function. Background and summary of the VMEA methodology is provided in this sub-section.

An important goal of engineering design, and within marine energy applications in particular, is to get a reliable product. In industry, the method of Failure Mode and Effect Analysis (FMEA) is often used for reliability assessments, where the aim is to identify possible failure modes and evaluate their effects, see e.g. (Stamatis, 2003). FMEA focuses on identifying and eliminating known or potential failures. However, it is a qualitative method, and it does not measure the resulting reliability. The failure modes are most often triggered by unwanted variation (Davis, 2006), and, thus, a general design philosophy, including all different sources of unavoidable variation, has been developed. This reliability and robust design methodology, named VMEA, was first presented in (Chakhunashvili et al., 2004; Johansson et al., 2006) and was further developed in (Chakhunashvili et al., 2009; Johansson et al., 2006; Svensson et al., 2009). A more general presentation of the methodology can be found in (Bergman, 2009; Johannesson et al., 2016, 2013; Johannesson and Speckert, 2013; Svensson and Johannesson, 2013). The VMEA concept takes the quantitative measures of failure causes into account. The method is based on statistics, reliability, and robust design, which can guide engineers to find critical areas of unwanted variation. The technique has been successfully implemented for fatigue design and maintenance in the automotive and aeronautic industries (Johannesson et al., 2009; Svensson et al., 2009), as well as in the marine energy field (Jia et al., 2017; Johannesson et al., 2022, 2019, 2016).

2.3.1 Generic Principles of VMEA

Generally, the VMEA method is described as evolving through three different phases during design, as illustrated in Figure 3.

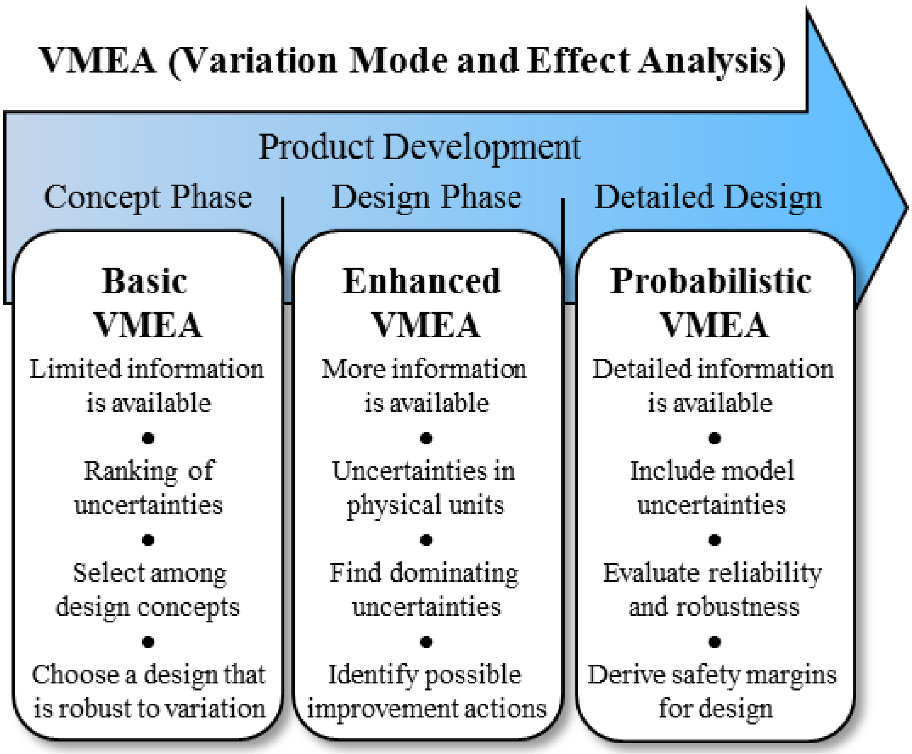

Figure 3: VMEA in different design stages.

The first phase is the basic VMEA, where sensitivities and uncertainty sizes are judged on a scale from 1 to 10. The basic VMEA is used in the early design stage when the knowledge of uncertainties is limited, and the assessment is often built upon engineering judgements from a cooperative brainstorm session. It aims to provide a high-level overview of the effect(s) of the different uncertainties, serving as a tool for identifying the major uncertainty contributions. The basic VMEA is primarily used to screen for uncertainty sources and can thus be used for prioritisation for further studies.

This project has received funding from the European Union's Horizon 2020 research and innovation programme under grant agreement No 101006927.

A refinement of the basic VMEA may be done by quantifying uncertainties, by judging their standard deviations by means of standard rules and by judging sensitivities by fundamental physical knowledge; again the assessment is typically based on engineering judgements. The analysis is called an enhanced VMEA and can be used for a preliminary assessment of the uncertainty sources and the resulting measurement uncertainty.

The final stage, called the probabilistic VMEA, is made possible when more information is available about the most critical uncertainty sources. Standard deviations are typically obtained by more detailed studies of empirical results. Sensitivity coefficients can be found from numerical sensitivity studies or differentiation of physical/mathematical models. The result of such an analysis gives an estimate of the resulting total uncertainty and a corresponding statistical safety factor.

The general procedure for performing a VMEA is common for all development phases. The work process can be split into four activities "Define-Analyse-Evaluate-Improve", as illustrated in Figure 4. These seven steps listed in Figure 4 will be described in more detail in Section 3.1.2.

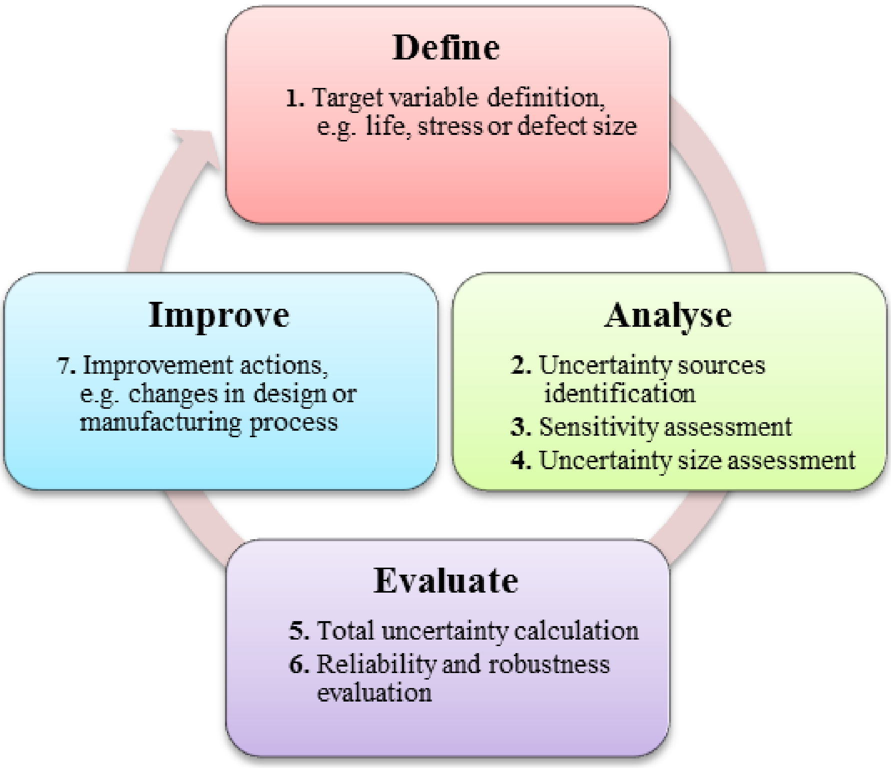

Figure 4: VMEA in the design and improvement cycle.

2.3.2 Mathematical and Statistical Principles of VMEA

The VMEA method represents a first-order, second-moment reliability method that studies the variation and uncertainty around a nominal design. The underlying mathematical and statistical principles of VMEA are presented in this sub-section.

The target function, often also referred to as the response function, can be defined as:

$$y = f(x_1, x_2, \dots, x_n) \tag{2}$$

where y is the target variable, also called response or output variable, and x_i are the input variables. The target function describes the relation between the input variables and the target variable, and it can be, for example, the fatigue life, the maximum stress, or the maximum defect size.

The evaluation of the statistical properties of the target variable is of interest, assuming that the input variables are random variables characterized by their mean and standard deviation. The Gauss' approximation formula is used, which is based on linearizing the target function:

$$\mathrm{y} = f(x_1, x_2, \ldots, x_n) \approx \sum_{i=1}^{n} c_i \cdot \mathrm{x_i} \tag{3}$$

where c_i is the partial derivative of the target function f with respect to x_i, namely:

$$c_i = \frac{\partial f}{\partial x_i}(x_{1,r}, x_{2,r}, \ldots, x_{p,r}) \tag{4}$$

evaluated at a reference point, typically chosen to be the mean value of the input variables. As stated above, the sensitivity coefficient c_i is formally the partial derivative of the target function f with respect to x_i; however, in practice, it is often best approximated by a difference quotient.

Using Gauss' approximation formula, the mean and standard deviation can be evaluated. The random variables corresponding to the target variable and the input variables are denoted by Y and X_i, respectively. The mean value of the target variable is evaluated as:

$$\mathrm{E}[Y] = \mathrm{E}[f(X_1, X_2, \ldots, X_n)] \approx f(\mathrm{E}[X_1], \mathrm{E}[X_2], \ldots, \mathrm{E}[X_n]) \tag{5}$$

where $\mathrm{E}[\cdot]$ denotes the expected value.

The standard deviation, being the square root of the variance, can then be approximated using Gauss' approximation formula:

$$\mathrm{Var}[Y] = \mathrm{Var}[f(X_1, X_2, \ldots, X_n)] \approx \sum_{i=1}^{n} c_i^2 \mathrm{Var}[X_i] + \mathrm{Covariances} \tag{6}$$

This formula gives the variance of the target variable Y as the sum of variance contributions (and possible covariances) from different influencing random variables X_i, each described by its own variance, $\mathrm{Var}[X_i]$, together with its influence by means of the sensitivity coefficient c_i. Covariances between the influencing variables may also contribute, however they can usually be neglected or avoided by re-formulating the model.

In summary, the VMEA method is based on characterising each uncertainty source by its mean and statistical standard deviation, which corresponds to a second-moment method. Further, it approximates the target function by means of its sensitivity coefficients with respect to the target variables, which corresponds to a first-order method. The nominal value of the target variable is evaluated according to Eq. (5). The total prediction uncertainty, here denoted by u_y in accordance with the standard notation in measurement uncertainty, is derived by using the root sum of squares of the uncertainties:

$$u_y = \sqrt{\sum_{i=1}^{n} u_{y,i}^2} = \sqrt{\sum_{i=1}^{n} c_i^2 \cdot u_i^2} \tag{7}$$

where $u_{y,i}$ is the resulting uncertainty from source i, and is calculated as the product of the sensitivity coefficient $|c_i|$ and the standard deviation u_i of source i. The total number of uncertainty sources is n. Note that the VMEA method is a so-called second-moment method, since it uses only the standard deviation to characterise the distribution of the uncertainty sources. Further, it approximates the target function by means of its sensitivity coefficients with respect to the input variables, which corresponds to a first-order method.

2.3.3 Evaluation of Reliability and Uncertainties

The results from the uncertainty assessment can be used for reliability evaluations and for deriving safety factors. Some assumption on the distribution of the target variable is necessary for the statistical analysis. Often the central part of the distribution of the target variable may be well approximated by a normal distribution. An approximate confidence interval for the target variable can then be calculated as $Y = y \pm k \cdot u_y$, compare Section 2.1.3. Often the target function is in logarithmic form, and then by taking the exponential of the confidence interval a corresponding safety factor can be obtained. Further discussions on these topics are found in Section 6.

This project has received funding from the European Union's Horizon 2020 research and innovation programme under grant agreement No 101006927.

3 Methodology for Uncertainty Quantification in Hybrid Testing

In hybrid testing, which involves both physical and numerical models, there is a need to assess the quality of the result. Therefore, the uncertainty of the output of the hybrid tests should the investigated, and the uncertainty should be evaluated in a systematic way.

The proposed methodology for UQ in accelerated hybrid testing is based on three methodologies presented in Sections 2.1-2.3:

- ISO recommendation GUM (ISO/TMBG, 2008), which was introduced in Section 2.1 and is described in detail in Section 4.
- UQ methodology in numerical simulations, which was introduced in Section 2.2 and methods reviewed in Section 5.
- VMEA, which was described in Section 2.3, and will here be adapted to the hybrid testing set-up.

The aim for this section is to present the methodology for UQ in hybrid testing. The general work process will follow the VMEA methodology, which is similar to that detailed in GUM. The main steps in the suggested methodology for UQ in hybrid testing are:

- Define the output quantity to be evaluated, i.e., the target variable.
- Identify the uncertainty sources, that are classified as random or systematic.
- Assess uncertainty sources in terms of their sensitivities and uncertainty sizes.
- Combine the uncertainty sources into a combined measurement uncertainty for the hybrid testing.

First, in Section 3.1, the general work process is described. The identification and classification of uncertainties are discussed in Section 3.2. The methodology implemented for the concept stage is described in Section 3.3, and is based on the basic VMEA approach, where the aim is to identify and assess, at a high-level, the major uncertainty sources. For the final design stage, the methodology for assessing the measurement uncertainty is detailed in Section 3.4, based on the probabilistic VMEA approach.

3.1 General Work Process

The general work process for VMEA adopted for UQ in hybrid testing is described in the following sub-sections.

3.1.1 Different Development Stages

Two stages of uncertainty quantification, as illustrated in Figure 5, are recommended for hybrid testing of critical components:

1. *Concept phase* – where the goal is to assess the main uncertainty sources for the concept or prototype test rig that is in development. In this phase the basic VMEA approach can be used.
2. *Finalized design phase* – where the goal is to assess the measurement uncertainty for the output quantities of hybrid test rig. In this phase the probabilistic VMEA approach can be used.

This project has received funding from the European Union's Horizon 2020
research and innovation programme under grant agreement No 101006927.

The IEA-OES guidance framework, (IEC TS 62600-103, 2018) for evaluation of ocean energy technology, also based on stage activities, describes Stage 1 as concept development and Stage 2 as design optimisation, which aligns with the two phases above. Moreover, there are suggested stage activities for assessing reliability.

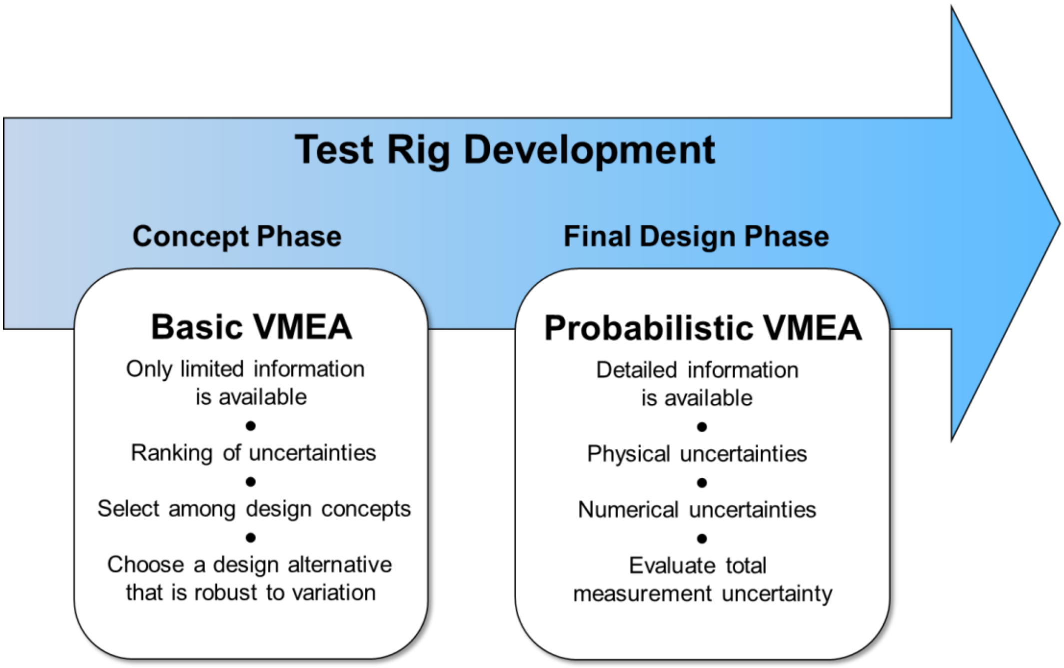

Figure 5: Test rig development stages, basic & probabilistic VMEA.

3.1.2 Work Process

Following the general VMEA work process described in Section 2.3 and illustrated in Figure 4, the work process for UQ in hybrid testing can be grouped into four activities "Define-Analyse-Evaluate-Improve". The work process is described by the following seven steps:

1. *Target variable definition*: The first step is to define the target variable, i.e., the property to be studied, which can. e.g., be the life of a component, the maximum stress or the largest defect.
2. *Uncertainty source identification*: In this step all sources of uncertainty that can have an impact on the target variable are identified and categorised into either load or strength group. The uncertainty sources may be classified as scatter, statistical and model uncertainties.
3. *Sensitivity assessment*: Here the task is to evaluate the sensitivity coefficients of the sources of uncertainty with respect to the target variable by numerical calculations, experiments, previous experience etc.
4. *Uncertainty size assessment*: Here the task is to quantify the size of the different sources of uncertainty by experiments, previous experience, engineering judgement etc.
5. *Total uncertainty calculation*: The final step of the core VMEA activity is to calculate the total resulting uncertainty in the output of the target function by combining the contributions from all uncertainty sources according to their sensitivities and sizes.

6. *Reliability and robustness evaluation*: The result of the VMEA can be used to evaluate the reliability and robustness in order to compare design concepts, find dominating uncertainties, derive safety factors etc.
7. *Improvement actions*: The last important step is to feedback results into the improvement process by identifying uncertainty sources that are candidates for improvement actions and evaluate their potential for reliability improvements.

Although the core VMEA methodology constitutes steps 2-5, the problem definition (step 1), reliability evaluation (step 6) and improvement work (step 7) are equally essential in the design process. Therefore, all seven steps are included in the overall VMEA methodology to cover the design and improvement cycle illustrated in Figure 4.

3.2 Identification and Classification of Uncertainty

The understanding of uncertainty sources is a key issue in assessing measurement uncertainty as well as in engineering design. Therefore, this section is devoted to the identification and classification of uncertainties.

3.2.1 Identification of Uncertainty Sources

Identifying the important uncertainty sources is a difficult task, where a combination of individual creativity and brainstorming could be recommended. To aid in the work of identification, it is often useful to have some kind of structure. In the automotive industry, five categories of uncertainties in engineering design are often used. These have been adopted to the hybrid testing for wave energy applications, and the following five categories of uncertainty sources are suggested:

- **Environmental conditions** – External environmental conditions that the products/devices are exposed to.
- **Physical test rig** – Uncertainties related to the physical test set-up.
- **Numerical test rig** – Uncertainties related to the numerical models and simulations test set-up.
- **Life modelling** – Uncertainties related to life and wear-out modelling including, e.g., acceleration methods, scaling methods and potential errors in life modelling.
- **Manufacturing** – Uncertainties related to manufacturing, assembly and mounting of component/product.

The five categories are illustrated in Figure 6, where they are also connected to the pre-processing, processing and post-processing steps introduced in VALID D1.1 (Bargiacchi et al., 2021). Below some guidance on typical uncertainty sources within the five categories is presented.

This project has received funding from the European Union's Horizon 2020 research and innovation programme under grant agreement No 101006927.

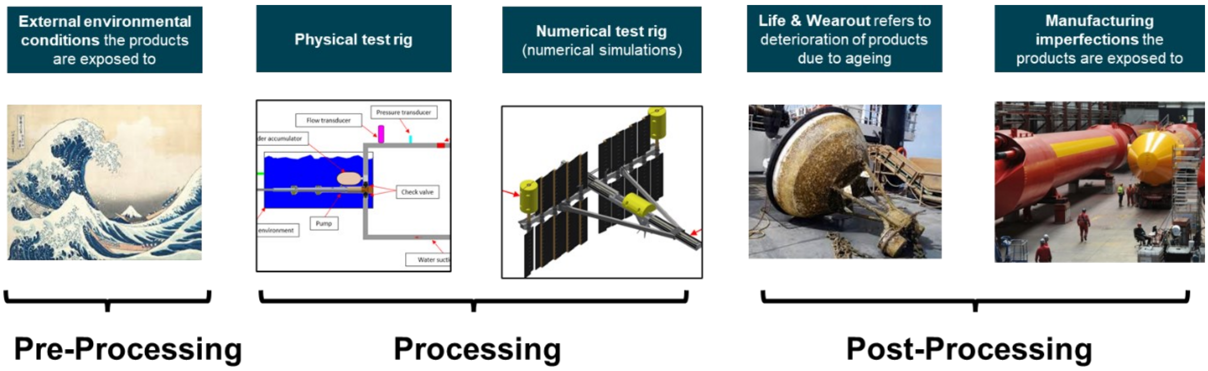

Figure 6: Five categories of uncertainty sources.

3.2.1.1 Environmental Conditions

This category contains uncertainty sources due to external environmental conditions that the products/devices are exposed to. Typical uncertainties to consider are:

- Waves conditions – characterized by e.g. wave height and period, $(H_s, T_p\ )$.
- Currents.
- Wind.
- Bio fouling.
- Sea water salinity.
- Sea water temperature.

3.2.1.2 Physical Test Rig

Uncertainties related to the physical test set-up. Typical uncertainties to consider are:

- Measurement uncertainty and control of signals, e.g., position, pressure, temperature.
- Mounting of specimen in test rig.
- Tolerances of specimen.
- Application of loads in test rig vs. real device operation.

3.2.1.3 Numerical Test Rig

Uncertainties related to the numerical models and simulations. Typical uncertainties to consider are:

- Modelling error.
- Domain error.
- Discretization error.
- Boundary conditions and load application.

3.2.1.4 Life Modelling

Uncertainties related to life and wear-out modelling including e.g., acceleration methods, scaling methods and potential errors in life modelling. Typical uncertainties to consider are:

- Modelling error in life model.
- Acceleration methods.
- Scaling methods.
- Marine growth effects.
- Corrosion effects.

3.2.1.5 Manufacturing

Uncertainties related to manufacturing, assembly and mounting of components. Typical uncertainties to consider are:

- Tolerances.
- Variation in material properties.
- Assembly and mounting of components.

3.2.2 Classification of Uncertainties

3.2.2.1 Random or Systematic Effects

In GUM (ISO/TMBG, 2008), the uncertainty sources that give rise to uncertainty in measurement are classified as:

- **Random** - where repeating the measurement gives a randomly different result. Hence, repeated measurements give more knowledge, and by averaging the results a better estimate is obtained through diminishing random errors.
- **Systematic** - where the same influence affects the result for each of the repeated measurements. In this case, nothing extra is learned by simply repeating measurements. Other methods are needed to estimate uncertainties due to systematic effects.

These types of uncertainties are important to distinguish, since random effects can be reduced by repeated measurements, while systematic effects will not diminish.

3.2.2.2 Aleatory and Epistemic Uncertainties

There are more detailed and systematic ways in which the types of uncertainties may be classified, see e.g. (Melchers and Beck, 2018) and (Ditlevsen and Madsen, 2007). The first classification is, as above, to distinguish between random and systematic effects, and these types of uncertainties are here called aleatory uncertainties and epistemic uncertainties. The first one refers to the underlying, intrinsic uncertainties, e.g., the scatter or random uncertainties that may originate from load variation or uncontrollable strength variation. The latter one refers to the uncertainties due to lack of knowledge, which can be reduced by means of additional data or information, better modelling and better parameter estimation methods.

In (Melchers and Beck, 2018) a detailed breakdown of different kinds of uncertainties is presented. In the uncertainty assessments, the focus is often on three kinds of uncertainties, also mentioned by (Ditlevsen and Madsen, 2007):

- *Random uncertainty* or physical uncertainty, which is an uncertainty identified with the inherent random nature of the phenomenon, e.g., the variation in strength between different components. Sometimes it is also called scatter, randomness or noise.
- *Statistical uncertainty*, which is an uncertainty due to the statistical estimation of model parameters based on available data, e.g., the estimation of the uncertainty of parameters in a regression model describing the life as a function of the load level. Generally, the observations of the variable do not represent it perfectly and as a result there may be bias in the data recorded. In addition, different sample data sets will usually produce different statistical estimates. This causes statistical uncertainty.
- *Model uncertainty*, which is the uncertainty associated with the use of one (or more) simplified relationships to represent the 'real' relationship or phenomenon of interest, e.g., a finite element model used for calculating stresses, is only a model for the 'real' stress state. Modelling uncertainty is often due to lack of knowledge, and can be reduced with research, refinement of models or increased availability of data.

The first type of uncertainty, *random uncertainty*, is an aleatory uncertainty, whereas the others should be regarded as epistemic uncertainties, as they can be reduced through better knowledge.

Another important kind of uncertainty is the uncertainties due to human factors. These are the uncertainties resulting from human errors or involvement in the design, system, use, etc. Failures caused by misuse, gross errors and human mistakes should primarily be subject to quality management procedures.

3.3 Concept Stage – Basic VMEA

The basic VMEA procedure, see (Chakhunashvili et al., 2004; Johansson et al., 2006), is detailed in this sub-section. Recall that the goal of the basic VMEA is to identify the most important sources of uncertainty, and the sizes of the sources of uncertainties as well as their sensitivities, which are evaluated on a scale from 1 to 10. The variation is characterized by the summing of the square of the product of the sensitivity and the uncertainty size. To conduct an adequate VMEA that incorporates different views and competences, a cross-functional team of engineers and experts should be formed. Such an analysis can indicate which part of the hybrid testing is most critical in terms of uncertainty, and hence, that needs special focus in the design and set-up of the testing.

3.3.1 Target Variable Definition

The first step in the procedure is to define the target variable, i.e., the output quantity of the experiment for which the measurement of the uncertainty shall be evaluated. For wave energy, the target variable is often some property of a critical component or sub-system, typically it can be the maximum stress, the life, or the friction force.

3.3.2 Uncertainty Sources Identification

The goal in this step is to identify all major sources of uncertainty that affect the target variable, and especially here it is recommended to have a cross-functional team of engineers. A previously performed Failure Mode, Effects and Criticality Analysis (FMECA) can give valuable input. When identifying uncertainty sources, it can be helpful to think about the different types of uncertainties. Uncertainties can be classified due to their nature. The first kind of uncertainty is due to random variation, while the second kind is due to the lack of knowledge, for example when modelling the product characteristics or estimating model parameters. In the basic VMEA the focus is on the random variation, but also other uncertainties, such as possible model errors, should be included. A detailed discussion on identifying and classifying uncertainties are found in Section 3.2.

This project has received funding from the European Union's Horizon 2020 research and innovation programme under grant agreement No 101006927.

A useful way to illustrate the uncertainties is through a fishbone (or Ishikawa) diagram, which is a graphical tool to explore and visualize the causes of a problem as well as the factors affecting the outcome of a process or the property of a product. An example of the application of fishbone diagrams to analyse cause-effect relationships and optimize manufacturing processes is described in (Johansson et al., 2006). In that case, the "effect" of interest was the inner diameter of a valve used in industrial refrigeration systems. A team of experts discussed the role played by several factors in the manufacturing process of the valve and visualized them as the fishbone diagram shown in Figure 7. Mapping out all the factors involved in the manufacturing process and their associated uncertainty provided a solid ground to estimate the expected uncertainty for the diameter of the valve and to design appropriate optimization strategies. That was an example of how the outcome of cause-effect analysis can facilitate the execution of VMEA.

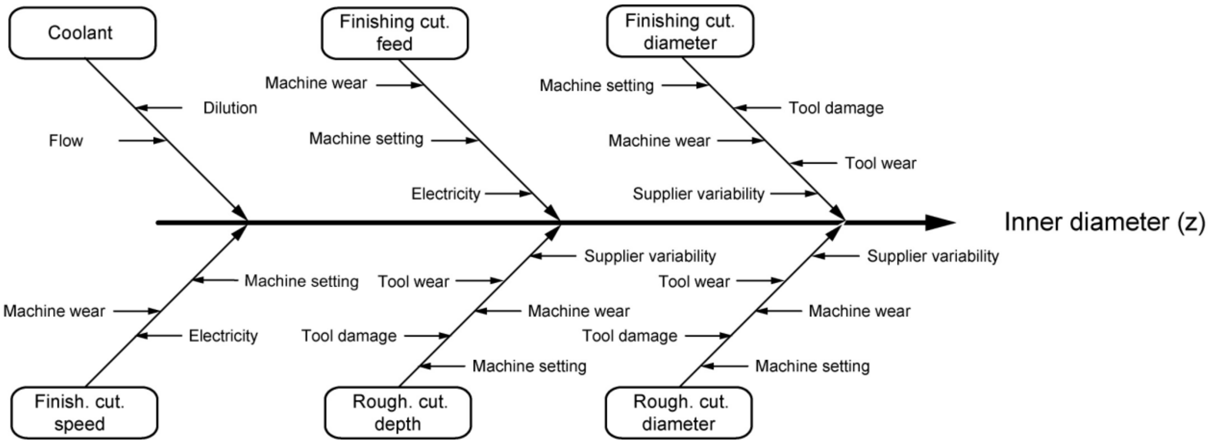

Figure 7: Example of complete fishbone diagram for a manufacturing problem; (Johansson et al., 2006).

3.3.3 Sensitivity Assessment

The sensitivity and uncertainty size assessments are often executed in parallel. The assessments are evaluated on a 1-10 scale, and are based mostly on engineering experience, judgements and informed guesses. The description by (Johansson et al., 2006) is followed.

In the second step of the VMEA procedure, engineers assess the sensitivity of the target variable to the influence of each identified uncertainty source. To assess sensitivities, engineers can use objective measures or subjective assessments based on their experience and theoretical knowledge. Since it is not always possible to obtain objective measures, especially in the early phases of development, subjective assessment is proposed for capturing engineering knowledge. The assessment is based on a scale ranging from 1 to 10, where 1 corresponds to very low sensitivity and 10 corresponds to very high sensitivity. The criteria are given in Table 1.

This project has received funding from the European Union's Horizon 2020 research and innovation programme under grant agreement No 101006927.

Table 1: Sensitivity assessment criteria for Basic VMEA.

Sensitivity	Criteria for assessing sensitivity	Score
Very low	The uncertainty is (almost) not at all transmitted	1—2
Low	The uncertainty is transmitted to a small degree	3—4
Moderate	The uncertainty is transmitted to a moderate degree	5—6
High	The uncertainty is transmitted to a high degree	7—8
Very high	The uncertainty is transmitted to a very high degree	9—10

3.3.4 Uncertainty Size Assessment

In the third step of the VMEA procedure, engineers examine uncertainty sources and assess their sizes in operating conditions. In Table 2 subjective assessment criteria are proposed for capturing engineering knowledge about the magnitude of uncertainty. The assessment is based on a scale ranging from 1 to 10, where 1 corresponds to very low uncertainty and 10 corresponds to very high uncertainty.

Table 2: Uncertainty size assessment criteria for Basic VMEA.

Uncertainty	Criteria for assessing sensitivity	Score
Very low	The uncertainty source is considered to be almost constant in all possible conditions	1—2
Low	The uncertainty source exhibits small fluctuations in all possible conditions	3—4
Moderate	The uncertainty source exhibits moderate fluctuations in all possible conditions	5—6
High	The uncertainty source exhibits high fluctuations in all possible conditions	7—8
Very high	The uncertainty source exhibits very high fluctuations in all possible conditions	9—10

3.3.5 VMEA Table and Total Uncertainty Calculation

The importance of the different sources in the basic VMEA is characterized by the so-called Variation Risk Priority Number (VRPN) which is calculated for each source:

$$VRPN = \sum_{i=1}^{n} VRPN_i = \sum_{i=1}^{n} c_i^2 \cdot u_i^2 \tag{8}$$

where $VRPN_i$ is the variation contribution due to source i, which is the square of the product of the sensitivity, c_i, and the uncertainty, u_i.

The result of the basic VMEA is well suited to be presented in a so-called VMEA table, see Table 3 below for an illustrative example, presenting the identified uncertainty sources together with the assessed sensitivities and uncertainty sizes. The resulting uncertainties and the VRPNs are presented together with the proportion of the variance contributions of the sources. The last row of the VMEA table presents the total uncertainty and VRPN.

This project has received funding from the European Union's Horizon 2020 research and innovation programme under grant agreement No 101006927.

Table 3: Example of a Basic VMEA for a dynamic seal.

Input			Result		
Uncertainty components	Sensitivity c_i (1-10)	Uncertainty input u_i (1-10)	Uncertainty output $\tau_i = c_i \cdot u_i$	Variation contribution VRPN τ_i^2	VRPN proportion
Physical test rig					
Total travelled distance (TTD)	6	2	12.0	144	3%
Lubrication oil flow and quality	6	4	24.0	576	13%
Diameter of seal and rod/piston	7	2	14.0	196	4%
Rod roughness	7	4	28.0	784	17%
Total			**41.2**	**1700**	**38%**
Virtual test rig (numerical simulations)					
Modelling errors	5	5	25.0	625	14%
Discretization errors	3	3	9.0	81	2%
Total			**26.6**	**706**	**16%**
Life & wearout					
Acceleration methods	5	7	35.0	1225	27%
Scaling methods	5	6	30.0	900	20%
Total			**46.1**	**2125**	**47%**
Total uncertainty			**67.3**	**4531**	**100%**

3.3.6 Evaluation and Improvement Actions

The result of the basic VMEA is mostly used to evaluate the robustness of the test rig design and set-up. Typical applications are to compare design concepts and to find dominating uncertainty sources. The feedback to the improvement process can be the dominating uncertainty sources that should be studied in more detail or that could be candidates for improvement actions.

The relative contribution of uncertainties should be studied in terms of VRPN (i.e., in terms of variance), which is shown in column "VRPN proportion" in Table 3. However, it is best illustrated in terms of graphs, e.g., using a pie chart as in Figure 8. Another alternative is to use a Pareto chart, see Figure 9, where the uncertainty sources are sorted according to their resulting VRPN and illustrated as a bar diagram together with a line showing the cumulative VRPN.

This project has received funding from the European Union's Horizon 2020 research and innovation programme under grant agreement No 101006927.

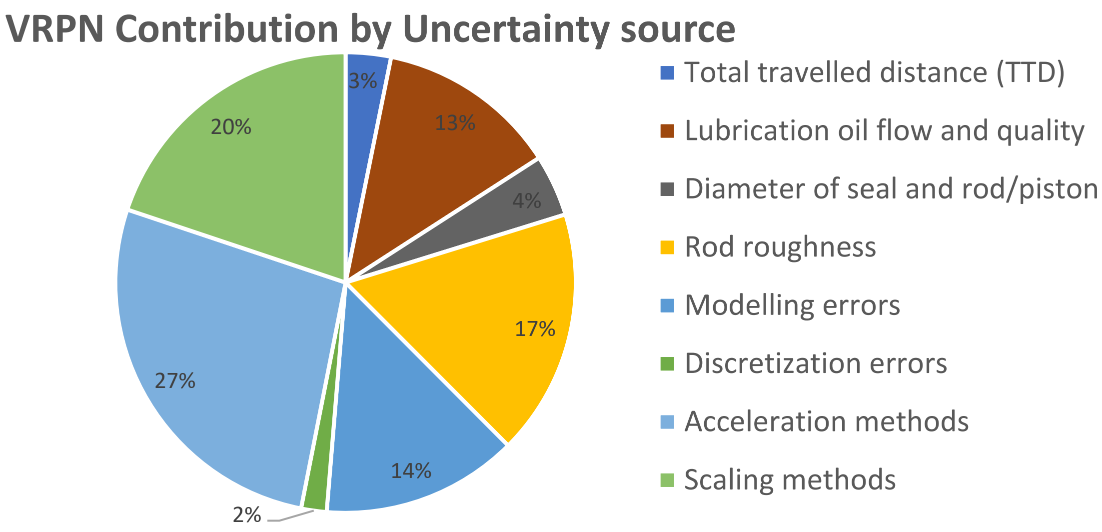

Figure 8: Pie chart of VRPN for dynamic seal example, Table 3.

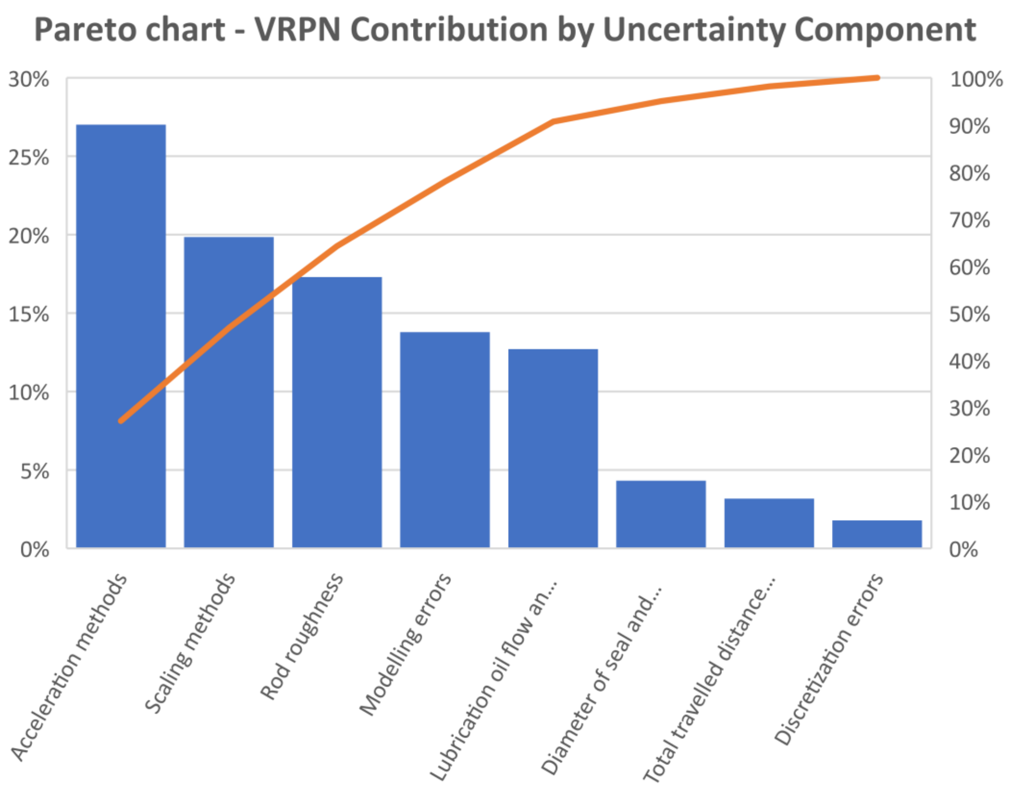

Figure 9: Pareto chart of VRPN for dynamic seal example, Table 3.

3.4 Final Design Stage – Probabilistic VMEA

The main difference between probabilistic and basic VMEA is that the probabilistic one evaluates final quantitative measures on uncertainty. The quantitative measures are the same as for the enhanced VMEA, namely, 1) sensitivities by means of mathematical *sensitivity* *coefficients* and 2) measures of uncertainty or dispersion by means of *statistical standard deviations*.

3.4.1 Target Function Definition

In this stage the target variable, also called measurand in the terminology of measurement uncertainty, needs to be specified in more detail, e.g., in terms of units of inputs and output variables.

Formally the target variable can be formulated as a target function of input variables:

$$y = f(x_1, x_2, \dots, x_n) \tag{9}$$

where y is the response and $f(\cdot)$ is the target function depending on the input parameters $x_1, x_2, \dots, x_n$, which represent the sources of uncertainty.

The output of the target function in the VMEA concept is regarded as a random variable and, in many cases, its logarithmic form makes the procedure more stable. There are mainly two reasons for this, namely 1) The linear approximation used when combining uncertainty sources often becomes more accurate, and 2) the uncertainty measure, the standard deviation, becomes more stable (constant) within the range of interest.

3.4.2 Uncertainty Sources Identification

Methods for finding all possible sources of uncertainties are the same for probabilistic VMEA as for basic VMEA. However, in order to evaluate the probabilistic VMEA each source of uncertainty must be represented by a measurable quantity that can be characterised by a nominal value and a standard deviation.

In the later design stages, it is important to consider all types of uncertainty, not only scatter sources, but also statistical uncertainties and possible model errors. The classification of the different types of uncertainties is recalled:

- ***Scatter*** or physical uncertainty which is that identified with the inherent random nature of the phenomenon, e.g., the variation in strength between different components.
- ***Statistical uncertainty*** which is that associated with the uncertainty due to statistical estimation of physical model parameters based on available data, e.g., estimation of parameters in a life model based on test data.
- ***Model uncertainty*** which is that associated with the use of one (or more) simplified relationship to represent the 'real' relationship or phenomenon of interest, e.g., a finite element model for the relation between outer loads and local stresses.

Scatter cannot be avoided, while the last two types of uncertainties can be decreased by gaining more data or by building better models. Further, in testing, random sources may be diminished by multiple measurements. Therefore, it is important to distinguish between random and systematic effects.

3.4.3 Sensitivity Assessment

The VMEA procedure, as well as GUM, is a simplification in mainly two respects. The first one is that the statistical evaluation is based only on second order moments, which means that only variances (or standard deviations) are used to specify the statistical property of an uncertainty component. The other important simplification is that the total variance is based on a linearization of the transfer function from influential variables to the target variable. These linear approximations make it sufficient to use a sensitivity coefficient for each variable.

This project has received funding from the European Union's Horizon 2020 research and innovation programme under grant agreement No 101006927.

Formally, the sensitivity coefficient with respect to the i:th uncertainty source, is the partial derivative:

$$c_i = \frac{\partial f}{\partial x_i}(\tilde{x}_1, \tilde{x}_2, \ldots, \tilde{x}_n) \tag{10}$$

where $\tilde{x}_i$ is the nominal value of the actual variable, and $f(\cdot)$ is the target function.

However, in practice it is often easier and more robust to evaluate the sensitivity coefficient using difference quotients, see (Svensson and de Maré, 2008). Then the sensitivity coefficient can be evaluated using a difference quotient, namely:

$$c_i = \frac{f(\tilde{x}_1, \ldots, \tilde{x}_i + u_i, \ldots, \tilde{x}_n) - f(\tilde{x}_1, \ldots, \tilde{x}_i - u_i, \ldots, \tilde{x}_n)}{2u_i} \tag{11}$$

where and u_i is the standard deviation of this variable. Note that the steps should be chosen in the order of typical variations of the input variable; here it is chosen to one standard deviation. More details on evaluating sensitivity coefficients are found in Sections 4 and 5.

3.4.4 Uncertainty Size Assessment

Each source of uncertainty needs to be characterised by means of its possible uncertainty. In probabilistic VMEA the standard deviation is used. The standard deviation is a statistical measure and defined as the square root of the *variance*. The variance in turn is formally defined as the mean of all squared distances from the mean value of the population.

In many situations a logarithmic transformation is useful, e.g., when studying positive quantities. The reason for using the standard deviation of the logarithmic property is twofold, 1) engineering relations are often very well described as straight lines in log-log diagrams and the variation around such a line has similar spread around it for the magnitudes of interest, 2) the standard deviation of the logarithmic property is approximately the same as the coefficient of variation of the property itself, namely:

$$\mathrm{std}(\ln X) \approx \frac{\mathrm{std}(X)}{\mathrm{E}[X]} \tag{12}$$

where std is the standard deviation and $\mathrm{E}[X]$ is the mean value (or population mean). This means that it is easy to use engineering judgements for estimates by means of *percentage uncertainty,* if a property has an uncertainty of 10%, the standard deviation of its natural logarithm is approximately 0.10.

Based on these statistical definitions, methods for estimating the uncertainties for input variables to the VMEA analysis can be outlined.

3.4.4.1 Type A: Evaluate Uncertainty from Statistical Observations

A standard uncertainty evaluated from a statistical sample is in GUM denoted type A uncertainty, see Section 4.4.1. Consider a sample from a population that is representative for the input variable. Then this sample may be used to estimate both its expected value, $\bar{x}$, and its standard deviation, s:

$$\bar{x} = \sum_{i=1}^{n} x_i, \quad s^2 = \sum_{i=1}^{n} (x_i - \bar{x})^2 \tag{13}$$

The average and standard deviation are uncertain themselves, and standard statistical theory is used to account for this. Namely, the standard deviation is multiplied with a constant which depends on the number of samples behind its estimation. This constant is based on the statistical *t*-distribution[1] and is found in Table 4. Thus, the uncertainty is estimated as:

$$u = t(n) \cdot s \tag{14}$$

Further, the uncertainty of the average value depends both on the standard deviation and the number of samples and equals the standard deviation divided by the square root of the number of samples.

Table 4: Values for the t-correction factor.

n	2	3	4	5	6	7-10	11-26	27-
$t(n)$	6.5	2.2	1.6	1.4	1.3	1.2	1.1	1.0

3.4.4.2 Type B: Evaluate Uncertainty from Interval Judgements

When no statistical sample is available, the standard deviation must be assessed in other ways, which is referred to type B uncertainty in GUM, see Section 4.4.2. A useful method in engineering is to estimate an interval that is assumed to contain most variation for a property. A typical situation for this application is for geometric tolerances. Such an interval may be transformed to a standard deviation by assuming that the statistical distribution of variation within the interval is uniform, i.e., the probability is the same for all points within the interval. This is often a somewhat conservative assumption, but without detailed knowledge about the distribution it is the most practical solution.

It can be convenient to assess a type B uncertainty from an independent input variable though direct estimation of its contribution to the uncertainty of the target variable. When it is difficult to quantify the input entity and/or the sensitivity coefficient, one can make an effort to estimate the variation in the target variable that is caused by the input uncertainty directly. Consider for instance the difficulty in quantifying the amount of pollution in the water and its influence on wear of a seal. Experience or judgment can be used to describe the variation in the wear directly and, consequently, set the sensitivity to one.

If a property is assumed to vary within the interval $x \pm d$, then, assuming a uniform distribution, the standard deviation is:

$$u = \frac{d}{\sqrt{3}} \tag{15}$$

Model errors are often hard but necessary to take into account. The solution is to use engineering experience and physical understanding to make judgements about the possible error that a certain approximation may introduce. The uniform distribution is an important tool to include possible model errors. Material specifications are usually found from laboratory experiments which differ from the conditions in service. Finite element procedures most often contain approximations by means of boundary conditions and resolution.

In most cases, judgements are best expressed as *possible percentage error*. If such an error is judged by means of the target variable, then it can be interpreted as a possible error interval, and by using the uniform distribution assumption it can be transformed to a standard deviation for the logarithmic properties, ±p% error is transformed to the standard deviation according to Eq. (15).

---

[1] The number is the 2.5% quantile in the statistical *t*-distribution with *n*-1 degrees of freedom divided by the 2.5% quantile in the normal distribution, which corresponds to the *t*-distribution with infinite degrees of freedom.

This project has received funding from the European Union's Horizon 2020 research and innovation programme under grant agreement No 101006927.

More details on evaluating uncertainty size are found in Sections 44 and 55.

3.4.5 Total Uncertainty Calculation

The total uncertainty, u_y, in the target variable, y, is calculated by combining all the contributions from all uncertainty sources:

$$u_y = \sqrt{\sum_{i=1}^{n} u_{y,i}^2} = \sqrt{\sum_{i=1}^{n} c_i^2 \cdot u_i^2} \tag{16}$$

where $u_{y,i}$ is the resulting uncertainty from source i, and is calculated as the product of the absolute sensitivity coefficient $|c_i|$, and the uncertainty u_i of source i. The total number of uncertainty sources is n.

The inputs and results of the uncertainty assessment can be presented in a VMEA table, also called uncertainty budget, where all uncertainty sources are listed together with assessment of sensitivity and uncertainty size, see Table 5 for an illustrative example of the life of a dynamic seal. The table also presents the total combined measurement uncertainty, and the variation proportion of the uncertainty sources.

Table 5: Example of a Probabilistic VMEA for a dynamic seal.

Input			**Result**		
	Sensitivity	Uncertainty input	Uncertainty output	Variation contribution	
				VRPN	VRPN
Uncertainty components	c_i	u_i	$\tau_i = c_i \cdot u_i$	τ_i^2	proportion
Physical test rig					
Total travelled distance (TTD)	1	5%	5%	0.0025	2%
Lubrication oil flow and quality	1	8%	8%	0.0064	5%
Diameter of seal and rod/piston	2	4%	8%	0.0064	5%
Rod roughness	1	6%	6%	0.0036	3%
Total			**14%**	**0.0189**	**15%**
Virtual test rig (numerical simulations)					
Modelling errors	1	15%	15%	0.0225	18%
Discretization errors	1	4%	4%	0.0016	1%
Total			**16%**	**0.0241**	**19%**
Life & wearout					
Acceleration methods	1	25%	25%	0.0625	49%
Scaling methods	1	15%	15%	0.0225	18%
Total			**29%**	**0.085**	**66%**
Total uncertainty			**36%**	**0.128**	**100%**

3.4.6 Reliability and Robustness Evaluation

Measurement uncertainty is often given as an interval $y \pm 2 \cdot u_y$, representing a confidence level of 95%. The term $2u_y$ is called the expanded uncertainty and is generally given by $U = k \cdot u_y$, where k is called the coverage factor for the chosen level of confidence.

The illustrative example in Table 5 studies the life of a seal, and the target variable is there defined as the logarithmic life, $Y = \ln N$. Thus, the assessment is in percentage uncertainty, and the measurement uncertainty is estimated to $u_y = 36\%$. The expanded uncertainty, corresponding to a 95% confidence level, is calculated to $U = 2 \cdot u_y = 72\%$. The uncertainty interval for the logarithmic life, $\ln N$, is thus:

$$\ln N = \ln \widehat{N} \pm 0.72 \tag{17}$$

where $\widehat{N}$ is the experimental life. Then, the interval in life is calculated as:

$$N = \exp\left(\ln \widehat{N} \pm 0.72\right) = \left[0.49 \cdot \widehat{N}\,; 2.05 \cdot \widehat{N}\right] \tag{18}$$

Note that in this case the uncertainty interval represents about a factor two in life.

The reliability target is often that the target function should exceed some limit with a proper safety margin. For more details, see Section 6.3.

3.4.7 Improvement Actions

An important part in the design process is the improvement stage, where the VMEA can be of help for identifying areas of improvement and evaluating their potential effects. The first task is to identify uncertainty sources that may be candidates for improvement actions.

Improvement measures should concern all three categories:

- **Physical test set-up:** A part of the test rig design phase is to set the tolerances. The VMEA can help to identify tolerances that have a large impact on the total uncertainty, and thus are candidated for improvements by tightening the tolerance. On the other hand, there may be tolerances that are set too tight and could be relaxed without giving an impact on the total uncertainty.
- **Numerical simulation:** The numerical part of the hybrid test set-up involves several types of uncertainties, including model simplifications, and numerical errors.
- **Life and acceleration models:** If the uncertainty in the life model is large, it can be motivated to perform tests on the specific component to improve the understanding of modelling. Especially, it is important to understand the acceleration and scaling models.

This project has received funding from the European Union's Horizon 2020 research and innovation programme under grant agreement No 101006927.

4 Uncertainty Quantification in Physical Testing

4.1 Hybrid Testing for Reliability Verification

Uncertainties affect all stages of a reliability verification process. There are uncertainties in the reliability requirement specification, in how well it represents the true environmental load in service during the required life span. Even if the service life could be described perfectly in terms of environmental loading, the reliability test requirement must have reduced complexity and accelerated loading exposure. This test requirement is also strongly connected to the test rig or simulation model and how accurate it applies the load. For instance, it can be difficult to achieve a good match in boundary conditions, when testing is performed on a sub-system. Finally, physical testing uses measurement technology that adds to the total uncertainty.

This section is primarily about guidance in MSA and the measurement uncertainty principles detailed in "ISO/IEC GUIDE 98-3:2008 *Uncertainty of measurement -- Part 3: Guide to the expression of uncertainty in measurement (GUM:1995)",* (ISO/TMBG, 2008). However, all uncertainties can be delt with in a similar way, i.e., by analysing each part, quantifying uncertainty, and then combining the uncertainties of parts.

4.2 Overview of Measurement Uncertainty

As introduced in Section 2.1, a measurement result y is not complete unless it is accompanied by an 'expanded uncertainty' with the purpose of quantifying an interval, centred around the measured value, that is likely to contain the true value of the measurand. One can then state, with a chosen degree of confidence, that the true value lies within the interval $[y - U, y + U]$.

The expanded uncertainty is based on the 'standard uncertainty' u which corresponds to the standard deviation of a random variable. The choice of 'coverage factor' *k* determines the width of the interval, as $U = ku$. Often a 95% level of confidence is used, which corresponds to a coverage factor of $k = 2$, so that $U = 2u$.

Experimental and mathematical analysis of a measurement chain or process to determine how much the variation within the measurement process contributes to overall process variability is called MSA. The overall process variability is causing the measurement process to show different measurement results each time the measurement is reproduced. The source of variation can be the measuring equipment, the operator, the environment, etc. and each variation will transfer through the measurement process and contribute to the overall measurement variability. Reduction of measurement variation is achieved through control of variation within the process, e.g., through calibration of equipment, using the same operator, keeping environmental factors constant, etc. The purpose of MSA is to qualify a measurement system by quantifying its variation, which is distorting accuracy (systematic error), precision (random variation) and stability (variation over time). The difference between accuracy and precision is illustrated in Figure 10.

This project has received funding from the European Union's Horizon 2020
research and innovation programme under grant agreement No 101006927.

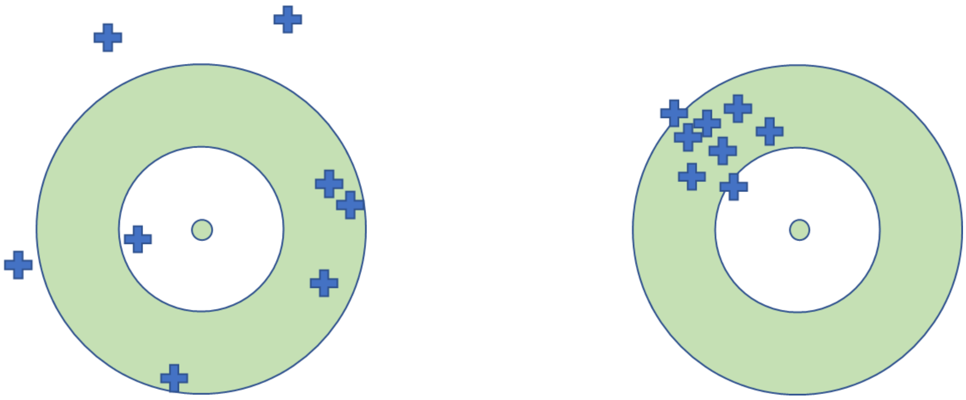

Figure 10: Two measurement outcomes with different type of variation from the true position in the centre. The left picture illustrates good accuracy but poor precision. Vice versa to the right.

GUM provides general rules for evaluating and expressing uncertainty in measurement. It presents eight steps to be followed, that are quoted and commented here:

1. *"Express mathematically the relationship between the measurand Y and the input quantities X_i on which Y depends: $Y = f(X_1, X_2, \dots, X_n)$. The function f should contain every quantity, including all corrections and correction factors, that can contribute a significant component of uncertainty to the result of the measurement."*

   This first step is the most important step, because the measurement uncertainty quantification will be wrong if only a single source of uncertainty is forgotten. It is also a difficult step. Thorough experience about the measurement process is needed.

   An alternative way to express the relationship is $Y = y + f(e_1, e_2, \dots, e_n)$. In this case the mean values are subtracted from each input quantity and represented by the mean of the measurand, $y = f(x_1, x_2 \dots, x_n)$. The resulting measurement variation is then expressed as a function of zero-mean input errors e_i.

2. "*Determine x_i, the estimated value of input quantity X_i, either on the basis of the statistical analysis of series of observations or by other means.*"

   The input quantities are grouped into two categories, depending on how the variation is quantified:

   Type A – input quantities that can be evaluated by statistical analysis of experiments.

   Type B – input quantities which variations are estimated by judgement or experience.

3. "*Evaluate the standard uncertainty $u(x_i)$ of each input estimate x_i.*"

   This is explained further in Section 4.4.

4. "*Evaluate the covariances associated with any input estimates that are correlated.*"

   Often input quantities can be treated as independent random variables, which simplifies the analysis of uncertainty. However, if some of the X_i are significantly correlated, the correlations must be considered. Covariance terms (or terms with correlation coefficients) are added to the equation of combined standard uncertainty $u_c(y)$ in step 6 (see Section 4.4).

5. "*Calculate the result of the measurement, that is, the estimate y of the measurand Y, from the functional relationship f using for the input quantities X_i the estimates x_i obtained in step 2.*"

6. "*Determine the combined standard uncertainty $u_c(y)$ of the measurement result y from the standard uncertainties and covariances associated with the input estimates.*"

   This is explained further in Section 4.4.

7. "*If it is necessary to give an expanded uncertainty U, whose purpose is to provide an interval $y - U$ to $y + U$ that may be expected to encompass a large fraction of the distribution of values that could reasonably be attributed to the measurand Y, multiply the combined standard uncertainty $u_c(y)$ by a coverage factor k, typically in the range 2 to 3, to obtain $U = ku_c(y)$. Select k on the basis of the level of confidence required of the interval.*"

8. "*Report the result of the measurement y together with its combined standard uncertainty $u_c(y)$ or expanded uncertainty U.*"

4.3 Different Types of Measurement Uncertainty

The result of a measurement usually depends on multiple sources. Every time a measurement is conducted, the result might deviate from previous measurements due to variability in different sources. The uncertainty of the sources will contribute to the overall uncertainty of the measurement. The sources of uncertainties can be subdivided into following categories:

- ***Item being measured**:* The item that is being measured can itself contribute to the uncertainty. The item could, for example, be unstable in nature. Imagine measuring the dimensions of an ice cube in a warm room or measuring the windspeed. The item could also be contaminated, which may affect the result of the measurement, for example, dirt particles that are adding extra weight to the item. The variation between different item samples may also contribute to uncertainty.
- ***Measuring instrument**:* The instrument that is used for measuring often holds multiple sources of uncertainties, e.g., error in calibration, bias, drift, electrical noise, aging, rounding errors, poor readability, just to name a few. It is also common that the measuring instrument affects the item being measured. For example, when measuring the temperature of an item, the thermometer may itself affect the measured temperature since the thermometer tends towards thermal equilibrium with the item. Another example is when measuring acceleration using an accelerometer, where the extra mass of the accelerometer is changing the dynamic behaviour of the item.

- ***Operator**:* The skill and judgement of the person(s) performing the measurement can affect the outcome of the result. How the operator is treating the measuring instrument and test item, and how well the operator is executing the measurement process, are also important aspects.
- ***Environment**:* The environment, such as temperature, air pressure, and humidity, can affect the measuring instrument as well as the item being measured. The environment may even have an impact on the operator.
- ***Measurement process**:* How and when the measurement is carried out is also an important aspect of uncertainty. The rigging and positioning of the item being measured and the measuring instrument, may also affect the outcome of the result. If the measurement process is complex to execute, the risk of human errors will most likely increase.

An overview of the subdivision of sources that contribute to measurement uncertainty is presented in Figure 11.

Note that this section presents measurement uncertainty categories in a general setting. It is different from the set of uncertainty categories that was adopted to the hybrid testing for wave energy applications, as suggested in Section 3.2.1.

The uncertainty of a measurement contains the combined uncertainty of multiple sources. The relation between measured quantity Y and sources X_i is given by a function $Y = f(X_1, \ldots, X_N)$, where arbitrary values of the sources X_i is mapped to the measurement Y. An illustration of this is presented in Figure 12 and Figure 13. The "true value" of a measurement is acquired if all sources is equal to their nominal values. Any deviation from the nominal value contribute to a measurement error. However, in some situations the measurement errors of different sources might cancel each other out.

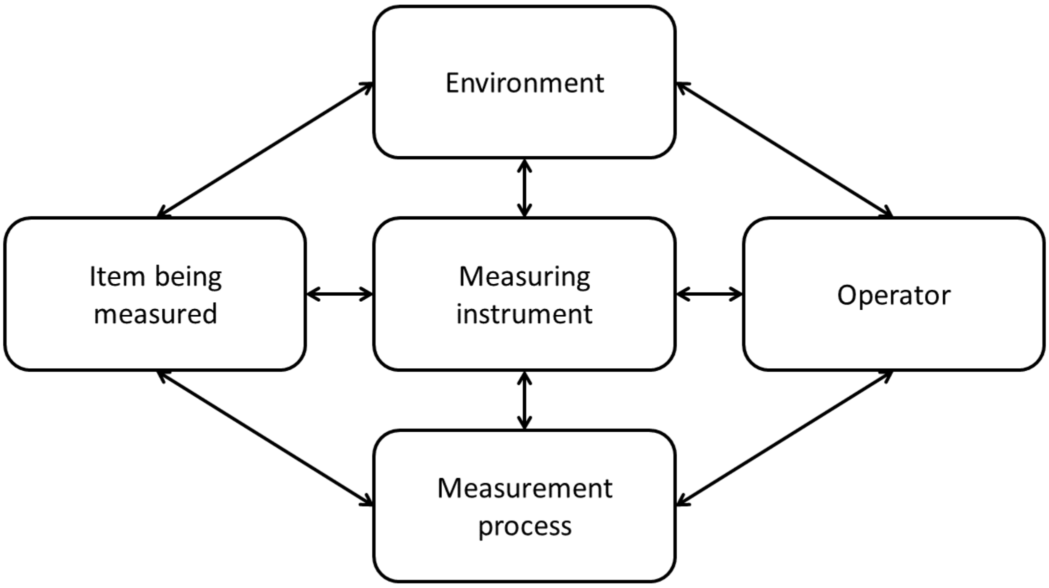

Figure 11: Different types of measurement uncertainties. The arrows denote the mutual influence between them.

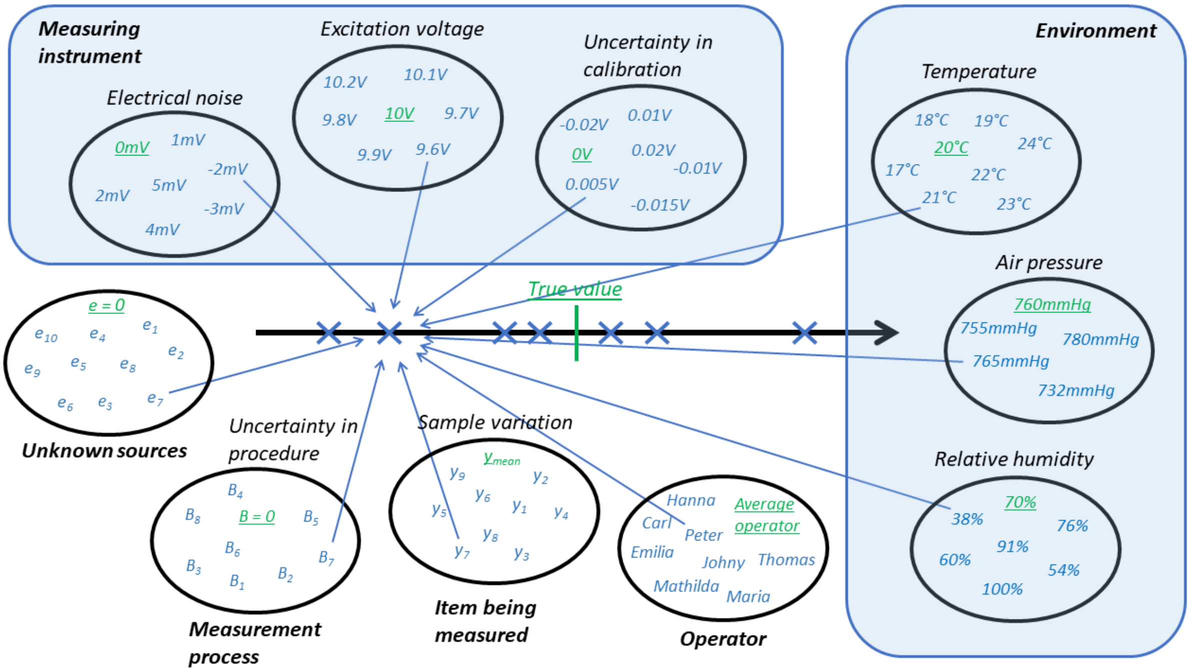

Figure 12: Different sources of uncertainties that decide the outcome of a measurement. The green value of each source denotes the nominal value.

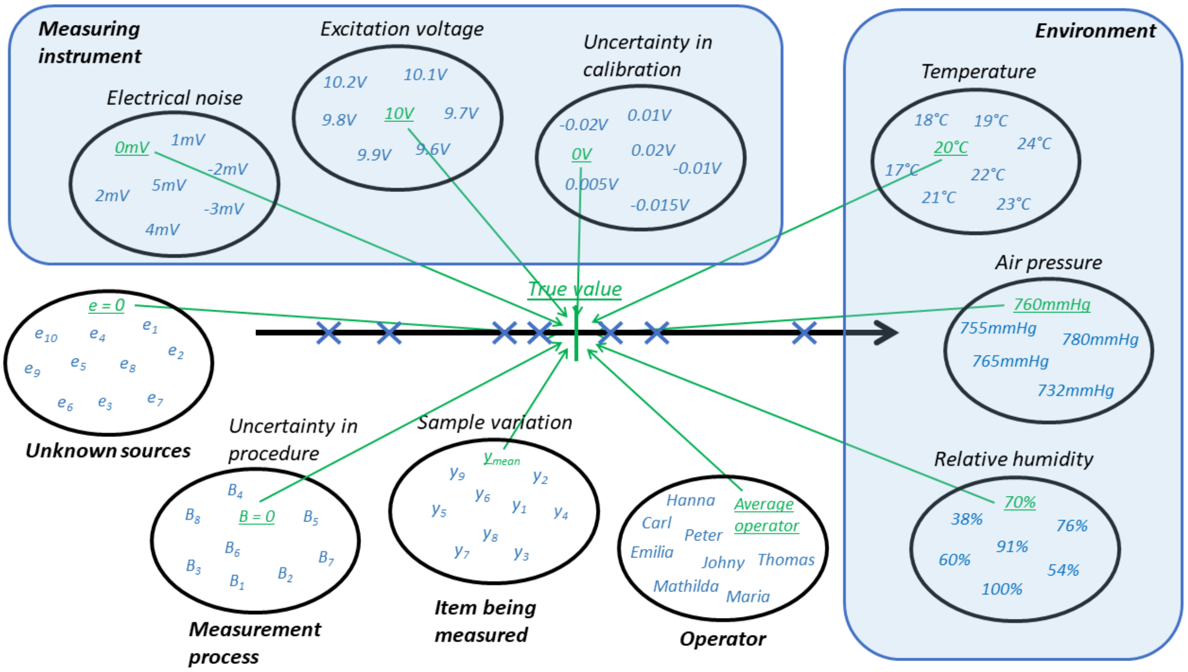

Figure 13: The nominal value of all sources is mapping to the true value of the measurement. The green value of each source denotes the nominal value.

4.4 Methods for Assessing Uncertainty

4.4.1 Evaluation of Standard Uncertainty Type A

Input quantity uncertainties of Type A are preferred as they can be evaluated using experiments and statistical analysis. The variation of each input quantity is studied from a population that represents the variation that is to be quantified. Every type of uncertainty, as presented in the previous sub-section, is not always included in the analysis.

The standard uncertainty, for uncertainty i, is estimated using the well-known equation for calculation of sample standard deviation, from a random trial:

$$u_i = \sqrt{\frac{1}{n-1}\sum_{j=1}^{n}\left(x_{i,j} - \bar{x}_i\right)^2} \tag{19}$$

where n is the sample size and $\bar{x}_i$ is the arithmetic mean estimate:

$$\bar{x}_i = \frac{1}{n}\sum_{j=1}^{n} x_{i,j} \tag{20}$$

from the n observations $x_{i,j}$ of the i:th input quantity. The number of degrees of freedom associated with the uncertainty estimate is $\nu_i = n - 1$.

Analysis of a random variation of an input quantity will benefit from a large sample size, as the uncertainty will reduce gradually with increasing n.

When the measurement system has poor accuracy, there is a systematic error (or bias) that will not reduce through averaging. Calibration experiments can be performed to quantify systematic errors, e.g., for a measurement instrument. Often an adjustment of the measurement output is done to reduce the error (and the uncertainty).

4.4.2 Evaluation of Standard Uncertainty Type B

It is not always possible or practical to perform the experiments needed to evaluate type A uncertainties. Even when it is possible, it may not be worth the effort compared to making conservative guesses when you can afford higher uncertainty (over-estimation).

In some cases, the uncertainty evaluation through judgement can be easier to motivate:

- when the uncertainty is known from experience
- when the uncertainty is given in equipment specification, calibration document, etc.
- when the effect from an error can be derived exactly, e.g., round-off error.

Uncertainties given in documents are often easy to recalculate to a standard uncertainty, if not given directly.

When an interval is given together with a probability of the input quantity X_i lying inside it, the standard uncertainty can often be derived through the standard deviation of a normal distribution with the corresponding confidence interval.

Type B uncertainties can also be expressed as estimated bounds outside which an input quantity is very unlikely to appear. In some cases with a bound $[a, b]$ one will consider any value inside the limits as equally probable. An assumption about uniform distribution is made with its standard deviation adopted as the standard uncertainty:

$$u_i = \sqrt{\frac{(b-a)^2}{12}} \tag{21}$$

In other cases with a bound $[a, b]$ one could consider outcomes close to the bounds less likely than outcomes close to the mid-value $(b + a)/2$. An assumption about a triangular distribution can then be made, symmetric or not. The standard uncertainty for the symmetric triangular distribution is:

$$u_i = \sqrt{\frac{(b-a)^2}{24}} \tag{22}$$

4.4.3 Evaluation of Sensitivity Coefficients

The measurand is a function of input quantities $Y = f(X_1, X_2, \ldots, X_N)$ and the uncertainty of each input quantity is now determined, as described above. Different input quantities can have similar level of standard uncertainty but still contribute to different amount of uncertainty in the measurement result y. How much uncertainty that is transferred through to the measurand, from each input quantity, is controlled by the function $f(X_1, X_2, \ldots, X_N)$. The combined standard uncertainty of the measurement result can be expressed with sensitivity coefficients c_i as:

$$u_y^2 = \sum_{i=1}^{n} c_i^2 u_i^2 \tag{23}$$

at least when there is no correlation between the input quantities. Each sensitivity coefficient is equal to the partial derivative:

$$c_i = \frac{\partial f}{\partial x_i} \tag{24}$$

The function $y = f(x_1, x_2, \ldots, x_N)$ is sometimes known and then the coefficients can be derived directly by derivation.

In many cases the function is not known, and sensitivity coefficients can then be determined from experiments, varying one input quantity by a small amount while keeping other inputs fixed. The ratio between the resulting difference in measurement output and the difference in input quantity is the sensitivity coefficient, for that input quantity. The experiment is then repeated with controlled variation of other input quantities, one by one. This difference propagation is evaluated keeping all but one input quantities constant, at the time, at a nominal value that should be close to each mean value.

If the variation applied for input quantity x_i is exactly one standard uncertainty up and down, from the nominal value $\tilde{x}_i$, $\tilde{x}_i + u_i$ and $\tilde{x}_i - u_i$, then the expression for calculating the i:th sensitivity coefficient is:

$$c_i = \frac{f(\tilde{x}_1, \ldots, \tilde{x}_i + u_i, \ldots, \tilde{x}_n) - f(\tilde{x}_1, \ldots, \tilde{x}_i - u_i, \ldots, \tilde{x}_n)}{2u_i} \tag{25}$$

When correlation between two or more input quantities does exist, the expression for the combined standard uncertainty of the measurement result becomes more complex:

This project has received funding from the European Union's Horizon 2020 research and innovation programme under grant agreement No 101006927.

$$u_y^2 = \sum_{i=1}^{n} c_i^2 u_i^2 + 2 \sum_{i=2}^{n} \sum_{j=1}^{i-1} c_i\, c_j u_i u_j r(x_i, x_j) \tag{26}$$

where the correlation coefficient $r(x_i, x_j)$ is the quotient between the square root of the sample covariance estimate, between x_i and x_j, and the product of individual standard deviation estimates:

$$r(x_i, x_j) = \frac{s(\,x_i,\ x_j)}{s(\,x_i)s(\,x_j)} \tag{27}$$

5 Uncertainty Quantification in Numerical Simulations

Section 5 aims to address UQ in numerical modelling. Similar to the discussion presented in Section 4 for physical testing, UQ in numerical simulation aims to introduce a stochastic approach to the design process, whereby the inherent variability in the estimates is considered, and where the likelihood of failure can be estimated by assessing the load and resistance profiles in a probabilistic sense. In Wave Energy Converter (WEC) design, such probabilistic approach may prove vital in avoiding under- and / or over-design of a range of critical sub-systems and components, which is more likely to occur should a deterministic design approach be followed, i.e., if an arbitrary factor is assumed to address both the variability and safety margin between the characteristic load and resistance.

The mainstream application of numerical models in WEC design, in particular at the technology readiness levels targeted by the VALID project, emphasises the importance that practical guidance related to the adoption of UQ best practices may bring to the conceptualisation of reliable WEC designs. It is beyond the scope of this section to provide an exhaustive review of all the applications of UQ in numerical simulations – thus a focus on aspects deemed relevant to WEC design is kept throughout the section. The interested reader is directed to e.g. (Ghanem et al., 2017; Soize, 2017) for overarching references that address UQ in a wider engineering context. The further interested reader is additionally invited to assess the implications of V&V procedures in numerical simulations, which are not addressed in detail in this section; however, the authors acknowledge that V&V procedures can have a critical role in mitigating uncertainties in numerical simulations, by ensuring that the dominant equations are solved in a correct manner (verification) and that the correct equations are solved (validation). Specific links between UQ and V&V are addressed in e.g. relevant publications by NAFEMS – see e.g. (Smith, 2021); a connection with simulation quality management guidelines can also be made, especially with regard to specific topics such as code verification – see e.g. (ASME, 2023).

The main objective of this section is to familiarise the reader with the principles of UQ in numerical simulation, in a format directly applicable to WEC design considerations. To address this objective, this section is divided in four sub-sections. The overall methodology and multiple stages associated with UQ in numerical modelling are introduced in Section 5.1. At a high-level, these include input, results and (output) analysis stages. Each of such stages is then sequentially addressed in Section 5.2 to 5.4, respectively.

5.1 Stages of UQ in Numerical Simulations

The definition and analysis of uncertainty in numerical simulations parallel the presentation of these topics for physical measurements in many respects. The true value of physical quantities is not accessible neither to measurements nor to simulations. What is practically feasible is to estimate a range where the true value is expected to fall with a certain likelihood, and that is what UQ is all about. The factors that cause the outcomes of numerical simulations to differ from reality are partly the same that also affect physical measurements. However, there are also elements that are specific to the uncertainty in numerical simulations.

For example, numerical simulations performed to support engineering design are largely deterministic; that is, they provide exactly the same output for given inputs. This is in contrast with physical experimentation, where the repetition of a measurement under nominally identical conditions might lead to different results. Randomness and variability in inputs have to be deliberately added to the computational models, and thus it becomes a part of the modelling process itself.

Statistical analysis of repeated measurements is a straightforward way to quantity the overall uncertainty of the measured variables. Such a direct approach to UQ on the output of

This project has received funding from the European Union's Horizon 2020 research and innovation programme under grant agreement No 101006927.

computational models is not possible. The closest example of purely statistical approach to UQ for numerical simulations is the Monte Carlo method (and its many variants) which, in essence, consists in the estimation of model output statistics based on a sample computed from an ensemble of randomly drawn input samples. The results of this statistical approach depend on the characterization of the variability of inputs, which requires modelling choices (typically, in terms of probability distributions) that contribute to overall uncertainty in a way that might be hard to quantify.

Uncertainty in numerical simulations can be characterized in several forms, which might be tailored to highlight specific aspects. Here, the categorization proposed in (Oberkampf and Roy, 2010) is followed, that breaks down the total uncertainty in model predictions into three contributions:

1. Model uncertainty.
2. Input uncertainty.
3. Numerical error.

Model uncertainty (sometimes denoted as "model form uncertainty") stems from the formulation of the model and the assumptions embedded in it. For example, the choice of a certain set of equations might leave out some physical phenomena that potentially affect the behaviour of the actual system. This source of uncertainty introduces a bias in simulation results that, in most applications, is hard to quantify. Validation data from the comparison of model results with experiments or alternative model formulations might provide indications on how to quantify this uncertainty.

Variability and imprecise knowledge in inputs (sometimes denoted as "parametric uncertainty") is by far the source of uncertainty that is most commonly considered in the literature. More details on the quantification of this source are presented in Section 5.2.

Numerical errors arise from the algorithmic implementation and numerical solution procedures. Discretization errors due to the use of a finite time step and spatial resolution fall within this category. A discussion of this source of uncertainty in the context of models used for WEC design is presented in Section 5.4.1.

At a high-level, the characteristic stages of UQ in numerical simulations match those of UQ in physical testing – noting that suitable adaptation likely apply per stage, e.g., a material (numerical) model may be replaced in physical testing by a material specimen. A schematic of such stages is illustrated in Figure 14, with these being organised in three key steps:

1. Inputs: characterisation of input uncertainty, i.e., environmental conditions, loads model (and related assumptions) and material / resistance model (and related assumptions).
2. Results: propagation of the input uncertainty through the computational model(s), leading to the numerical results.
3. Analysis: assessment(s) of the uncertainty associated with the model outputs.

The overall uncertainty of numerical simulations δ_{sim} resulting from step 3 above may be expressed as the sum of three components to better understand the relative contribution of different categories of elements that build up the simulations (Oberkampf and Roy, 2010):

$$\delta_{sim} = \delta_{input} + \delta_{num} + \delta_{model} \tag{28}$$

where δ_{input} represents the contributions from input signals, parameters, and boundary conditions, δ_{num} is the sum of all the numerical errors associated to the approximate solution of model equations, and δ_{model} is the uncertainty generated by assumptions and simplifications in model form.

This project has received funding from the European Union's Horizon 2020
research and innovation programme under grant agreement No 101006927.

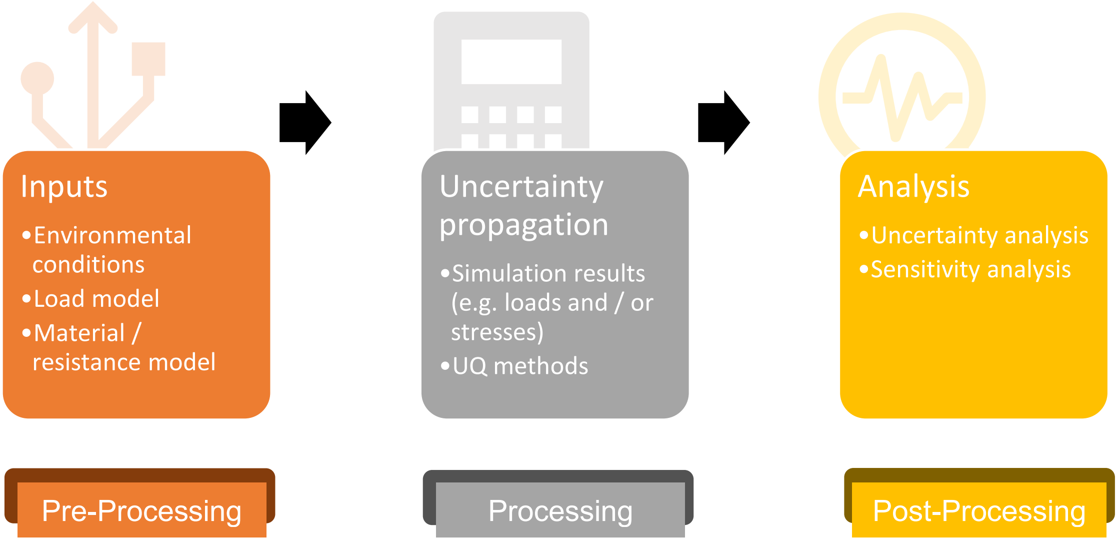

Figure 14: Main stages of UQ process in numerical simulations.

In the context of the VALID project, a direct analogy between each stage of UQ in numerical simulations and the methodology for hybrid life testing developed in VALID can be established. As also illustrated in Figure 14, the *Inputs*, *Results* and *Analysis* stages can be directly associated with the *Pre-Processing*, *Processing* and *Post-Processing* pillars of the VALID methodology, as originally identified in VALID D1.2, (Ruiz-Minguela et al., 2021). Each of the UQ stages is addressed sequentially in Sections 5.2 to 5.4, where details about stage-specific options and steps associated with UQ are documented.

An aspect of particular relevance in the context of hybrid life testing is the complexity and computational effort associated with the numerical model(s). An exhaustive review of generic guidelines associated with UQ in complex, computationally expensive models is outside the scope of this report – the interested reader is directed to e.g.: the deliverables of the European Metrology Research Programme (EMRP) *Novel mathematical & statistical approaches to uncertainty evaluation* project – see e.g. (Allard et al., 2015)-: the provisions listed in the *National Research Council* (NRC) *Assessing the Reliability of Complex Models: Mathematical and Statistical Foundations of Verification, Validation, and Uncertainty Quantification* book (Council, 2012).

Some cross-cutting considerations that are, in the opinion of the authors of this report, relevant, include:

- Uncertainty related to the model inputs (see Section 5.2) will affect the uncertainty associated with the model outputs (Section 5.4). By propagating the model input uncertainties through the model, an UQ exercise can be completed. Several methods may be followed to implement uncertainty propagating procedures (see Section 5.3).
- It is important to distinguish *error* from *uncertainty*. While in the former there is certainty regarding a flaw in the modelling process, in the latter such certainty does not apply.
- Complex, computationally expensive models may not allow a Monte Carlo sampling approach for UQ (see also Section 5.3). In such scenarios, an understanding of a feasible upper limit to the number of evaluations is beneficial (if not required) when initiating the UQ process.
- In wave energy applications, and as reviewed in VALID D1.2, (Ruiz-Minguela et al., 2021), fluid-structure interaction solvers are likely to be used to estimate the solution(s) of the

This project has received funding from the European Union's Horizon 2020 research and innovation programme under grant agreement No 101006927.

wave-structure interaction problem(s). While noting that a range of formulations may be used in such solvers, specific references have addressed the main sources of uncertainty affecting Computational Fluid Dynamics (CFD) solvers - see e.g. the Institute for Computer Applications in Science and Engineering report on uncertainty analysis for fluid mechanics with applications (Walters and Huyse, 2002). A summary of main sources of uncertainty and error in CFD is presented in Table 6, following (Oberkampf et al., 2001). At a high-level, the selection of core formulation (and of the related assumptions) is likely to have a large contribution to the overall uncertainty; in 'pure' CFD formulation such as Reynolds-Averaged Navier Stokes (RANSE) solvers it is accepted that discretisation error, geometric uncertainty and turbulence model uncertainty can have the most significant contributions to the overall uncertainty (Walters and Huyse, 2002).

Table 6: Sources of uncertainty and error in fluid-structure interaction solvers – adapted from (Oberkampf et al., 2001).

Source	Examples
Core model formulation	Boundary element method, RANSE, smoothed particle hydrodynamics, …
Core model assumptions	Inviscid / viscid flow, incompressible / compressible flow, …
Auxiliary model assumptions	Turbulence model, thermodynamic properties, …
Boundary conditions	Free-surface, wall conditions, far-field conditions, …
Discretization and solver settings	Geometry representation, iterative convergence, truncations error, …
Round-off error	Numerical precision, …
Programming / user error	-

As a concluding remark, and focusing on the underlying characteristics of hybrid life testing, recommended steps to quantify the uncertainty in the virtual (numerical) part of the test procedure include:

1. Mapping of the virtual and physical components in the test procedure, and of the associated interfaces, i.e., what is simulated, what is physical and how the two environments interact with each other. If several models are connected into a system or sub-system, the identification of the 'building blocks' that comprise each model and of the input / output interfaces between them is also critical – see also e.g. VALID D1.2, (Ruiz-Minguela et al., 2021).
2. For each numerical model / virtual component, the uncertainty analysis may be performed according to the general process defined in Figure 14, from the characterisation of the input uncertainty, its propagation across the solver stage, and the analysis of the model outputs.

5.2 Model Inputs

At a high-level, it is convenient to categorise the different sources of uncertainty in aleatory (i.e., intrinsic randomness) and epistemic (i.e., lack of knowledge). The practical consequence of this categorisation is the identification of which uncertainties are reducible by acquiring more data and / or by refining the models (i.e., epistemic) and which ones are irreducible (i.e. aleatory). Furthermore, the nature of available data (or lack thereof) as well as allocated

This project has received funding from the European Union's Horizon 2020 research and innovation programme under grant agreement No 101006927.

computational resources largely determine which methods are more appropriate to quantify the uncertainty.

A generic categorisation of uncertainty sources in input factors can take the following form:

i. Numerical parameters describing material and physical properties, geometric dimensions, loads models, etc.

ii. Model structure, e.g., which physical phenomena are taken/not taken into account, boundary conditions, initial conditions, etc.

iii. Numerical errors, e.g., discretisation, truncation errors, solver settings, etc.

In relation to items i. and ii., a reduced number of references connected to such uncertainty sources has focused on WEC design aspects. Examples of such references include e.g. (Ambühl, 2015), where an assessment of WEC reliability is considered using a probabilistic approach. In (Ambühl, 2015), and in addition to an overview of the differences between deterministic and probabilistic design principles, model uncertainties related to input factors are discussed, with environmental conditions, load and stress calculation models being identified as the categories of most interest. The different input categories suggested in (Ambühl, 2015) were used as a starting point in Table 7, which adapts and expands the overview of modelling options in a Highly Accelerated Life Test (HALT) context.

Table 7: Sources of modelling uncertainty at input level.

Input Category	Typical Modelling Options (HALT context)	Notes
Characterisation of the environmental conditions	Contour discretisation. Full environmental characterisation (response based).	Type of data source also affects underlying uncertainty (e.g., if field data is used, quality checking is required – but validation of the underlying numerical model does not apply).
Load calculation model(s)	Local / uncoupled or global / coupled model (e.g., does the model aim to mimic the WEC response, or just provide actuation loads to the test rig?). Formulation (potential flow, Morison, RANSE, etc.). Post-processing method to derive e.g., extreme loads. Accelerated testing models e.g., based on increased load amplitude, load frequency or displacement.	Model structural / numerical errors affect each option differently. V&V activities to be considered a precursor to any inclusion in a HALT environment – see e.g. (C/S2ESC, 2018). General assumption is that sub-system / component under test will replace part (or all) the simulation, with results allowing further, more detailed model development.

This project has received funding from the European Union's Horizon 2020 research and innovation programme under grant agreement No 101006927.

Input Category	Typical Modelling Options (HALT context)	Notes
Resistance and wear model(s)	Process-structure-property models to e.g. understand the cause-effect relationship between material structure and properties – see e.g. (Wang and McDowell, 2020). Structural / materials / stress models (e.g., finite element analysis) Wear / damage models, e.g. Palmgren-Miner rule and the rainflow cycle counting (Downing and Socie, 1982), fatigue stiffness degradation models (Sanchez-Sardi et al., 2016), spectral fatigue methods (Ragan and Manuel, 2007).	Testing may assist numerical modelling activities by e.g. establishing ultimate resistance / serviceability properties of structural components, obtaining specific material properties, calibrating and / or validating numerical models etc. – see e.g. Annex D of (CEN/TC 250, 2002).

As in (Ambühl, 2015), it can be noted that the model uncertainties associated with resistance and wear models are predominantly of a generic nature, i.e. they are not specific to WEC design. In contrast, model uncertainties associated with either the characterisation of the environmental conditions and load calculation models are likely to have elements where their relative importance in the overall uncertainty may differ between WEC design and other offshore engineering applications. Recent examples of relevant assessments include e.g.:

- The influence of a range of methods to estimate environmental contours was documented in (Haselsteiner et al., 2021), which highlights the potential impact of the method selection in long-term estimates of key environmental parameters, which may in turn influence related extreme load estimates. Furthermore, a subsequent application of different to load estimates in a fixed offshore wind turbine support structure was presented in (Haselsteiner et al., 2022), where contour and response-based methods yielded significantly different load estimates (up to 28% difference reported).
- In (Ambühl, 2015) the uncertainty associated with load characterisation was identified as having the highest (relative) importance in the overall model input uncertainty. A similar finding was reported in (Atcheson et al., 2019), where the post-processing methodology applied when deriving the Ultimate Limit State (ULS) load was the variable that mostly contributed to the overall uncertainty in the ULS estimate. Examples where different post-processing methods were used to derive ULS load estimates include e.g. (Coe et al., 2018; Shahroozi et al., 2022).
- A sensitivity analysis focused on the uncertainty associated with extreme load estimates associated with a point absorbed WEC was performed in (Eskilsson et al., 2022). A surrogate model based on the generalised polynomial chaos approach was created to minimise the computational effort. The resulting sensitivities were ranked using the Sobol index method. The relative importance of different input sources to the target metrics differed between the regular and irregular wave cases studies. Other recent studies were also performed targeting additional outputs variables, such as mooring line dynamics – see e.g. (Moura Paredes et al., 2020).

This project has received funding from the European Union's Horizon 2020 research and innovation programme under grant agreement No 101006927.

For other applications, including offshore wind, examples of assessments related to uncertainty in environmental characterisation and / or load models include e.g.:

- A Sobol global-sensitivity approach was adopted in (Nispel et al., 2021) to identify the most and least important parameters (including environmental parameters) that contribute to the fatigue life of the support structure of an offshore bottom-fixed wind turbine. The most influential parameters were found to be the mean wind speed and the air density, for which the authors recommended accurate data collection and statistical analysis to reduce uncertainty propagation in fatigue life assessments.
- The uncertainty in the Annual Energy Production (AEP) for a range of offshore wind farms was assessed in (Richter et al., 2022) based on the uncertainty propagation models related to mean wind speed, wake effects, thrust curve, surface roughness, power curve and plant performance. Overall, it was found that uncertainties in the mean wind speed have the greatest influence on uncertainty in AEP estimates; however, it was noted that farm layout, turbine types and farm locations may make some wind farms more sensitive to specific parameters than others.

Finally, generic examples of studies that address the uncertainties related to accelerated testing, resistance and wear models include:

- If conducted numerically, the future adoption of accelerated testing principles based on e.g., increased load amplitude and / or frequency may require assessing the validity of the underlying assumptions of the considered load model(s). For example, the use of a hydrodynamic model based on e.g., linear wave theory implies that the resulting dynamics are small when compared to the dominant wavelength, and that wave-induced loads are proportional to the wave amplitude. If an increased displacement amplitude is simulated to e.g. virtually accelerate the wear failure mechanism, this may violate the fundamental principles of linear wave theory – see e.g. (Faltinsen, 1990).
- In (Hu and Mahadevan, 2017) UQ modelling techniques are applied to predict material properties during additive manufacturing, based on a process-structure-property approach – see e.g. (Wang and McDowell, 2020). In particular, the study focuses on estimating the uncertainty of the ultimate tensile strength of a structure obtained from laser sintering of nanoparticles. Uncertainty sources are identified as both aleatory (variability of particle radii, sintering temperature, and the gap between the particles due to packing of the powder bed) and epistemic (the simulation model). Uncertainty propagation is based on a surrogate model (see also Section 5.3.3), which was used to derive 1,000 realizations of the stress-strain curve of the material to assess the uncertainty in the ultimate tensile strength of the material. Such study provides an example of UQ for the mechanical properties of a specific material, in the context of a process-structure-property framework aiming to investigate the uncertainties in the modelling of a manufacturing process, which may relate to the 'resistance' models alluded to in Table 7.
- The advantages and disadvantages of the Rainflow cycle counting algorithm (used in conjunction with the Palmgren-Miner rule) and a fatigue stiffness degradation model are discussed in (Sanchez-Sardi et al., 2016), with reference to the fatigue life assessment of a wind turbine blade. In particular, fatigue stiffness models associate the fatigue damage of a component to an overall degradation of its stiffness properties – as such models initially were developed for composite materials. The stiffness degradation phenomenon is generally modeled as a function of material properties (including the ultimate compression static strength), and the stress acting on the component. Although the study in (Sanchez-Sardi et al., 2016) does not provide quantitative, comparable results, it does stress that uncertainty may be associated following either model – with such uncertainty mostly related to input parameter estimation via physical modeling.

This project has received funding from the European Union's Horizon 2020
research and innovation programme under grant agreement No 101006927.

- In (Ragan and Manuel, 2007) Dirlik's spectral method was compared to a classical time-domain method (based on the Rainflow cycle counting algorithm) for the estimation of the fatigue loads acting on a wind turbine. Overall, the study concluded that the spectral method is more conservative than the time-domain method. Furthermore, it was noted that the spectral method was able to replicate the results of the time-domain methods more accurately for some type of loads e.g., tower bending moments than for others e.g. blade edgewise bending moment. The study suggests that Dirlik's spectral method performs poorly in estimating the fatigue damage when "*large [loading] periodic components*" occur, which is the case for blade loads due to e.g., centrifugal loads and gravity loads. The study included an analysis on the different types of inputs on which the two methods rely, and highlighted how reducing uncertainty in input data to the fatigue models is key in deriving accurate estimates of damage.

The quantitative evaluation of uncertainty in input factors can be based in the assessment of intervals (minimum and maximum values), statistical moments (typically measurements of central tendency and dispersion) and probabilistic distributions. Additionally, a range of methods for uncertainty propagation, particularly those under the denomination of "Sampling methods" in Section 5.3, explore the design space by selecting input values according to certain rules, thus resulting in structured patterns which resembles those derived from the techniques of Design of Experiments (DoE). There are some differences between physical and computational DoE, with the latter being underpinned in the principle of adequate coverage of the design space while minimising the amount of (possibly expensive) model evaluations.

To conclude, a more widely applicable set of references is dedicated to item iii (numerical errors). In general, numerical errors might be perceived as conceptually different from uncertainty, as they do not originate from natural variability or lack of knowledge. They can be intuitively assimilated to a bias, or systematic error as they entail the deviation of the computed solution from its true value (which, however, cannot always be proven to exist). Additionally, discretization errors and solver settings play an important role to determine the overall range of model output, therefore they should be at least noted at the input stage and estimated a priori whenever possible. However, in most cases, proper quantification of numerical solution errors can be performed only a posteriori, that is at the output stage (see Section 5.4).

5.3 Uncertainty Propagation

The propagation of uncertainty through numerical models may be addressed following several methods. In general, uncertainty propagation may be described by a (non)-linear function, $g(\times)$, which transfers one input variable, ζ , to the quantity of interest, η, as:

$$\eta = g(\zeta) \tag{29}$$

It is noted that the function $g(\times)$ may link more than one input variable to more than one quantity of interest; however, for simplicity of notation and without loss of generality, only one input variable and one quantity of interest are considered, to formulate illustrative equations in this section.

A non-exhaustive list of methods to assess uncertainty propagation through numerical models is outlined in Table 8. A brief description of each method is then proposed in the following subsections.

This project has received funding from the European Union's Horizon 2020 research and innovation programme under grant agreement No 101006927.

Table 8: Non-exhaustive list of methods to assess uncertainty propagation through numerical models.

Method Category	Method Type	Sample Reference(s)
Analytical methods	Taylor expansion	(Schenkendorf, 2014)
Sampling methods	Random sampling (Monte Carlo)	(Allard et al., 2015) (Nguyen et al., 2019)
	Importance sampling	(Allard et al., 2015) (Mckay et al., 2000)
	Stratified sampling	(Allard et al., 2015) (Mckay et al., 2000)
Surrogate methods	Nearest-Neighbour	(Allard et al., 2015)
	Polynomial Chaos Expansion	(Allard et al., 2015) (Nguyen et al., 2019) (Wiener, 1938)
Inference methods	Bayesian models	(Elster et al., 2015)
	Dampster-Shafer theory	(James C. Hoffman and Robin R. Murphy, 1993)

5.3.1 Analytical Methods

Analytical methods aim to formulate approximate analytical expressions of the function $g(\times)$ via the use of e.g. Taylor expansion (Schenkendorf, 2014). For example, the first-order Taylor approximation of Eq. (29), calculated at $\zeta = \bar{\zeta}$, may be expressed as:

$$\eta = g(\zeta) \approx g(\bar{\zeta}) + \left.\frac{\partial g}{\partial \zeta}\right|_{\zeta=\bar{\zeta}} (\zeta - \bar{\zeta}) \qquad (30)$$

Such an approximation would easily support the assessment of statistical moments of the quantity of interest, e.g., mean, standard deviation etc. However, a first-order Taylor series expansion is able to accurately represent $g(\times)$ only if the latter is close to being linear in the region of interest. While higher-order terms in the expansion may in principle gradually improve the modelling accuracy, higher than second-order approximations are seldom used practically (Schenkendorf, 2014). In addition, the adoption of a Taylor expansion scheme assumes that the mapping function $g(\times)$ is differentiable, which may not always be the case e.g. if the mapping function is a maximum function (Schenkendorf, 2014). Finally, and with particular significance for practical applications, the use of analytical methods is prevented when the mapping function is unknown, or it is not expressible in closed form.

This project has received funding from the European Union's Horizon 2020
research and innovation programme under grant agreement No 101006927.

5.3.2 Sampling Methods

Sampling methods consist in generating several samples of the input variable, ζ and assess the output, η, for each input sample to eventually estimate statistical properties of the quantity of interest (Allard et al., 2015). When the input variables are generated according to a random uniform distribution, the sampling method is also known as Monte Carlo method. In general, the Monte Carlo method requires a large number of simulations to be performed, in order to get statistically representative information about the quantity of interest (Allard et al., 2015).

In the field of wave energy, the Monte Carlo method has been applied in (Nguyen et al., 2019) to assess the long-term extreme response of a point absorber-type WEC. In this study, the input variables consisted in the significant wave height, H_s, and the peak wave period, T_p while the quantities of interest were represented by the Power Take Off (PTO) extension and the heave force acting on the prime mover of the WEC. The samples of H_s were randomly drawn from a three-parameters Weibull distribution, $F_{H_s}(h)$, while the samples of T_p were randomly drawn from a log-normal conditional distribution $F_{T_p|H_s}(t|h)$. A total of 10^5 input samples were generated, and simulations were run via a time-domain, point-load, coupled WEC model. In addition, to take into account the short-term variability of the wave conditions, each simulation was repeated 10 times with a different random wave phase vector, thus bringing the total number of simulations to 10^6. It is noted that such a number of simulations is in line what is recommended in other guidance documents e.g. (Allard et al., 2015). Figure 15 illustrates the extreme PTO extension (left-hand side) and heave force (right-hand side) acting on the WEC calculated via Monte Carlo simulations.

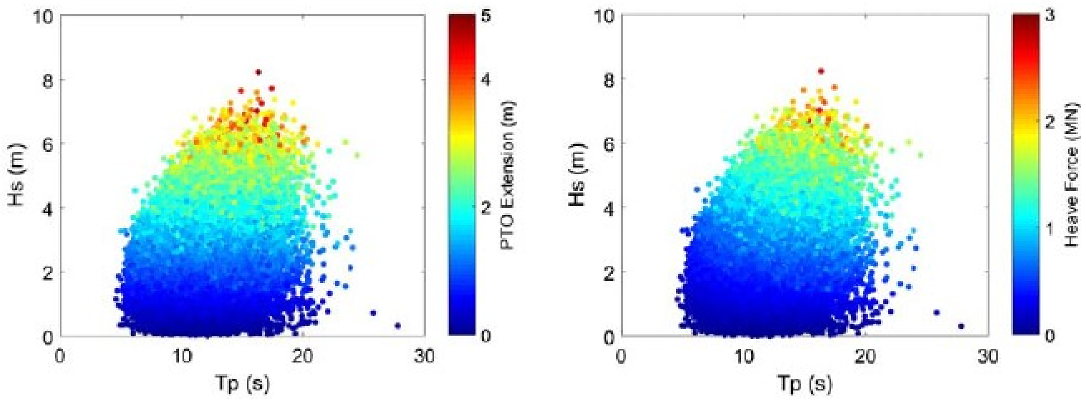

Figure 15: Extreme PTO extension (left) and heave force (right) on a point-absorber type WEC based on Monte Carlo simulations (Nguyen et al., 2019).

A potential disadvantage of a random sampling approach is that it does not ensure that specific regions of the input space are covered to an adequate level. This implies that areas of the input space related to critical values of the output quantities, e.g., powerful sea states may not be appropriately sampled (or not sampled at all), while less critical areas, e.g., mild sea states are sampled repeatedly. To potentially overcome this drawback, alternative sampling methods have been proposed, such as:

- *Importance sampling*. In this approach, the input samples generation includes the use of an importance sampling density function which essentially ensures that specific regions of interest of the input space are sampled – see (Allard et al., 2015; Owen and Zhou, 2000). Figure 16 provides an example of sampling density function, which aims to sample the regions around values $\zeta = 0.25$ and $\zeta = 0.75$.

This project has received funding from the European Union's Horizon 2020
research and innovation programme under grant agreement No 101006927.

- *Stratified sampling*. In a stratified sampling approach, the input space is divided into a number of distinct, non-overlapping regions where the number of samples can be controlled based on tunable parameters – see (Allard et al., 2015; Mckay et al., 2000).

The main drawback of sampling methods is that, most often, they require a significant number of model evaluations to be performed. If the model is computationally expensive, the overall effort may become unaffordable.

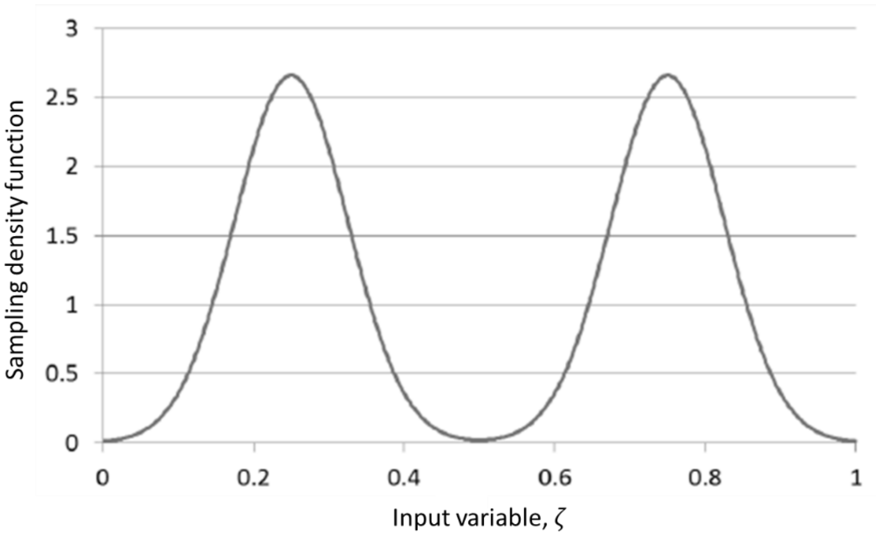

Figure 16: Example of sampling density function for application of the importance sampling method, adapted from (Allard et al., 2015).

5.3.3 Surrogate Methods

To reduce the overall computational effort and thus accelerate the assessment of uncertainty propagation through numerical models, methods based on surrogate models have been developed. A surrogate model is a simplified model that aims to capture the I/O relationship of the original model, for a certain range of the input quantities. As such, a surrogate model essentially replaces Eq. (30) with the following:

$$\eta = g(\zeta) \approx s(\zeta, \beta_1, \beta_2, \dots, \beta_N) \tag{31}$$

Where the function $s(\times)$ defines the surrogate model itself. Most often, a surrogate model is not linked to the physics of the modelled phenomena but is rather constructed from simple, computationally-efficient high-dimensional functions (Allard et al., 2015). In Eq. (31), the terms β_n represent model-specific parameters which are usually determined based on a set of training point outputs η_i associated with a set of training point input values ζ_i. Most often, the training point outputs are calculated by using the original numerical model.

In the nearest neighbour interpolation method, the value of $s(\times)$ at some arbitrary point is given by the function value at the closest training point (Allard et al., 2015). Although simple and easy to implement, the nearest neighbour method may require a significant number of training points to allow a sensible approximation of the original function.

A potentially more accurate and more widely adopted approach is based on the Polynomial Chaos Expansion (PCE) method – see e.g. (Allard et al., 2015; Wiener, 1938). In this approach, the output quantity of interest is approximated by a weighted sum of orthogonal polynomials of random variables, as:

This project has received funding from the European Union's Horizon 2020
research and innovation programme under grant agreement No 101006927.

$$\eta = g(\zeta) \approx \sum_{i=0}^{M-1} a_i \psi_i(q) \tag{32}$$

where:

- The terms a_i represent the weights of the polynomial functions.
- The terms ψ_i represent multivariate orthogonal basis functions.
- The term q is a random variable, which is mapped from the original input variable ζ.
- M is the number of polynomial terms.

Various methods exist for the estimation of the coefficients a_i, including spectral projection and linear regression (Sudret, 2008). In the field of wave energy, the PCE method was adopted in (Nguyen et al., 2019) to assess the extreme response of a point absorber-type WEC, which was then compared to that calculated via a Monte Carlo approach (see also Section 5.3.2). In this study, the input variables H_s and T_p were mapped to a pair of variables Q_1 and Q_2 following a Gauss-Laguerre quadrature scheme. A total of 7 x 7 = 49 input points were mapped and used as training points. Figure 17 illustrates the sea states selected as training points in the original input space (left-hand side) and the mapped input space (right-hand side).

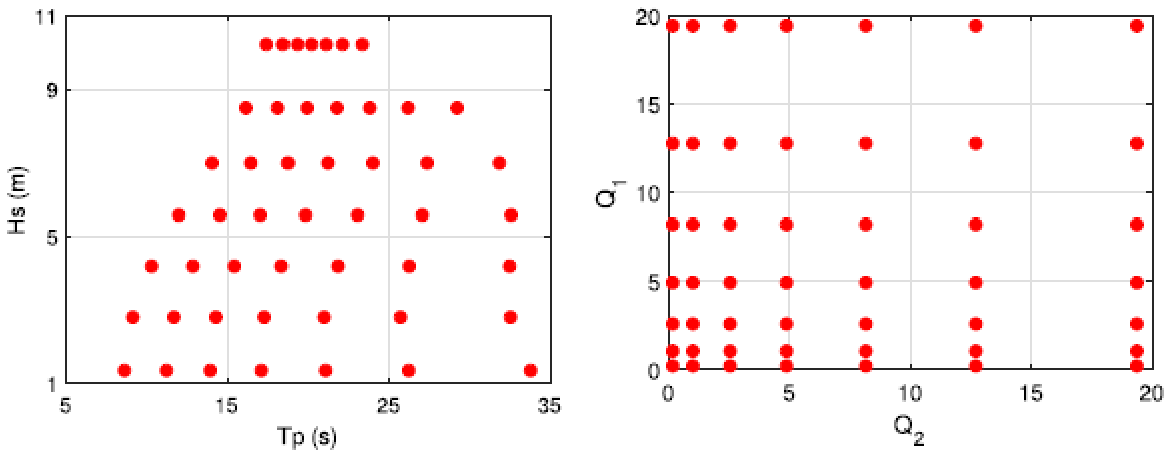

Figure 17: Sea states selected as training points in (Nguyen et al., 2019): original input space (left) and mapped input space (right).

A six-order PCE model was developed and used to assess the extreme PTO extension and the heave force acting on the prime mover of the WEC. Results were compared to those provided by a Monte Carlo method, which considered as that providing the "true" estimate of the extreme responses. Figure 18 illustrates the probability of exceedence of the PTO extension (left-hand side) and heave force (right-hand side), for the PCE model (blue curves) and the Monte Carlo simulations (red curves). For each method, 10 curves are illustrated as corresponding to 10 different random wave vectors associated with the input variables.

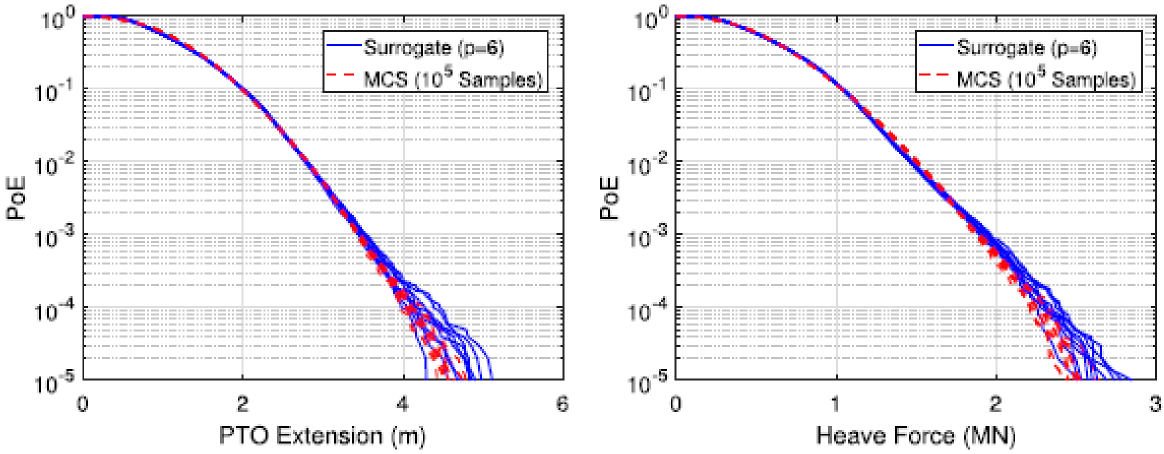

Figure 18: WEC long-term response probability of exceedence plots based on Monte Carlo simulations (in legend denoted as MCS) and PCE: (left) PTO extension and (right) heave force; (Nguyen et al., 2019).

Figure 19 outlines the response statistics (mean and standard deviation) of the extreme PTO extension (left-hand side) and heave force (right-hand side), for different probability levels. A good agreement between the PCE and the Monte Carlo methods was observed, down to a probability of exceedence of 10^{-5}.

Probability level	Response statistic	MCS	PCE ($p = 6$) $N = 10$
10^{-3}	μ (m)	3.45	3.47
	σ (m)	0.03	0.03
10^{-4}	μ (m)	4.10	4.20
	σ (m)	0.09	0.10
10^{-5}	μ (m)	4.59	4.71
	σ (m)	0.11	0.24

Probability level	Response statistic	MCS	PCE ($p = 6$) $N = 10$
10^{-3}	μ (MN)	1.89	1.94
	σ (MN)	0.02	0.02
10^{-4}	μ (MN)	2.26	2.29
	σ (MN)	0.05	0.06
10^{-5}	μ (MN)	2.50	2.56
	σ (MN)	0.07	0.13

Figure 19: Mean and standard deviation of extreme PTO extension (left) and heave force (right) for the Monte Carlo method (here denoted as MCS) and the PCE method (adapted from (Nguyen et al., 2019)).

Often, however, the surrogate model created is used in connection with a sampling method. An example of this approach was presented in (Eskilsson et al., 2022) for evaluating the sensitivity of the maximum mooring tension to uncertainty in environmental variables as well to uncertainties in the mooring/PTO system. The case study was the Uppsala University WEC which is made up of a point-absorber tightly moored to a linear generator placed on the sea floor. After an initial basic VMEA, five input variables were chosen to be the most important, and these were used in the study. For these five variables 1-dimensional PCE surrogate models were first created using numerical models run on the quadrature points. Checking that a polynomial order of 4 was sufficient (see Figure 20), the study proceeded to the multi-dimensional case.

This project has received funding from the European Union's Horizon 2020
research and innovation programme under grant agreement No 101006927.

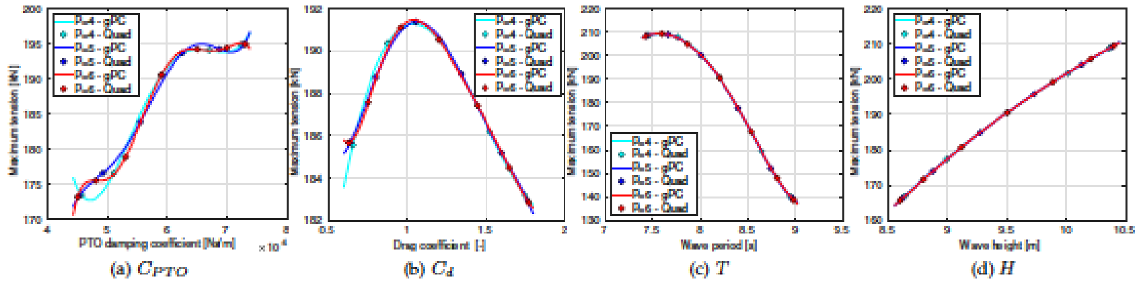

Figure 20: 1-dimensional PCE surrogate models for maximum mooring tension for (a) PTO damping coefficient, (b) drag coefficient, (c) wave period and (d) wave height. From (Eskilsson et al., 2022).

It should be mentioned that PCE suffers from the "curse of dimensionality". While the exponential convergence associated with higher order polynomials make PCE fast, for higher dimensions the required number of sampling points grows very fast as well. Thus, only a 5-dimensional case could be investigated, and 100 sampling points were created using the Latin hyper cube. Note that the issue of random phase angles was not treated with PCE but with the standard approach of 10 realizations. In total 1000 simulations were performed, using the software WEC-SIM, to create the 5-dimensional PCE surrogate model of the maximum tension. The PCE surrogate model directly holds the mean and variance of the solutions (and thus also global sensitivity indices), while probability density functions are usually created by a sampling method. The surrogate model was then used in a standard Monte Carlo simulation using one million random inputs to yield the probability density distribution, as well as sensitivity analysis using Sobol indices, see Figure 21. It can be observed that for the Uppsala WEC, the drag coefficient gives the largest contribution to the uncertainty.

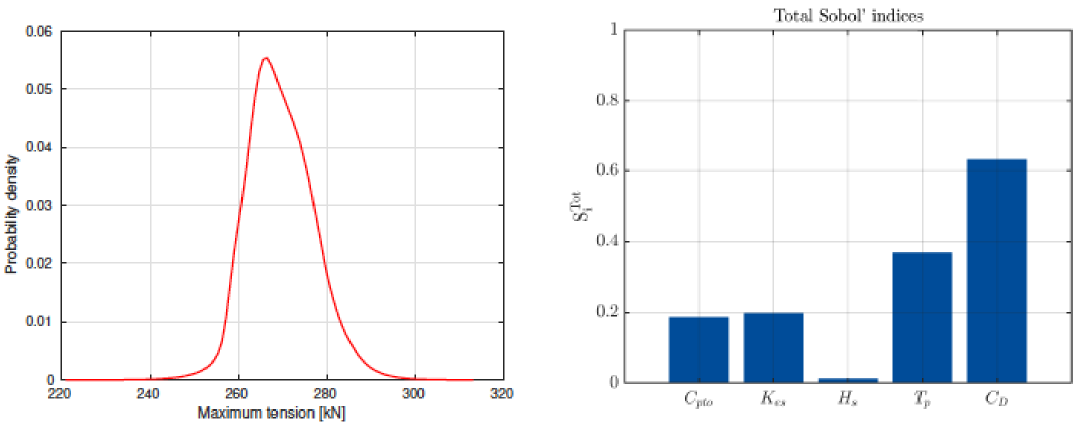

Figure 21: 5-dimensional PCE surrogate model for the maximum tension for a 100-year sea state. Right: Probability density function, and left: Sobol sensitivity indices; (Eskilsson et al., 2022).

5.3.4 Inference Methods

Statistical inference methods aim to infer the properties of an entire data population, for example by testing hypotheses and deriving estimates – differently from descriptive statistic methods, which solely deal with the properties of the observed data.

The Bayesian method is an inference approach based on Bayes' theorem, which can be expressed by the following equation:

$$P(H|E) = \frac{P(E|H)P(H)}{P(E)} \tag{33}$$

where:

- H represents a hypothesis, based on previous evidence, whose probability may be affected by current evidence ("hypothesis").
- $P(H)$ represents the estimate of the probability of H based on previous evidence, i.e., before the current evidence (data), E, is observed ("prior probability").
- $P(E|H)$ is the probability of observing E given H ("likelihood").
- $P(H|E)$ is the probability of H after E has been observed ("posterior probability").

The Dempster-Shafer theory provides an alternative to the Bayesian approach, from which it essentially differs on a number of major conceptual parts (James C. Hoffman and Robin R. Murphy, 1993). Among such differences:

- The computation of evidence in Dempster-Shafer theory does not require prior distributional information.
- The Dempster-Shafer theory avoids the Bayesian restriction that commitment of belief to a hypothesis implies commitment of the remaining belief to its negation, i.e., the Dempster-Shafer theory can explicitly represent any ambiguity or ignorance about what has been observed.

The study in (James C. Hoffman and Robin R. Murphy, 1993) provides a comparative application of the Bayesian approach and the Dempster-Shafer theory, concluding that "*both methods for dealing with uncertainty yield similar results if analysis is based on equivalent problem formulations. […] We believe that Bayesian theory is best suited to applications where there is no need to represent ignorance, where conditioning is easy to extract through probabilistic representations and prior odds are available*".

5.4 Model Output Analysis

Depending on the selected method for the analysis, the uncertainty of model output can be expressed as a (multivariate) probability distribution, statistical moments (e.g., mean and variance), interval, etc.

5.4.1 Numerical Uncertainties

Every numerical simulation contains errors and uncertainties. The terms error and uncertainty are linked but not synonyms. Error (δ) refers to the difference between a numerical solution (ϕ_i) and the exact solution (ϕ_0):

$$\delta = \phi_i - \phi_0 \tag{34}$$

Uncertainty (U_{ϕ_i}) defines an interval that should contain the exact solution with a certain degree of confidence:

$$\phi_i - U_{\phi_i} \leq \phi_0 \leq \phi_i + U_{\phi_i} \tag{35}$$

In the general CFD community many standards for assessing the of quality of the numerical solutions have been developed (AAIA, 1998; ASME, 2009; ITTC, 2017) The overarching terminology is verification and validation (V&V). As the name suggests there are two main steps: (1) the verification step and (2) the validation step.

The verification stage is commonly understood as making sure that the numerical code is working correctly, so-called code verification. By comparing against exact solutions – typically relying on simplified equations having the same numerical operators or on manufactured solutions – the implementation of the numerical schemes is verified to be correct. If using already available numerical models, the code verification task should already have been performed by the developers and is nothing for software user to be concerned about. The exception is for bespoke code development for WEC modules, e.g., PTO and control algorithm implementations. Any such development should go through the code verification step.

In the validation stage, it is vital to make sure that the underlying mathematical models approximate the problem under investigation. Validation is usually done by comparing numerical results to experimental test data. The literature on the validation of numerical models for WECs is quite vast. Almost all studies of WECs using high-fidelity tools have been focused on the validation, although a few studies have used proper V&V, see e.g. (Brown et al., 2021; Wang et al., 2018).

Additionally, there is a second part of the verification stage that is often omitted but should ideally be performed for every computational case by the software user: the solution verification. Solution verification is described by (Eça and Hoekstra, 2014) as how to

> *'estimate the error/uncertainty of a given calculation, for which in general the exact solution is not known'.*

It is important to stress that solution verification is not the same as making sure the numerical solution is 'grid independent'. That a solution appears grid independent neither implies that the solution is properly converged nor that the errors are insignificant and can be disregarded. Nevertheless, basic grid convergence studies, given in the eyeball norm, are still widely used to illustrate that the solutions are accurate. However, with relatively little extra effort, a proper solution verification can be performed, linking the errors of grid convergence to actual convergence rate and to estimates of the numerical uncertainty. It is generally accepted that the numerical uncertainties should be below 5% for the solutions to be acceptable and reliable (Eça et al., 2010; Stern et al., 2001).

As mentioned above the total numerical error (ε_T) arise from modelling error (ε_M), input error and numerical error (ε_N):

$$\varepsilon_T = \varepsilon_M + \varepsilon_I + \varepsilon_N \tag{36}$$

The numerical error is in turn made up of several parts:

$$\varepsilon_N = \varepsilon_d + \varepsilon_{it} + \varepsilon_{ro} + \varepsilon_{st} \tag{37}$$

where ε_d is the numerical discretization error, ε_{it} is the iteration error, ε_{ro} is the round-off error and ε_{st} denotes the statistical errors. Using double precision in the simulations, the round-off errors can usually be disregard. This is true most of the time, but we note that especially GPU applications might be using single precision. Statistical errors are linked to the simulation length and the choice of window for evaluating integral properties. Iterative errors are linked to the

This project has received funding from the European Union's Horizon 2020 research and innovation programme under grant agreement No 101006927.

solution of the nonlinear equation systems. As a rule of thumb this error can be disregarded if the residuals are kept two orders below the discretisation error (Eça and Hoekstra, 2009). However, that rule of thumb applies to simulations with fixed objects. For moving objects, the iterative errors include errors associated with convergence of the moving body, and this error might be significant. Nevertheless, most of the time the discretization error is the dominant error and the main part of the solution verification.

There exist several approaches to V&V for CFD, which differ slightly. The classical solution verification method is the grid convergence index by (Roache, 1998). The original grid convergence index only requires two grids but has a shortcoming in that it requires monotonic convergence. The (ITTC, 2017) recommendations are based on the method of (Stern et al., 2001). However, the solution verification method that has been used perhaps most frequently in the marine renewables is due to (Eça and Hoekstra, 2014). The Eca and Hoekstar method follows from the original grid convernegnce index method but evaluates the convergence in a least-square sense. We outline the Eca and Hoekstra approach below.

All solution verification methods rely on finding out how the solution changes for different resolutions in time and space. Let h denote the grid size and subsequently define a sequence of n grids as $h_1 < h_2 < \cdots < h_n$, where h_1 denotes the finest grid size. The grid refinement ratio h_i/h_1represents the ratio of cell size between grids with different densities. For structured grids the grid size is straightforward, while for unstructured grids we approximate the grid size as:

$$h_i = \left(\frac{N_1}{N_i}\right)^{1/d} \tag{38}$$

where N_i is the total number of degrees of freedom for grid i and d is the dimension of the problem.

Using Richardson extrapolation, the numerical error can be estimated as:

$$\varepsilon_d \approx \delta_{RE} = \phi_i - \phi_0 = ah_i^p \tag{39}$$

in which p is the numerically obtained order of convergence and a is a case specific constant. Assuming second order convergence as well as a mixture of first and second order convergence we additionally have:

$$\delta_{RE}^{02} = \phi_i - \phi_0 = a_{02}h_i^2 \tag{40}$$

$$\delta_{RE}^{12} = \phi_i - \phi_0 = a_{11}h_i^1 + a_{12}h_i^2 \tag{41}$$

Using a least square approach we then evaluate ϕ_0, p as well as the constants to obtain the errors.

Following (Roache, 1998) the numerical errors are converted into uncertainties by means of safety factors:

$$U_\phi = F_S|\varepsilon| \tag{42}$$

The values of the applied safety factors follow from the convergence. If $p > 0$ the convergence is monotone, otherwise it is oscillatory. If in addition the convergence is in the asymptotic range ($0.95 \leq p \leq 2.05$, for a standard second-order scheme) the safety factor is set to 1.25. If the convergence is monotonic but not in the asymptotic range, then the safety factor is set to 3. To summarize, the uncertainties can be evaluated as:

$$U_\phi = 1.25\delta_{RE} + U_S \quad \text{if } p \in [0.95,\, 2.05] \tag{43}$$

$$U_{\phi} = \min(1.25\delta_{RE} + U_S,\ 3\delta_{RE}^{12} + U_S^{12}) \text{ if } p < 0.95 \tag{44}$$

$$U_{\phi} = \max\left(1.25\delta_{RE} + U_S,\ 3\delta_{RE}^{02} + U_S^{02}\right) \text{ if } p < 2.05 \tag{45}$$

where U_S, U_S^{02} and U_S^{12} are the standard deviations obtained from the least square fits. In the case of oscillatory convergence, a range-based estimate is employed:

$$U_{\phi} = 3\delta_{\Delta M} \tag{46}$$

in which the error between the maximum and minimum is obtained as:

$$\delta_{\Delta M} = \frac{\max\left|\phi_i - \phi_j\right|}{\left(h_{N_g}/h_1\right) - 1} \quad 1 \leq i, j \leq N_g \tag{47}$$

We exemplify the use of the Eca and Hoekstra method for the case of estimation of drag coefficient for a case of Detached-Eddy simulations of flow over an infinitely wide plate with rounded edges (Andersen and Eskilsson, 2023), see Figure 22.

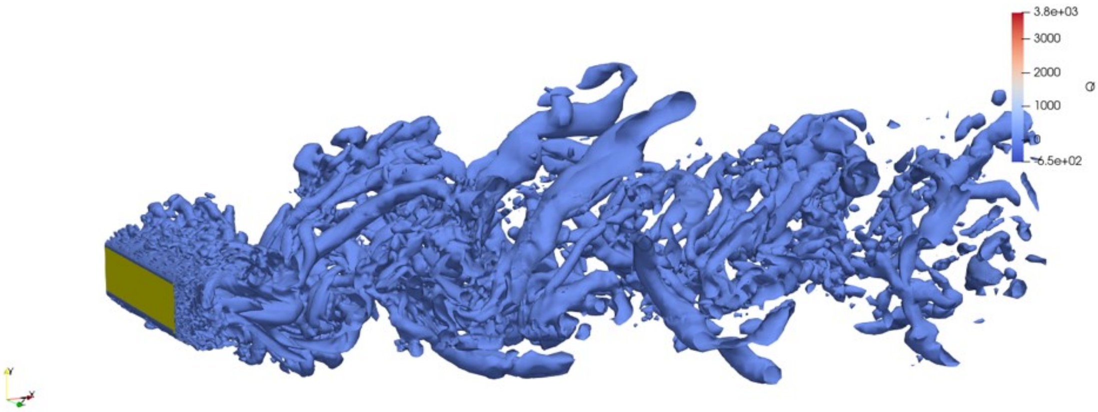

Figure 22: The iso-contour showing the vortex shedding after an infinitely wide plate with rounded edges. Flow is from left to right. From (Andersen and Eskilsson, 2023).

Using seven levels of spatial resolution, as presented in Table 9, we get a monotonic convergence in the asymptotic range (Figure 23). The associated level of uncertainty thus becomes low, and using the rule-of-thumb of 5% uncertainty we can with confidence use the 4.5M cell setup for the further analysis.

This project has received funding from the European Union's Horizon 2020 research and innovation programme under grant agreement No 101006927.

Table 9: Investigated spatial and temporal resolutions. N_z denotes the number of cells in the spanwise direction. From (Andersen and Eskilsson, 2023)

Case	h_i/h_1 [-]	N_{cells} [1e6 cells]	N_z [cells]	$\Delta t u_0/h$ [-]	$\langle C_D \rangle_t$ [-]	Δ_{rel} [%]	$U_{\langle C_D \rangle_t}$ [%]
1	1.00	10.3	48	6e-4	2.28	0.0	2.7
2	1.29	6.0	48	6e-4	2.28	0.2	3.7
3	1.49	4.5	48	6e-4	2.26	0.6	4.6
4	1.66	3.6	48	6e-4	2.23	2.1	5.4
5	2.08	2.3	48	6e-4	2.23	2.1	7.8
6	2.58	1.5	48	6e-4	2.10	8.0	11.3
7	3.16	1.0	48	6e-4	2.05	9.9	16.4

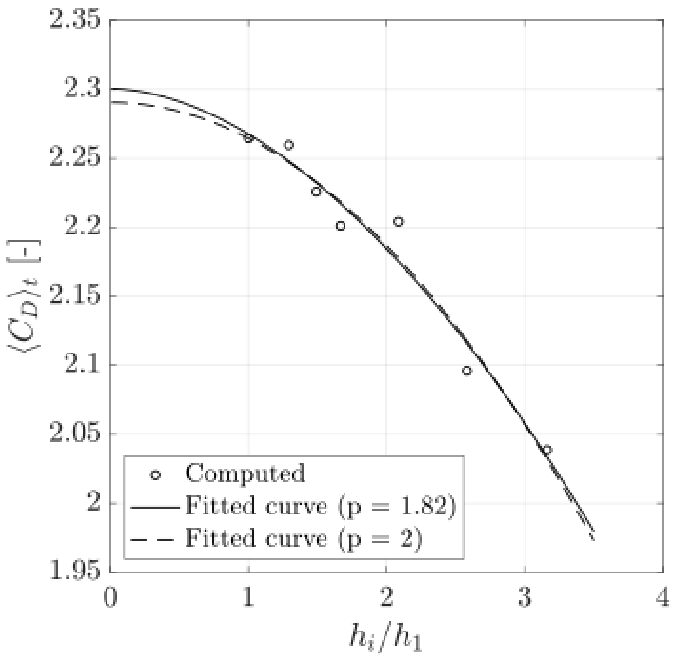

Figure 23: Estimated convergence of time averaged drag coefficient $\langle C_D \rangle_t$ from spatial resolution in the xy-plane. From (Andersen and Eskilsson, 2023).

While the use of solution verification greatly assists in assessing and improving the reliability of the numerical solutions there are still issues with regard to its implementation for wave energy applications. The most pressing would be how to apply this to standard linear potential flow applications. Here the numerical errors are likely to be of less importance compared to the modelling errors. How then to assess ϕ_0? For high-fidelity simulations of wave energy devices, we still have problems for cases with irregular/non-harmonic response. What parameters should we use when assessing the uncertainty?

This project has received funding from the European Union's Horizon 2020 research and innovation programme under grant agreement No 101006927.

5.4.2 Sensitivity Analysis

The result of the uncertainty analysis is an estimate of the range in which the model outputs is likely to fall, as a consequence of the uncertainty in all relevant input and solver characteristics and assumptions. This estimate can be further analysed in a Sensitivity Analysis (SA), which can be defined as (Saltelli et al., 2007)

> *'The study of how uncertainty in the output of a model (numerical or otherwise) can be apportioned to different sources of uncertainty in the model input'*

The purpose of SA is to screen how uncertain inputs contribute to the output uncertainty, thereby giving some indication on how to to reduce it. The quantitative ranking of input parameters according to some sensitivity index provides a rationale to focus the available resources on the most significant design variables. An SA can be said to be either local or global. Fundamentally, a local SA looks at the effect of an infinitly small perturbation of a single input parameter while the other part does not change, yielding a gradient of the function. For a nonlinear function, the derivative will vary, so a local SA is only applicable in a small range (Saltelli et al., 2007), A global SA, however, looks at the entire parameter space with the combined effects of several input parameters. Thus, the global SA is typically the preferred method, but can carry a high computational cost. While SA might seem straightforward, many reported SA falls below the acceptable criteria (Saltelli et al., 2019).

In the following we let $g(X)$ denote a function and S_i the sensitivity index of the ith model input x_i. Different approaches to SA are discussed below (Borgonovo and Plischke, 2016; Reed, Patrick M. et al., 2023; Saltelli et al., 2007):

Derivative-based methods. Using a one-at-a-time approach, the sensitivity index is simply evaluated as:

$$S_i(\bar{x}) = \frac{g(\overline{x_1}, \dots, \overline{x_\iota} + \Delta_i, \dots, \overline{x_N}) - g(\overline{x_1}, \dots, \overline{x_\iota}, \dots, \overline{x_N})}{\Delta_i} c_i \tag{48}$$

in which $\Delta_i$is the perturbation and c_i a scaling factor. This is a local method, and while computationally cheap, it can not investigate the entire parameter space in addition to missing out on any interaction effects.

Elementary effect methods. Elementary effect is an extension of the derivative-based method. While still using the one-at-a-time approach, elementary effect allows us to cover the entire parameter space. This is accomplished by dividing the parameter space into r trajectories (or sample repetitions), and use the sampling methodology of (Morris, 1991). Thus, the sensitivity index can be estimated as:

$$S_i = \mu_i = \frac{1}{r}\sum_{j=1}^{r} EE_i^j = \frac{1}{r}\sum_{j=1}^{r} \frac{g(\overline{x_1}, \dots, \overline{x_\iota} + \Delta_i, \dots, \overline{x_N}) - g(\overline{x_1}, \dots, \overline{x_\iota}, \dots, \overline{x_N})}{\Delta_i} c_i \tag{49}$$

In addition to the mean of elementary effects, the variance can be found as:

$$\sigma_i = \sqrt{\frac{1}{r}\sum_{j=1}^{r}\left(EE_i^j - \frac{1}{r}\sum_{j=1}^{r} EE_i^j\right)^2} \tag{50}$$

It is customary to plot μ_i against σ_i in a scatter plot, referred to as Morris plot. Parameters close to the origin are unimportant. A large μ_i means that the parameter has a high sensitivity, while a large σ_i means that we have interaction or nonlinear effects and thus often hard to estimate correctly.

Regression-based methods. By using a least-square approach we can fit a linear regression relation between the input vector x and the output vector y:

$$y = b_0 \sum_{i=1}^{N} b_i x_i \tag{51}$$

where b_i are the regression coefficients. Then the standardized regression coefficients (SRC) can be used as sensitivity indices and computed as:

$$S_i = SRC_i = b_i \frac{\sigma_i}{\sigma_y} \tag{52}$$

in which σ_i and σ_y are the variances of the ith input and the output. There exist versions of the SRC such as Pearson correlation coefficient (PCC) and Spearman's rank correlation coefficient (SRCC), see (Reed, Patrick M. et al., 2023). The regression-based methods are global methods but have a clear disadvantage of showing poor performance for nonlinear models.

Variance-based methods. Variance-based methods decompose the output variance into parts associated with input and interpret this as a measure of sensitivity. While there exist different types of variance-based methods, like the Fourier amplitude sensitivity test, the most widely used is the Sobol method (and variants thereof) (Sobol, 1993). Sobol's method gives three different sensitivity indices: first-order, higher-order and total Sobol sensitivity indices. The first-order sensitivity index gives the percentage of output variance due from a single input as:

$$S_i^1 = \frac{V_{x_i}\left[E_{x_{\sim i}}(x_i)\right]}{V(y)} \tag{53}$$

where E is the expected value and V is the variance. $x_{\sim i}$ denotes all values except x_i. Higher-order indices give information about interaction between two or more parameters that contribute to model output variations. The computations are tedious and most often just the second-order indices are computed:

$$S_{i,j}^2 = \frac{V_{x_{i,j}}\left[E_{x_{\sim i,j}}(x_i, x_j)\right]}{V(y)}, \quad i \neq j \tag{54}$$

Finally, the total Sobol indices is computed as:

$$S_i^T = \frac{E_{x_{\sim i}}\left[V_{x_i}(x_{\sim i})\right]}{V(y)} = 1 - \frac{V_{x_{\sim i}}\left[E_{x_i}(x_{\sim i})\right]}{V(y)} \tag{55}$$

It is often the best measure of sensitivity as it includes all individual and interaction effects.

5.4.3 Software Tools

There exist a fair number of open-source UQ and SA frameworks, see Figure 24.

This project has received funding from the European Union's Horizon 2020 research and innovation programme under grant agreement No 101006927.

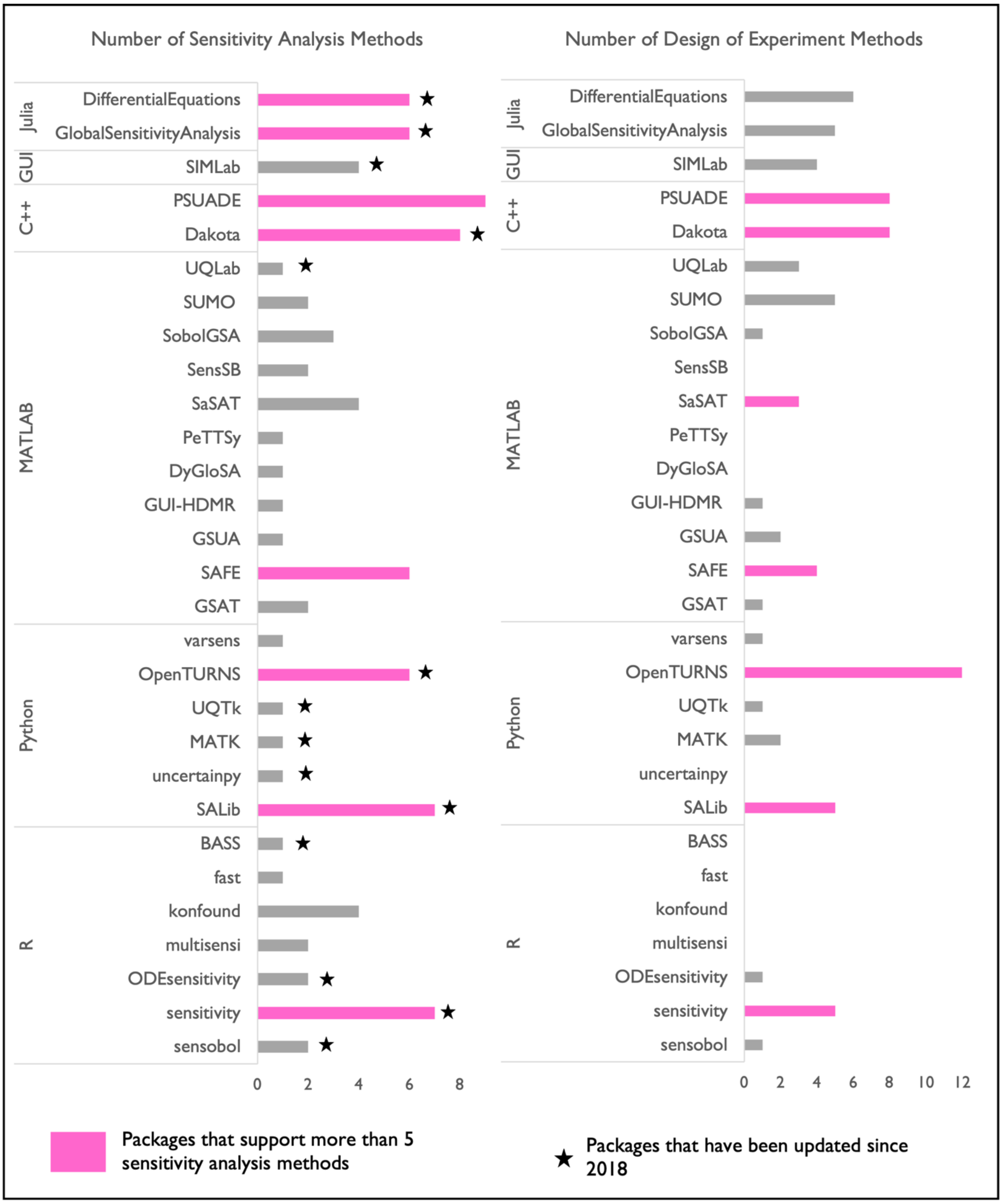

Figure 24: Sensitivity analysis packages available in different programming language platforms (R, Python, Julia, MATLAB, and C++), with the number of methods they support. Packages supporting more than five methods are indicated in pink. Packages updated since 2018 are indicated with asterisks (Reed, Patrick M. et al., 2023).

The most well-known are UQLab, Dakota and OpenTurns, which are complete frameworks covering DoE, sampling methods, surrogate models, reliability and sensitivity models.

UQLab (Marelli and Sudret, 2014) is a MATLAB-based UQ framework, with extensive documentation and tutorials, developed by ETH Zurich. UQLab is divided into 18 different

This project has received funding from the European Union's Horizon 2020
research and innovation programme under grant agreement No 101006927.

scientific modules, all with their individual documentation. UQLab supports PCE, Gaussian process (Kriging), combinations thereof, support vector machines, reliability analyses and sensitivity analyses, etc. As it is based on MATLAB the framework is rather easy to get started.

Dakota (Adams et al., 2021) is a UQ and optimization software written in C++ by Sandia. Initiated already in 1994, it is a mature tool for production. Dakota supports sampling-based approaches, local and global reliability methods, and stochastic expansion (polynomial chaos expansions, stochastic collocation, and functional tensor train) approaches. Due to its C++ API DAKOTA is easier to create direct interfaces between the UQ framework and numerical simulation models.

OpenTurns (Baudin et al., 2015) is a developed in python the French companies Airbus, EDF, IMACS, ONERA and Phimeca. OpenTurns includes tools for probabilistic modelling, uncertainty propagation through sampling, sensitivity analysis, surrogate models (Kriging, Karhunen-Loève, Polynomial Chaos) etc. OpenTurns has an extensive examples section and has a text-based code coupling facility.

This project has received funding from the European Union's Horizon 2020 research and innovation programme under grant agreement No 101006927.

6 Design and Reliability Assessment

Section 5 gives a general overview of design and reliability methods connected to UQ in hybrid testing. The aim is to provide a few fundamental applications of UQ in the test evaluation, decision making and reliability evaluation stages.

6.1 Test Evaluation

As introduced in Section 2, and detailed in Sections 3 and 4, measurement uncertainty should quantitatively be expressed as the standard deviation of the measurement. First, the basics of measurement uncertainty will be summarized, and then some basic applications will be discussed.

6.1.1 Expression of Measurement Uncertainty

The result of the measurement process should not be expressed by a single value, rather it should also be associated with its uncertainty. The measurement uncertainty of a measured quantity, y, is quantified in terms of its standard uncertainty, u_y, which is the standard deviation of measurement, y. Moreover, the measurement uncertainty is often expressed as an uncertainty interval, which is interpreted as the range of values where the true value of the measured quantity is expected to fall in with a chosen confidence. The interval is expressed as:

$$y \pm U \tag{56}$$

where y is the measured value, and U is the so-called "expanded uncertainty". Often a 95% confidence level is used, which results in an expanded uncertainty as $U = 2u_y$, using the quantile of the normal distribution. Other confidence levels may be chosen, and the expanded uncertainty is then adjusted correspondingly. This is handled by formulating the expanded uncertainty as $U = k \cdot u_y$, and using the normal distribution to calculate the coverage factor, k, according to the specified confidence level. Table 10 shows commonly used confidence levels and their corresponding coverage factors. For the full justification of Eq. (56) , the reader is referred to Sections 3 and 4 and the references therein.

Table 10: Confidence levels for expanded uncertainty and their corresponding coverage factors.

Confidence level	80%	90%	95%	98%	99%	99.8%	99.9%
Coverage factor, $\boldsymbol{k}$	1.28	1.64	1.96	2.33	2.58	3.09	3.29

6.1.2 Averaging Results

A standard method to reduce the measurement uncertainty is to repeat the measurements and then average the results. In such a scenario, repeated measurements (n) of the same property are performed, and the mean of the results is calculated:

$$\bar{y} = \sum_{k=1}^{n} y_i \tag{57}$$

Generally, the rationale for multiple tests is to obtain more certain estimates of the property in question, by reducing the random part of the measurement uncertainty from the testing.

This project has received funding from the European Union's Horizon 2020
research and innovation programme under grant agreement No 101006927.

First consider the case when all input variables are purely random, and thus no systematic errors are present in the measurement. Assuming statistically uncorrelated measurements gives the standard uncertainty for the mean as:

$$u_{\bar{y}} = \frac{u_y}{\sqrt{n}} \tag{58}$$

where it can be observed that the measurement uncertainty is inversely proportional to the square root of the number of measurements. Consequently, increasing the number of measurements by a factor four will reduce the standard uncertainty to half.

However, often a part of the measurement uncertainty consists of systematic errors that will not be reduced when averaging. In this situation it is important to distinguish between random and systematic effects in the standard uncertainty, which can be formulated as:

$$u_y^2 = u_{y,random}^2 + u_{y,systematic}^2 \tag{59}$$

where $u_{y,random}$ is the random part, and $u_{y,systematic}$ is the systematic part of the standard uncertainty u_y. Note that uncertainties should be summed in squares. The standard uncertainty for the average can then be calculated as:

$$u_{\bar{y}} = \sqrt{\frac{u_{y,random}^2}{n} + u_{y,systematic}^2} \tag{60}$$

It can be observed from Eq. (61) that the random contribution to the uncertainty in the average diminishes as the number of tests increases, while the systematic contribution remains unchanged.

6.1.3 Identifying Weak Spots in Testing

It is important to systematically work on the quality and improvement of the testing. MSA is such a tool, where a systematic assessment of measurement uncertainty will enable the identification of weak spots in the test set-up and in the execution of the testing. It allows the identification of the major sources of uncertainty and, thus, guides improvement work in order to systematically increase the accuracy of the measurements. This topic is discussed in detail in Section 3.

6.2 Decision Making

Testing is often performed in order to support the design process or to fulfil some requirement. Typical applications can be to make sure that the product requirements are fulfilled with a given confidence. Other cases include comparing two different products, or comparing two material choices for the same product.

6.2.1 Comparing to a Limit

The expanded uncertainty interval can be used when comparing the result to a limit, according to the two following cases:

1. If a measured value should be compared to an upper limit, then the tested product is accepted if the result plus the expanded uncertainty is below the limit, see Figure 25(a).
2. If a measured value should be compared to a lower limit, then the tested product is accepted if the result minus the expanded uncertainty is below the limit, see Figure 25(b).

This project has received funding from the European Union's Horizon 2020
research and innovation programme under grant agreement No 101006927.

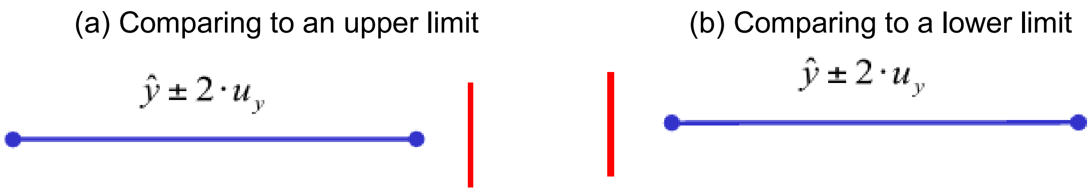

Figure 25: Comparing to a limit.

6.2.2 Comparing Two Products

If two measured values should be compared, then the uncertainty of the difference shall be evaluated. The confidence interval for the difference is calculated according to:

$$y_2 - y_1 \pm \sqrt{U_{y_1}^2 + U_{y_2}^2} \tag{61}$$

where U_{y_1} and U_{y_2} are the expanded uncertainties of the two measurements, representing the same confidence level. Thus, there is a significant difference only if the difference between the measured values is larger than the square root of the square sum of the individual expanded uncertainties.

6.3 Reliability Evaluation

Reliability can generally be defined as the ability of a product, system, or service to perform its intended function adequately for a specified period of time and under specified operating conditions; following (Hodges et al., 2021) and VALID D1.1 (Bargiacchi et al., 2021). Reliability may be quantified by a probability; however, in engineering design it is often more convenient to express the reliability requirements in terms of a reliability index, which can be related to safety distances or safety factors.

A reliability assessment takes both the load and strength into account. Thus, it includes uncertainties not only from the strength testing, but also uncertainties related to e.g. the environmental loads, the usage in operation, and the manufacturing and assembly process; see e.g. the five categories of uncertainties in Figure 6, Section 3.2. The load and strength may be illustrated as statistical distributions, see Figure 26.

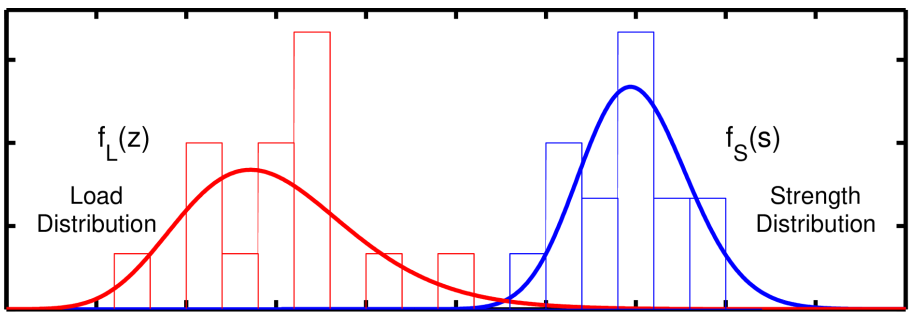

Figure 26: Illustration of interaction of load and strength.

The aim of this section is to illustrate some methods for reliability evaluation, rather than to give a detailed review of the topic. For the interested reader, there is a vast literature on reliability, e.g. (O'Connor and Kleyner, 2012), (Melchers and Beck, 2018) and (Ditlevsen and Madsen, 2007), and also relevant standards and design codes, e.g. Eurocode (CEN/TC 250, 2002) and (JCSS, 2001).

This project has received funding from the European Union's Horizon 2020 research and innovation programme under grant agreement No 101006927.

6.3.1 Characteristic Strength

The characteristic strength can be defined as that level of strength below which not more than a specified proportion of all test results is expected to fail. Often this proportion is chosen to be 5%, in e.g. the Eurocode standard, (CEN/TC 250, 2002). The mean or nominal strength is defined as the strength below which 50% of the test results are expected to fail.

The characteristic strength may be calculated as:

$$S_\alpha = S_{nom} - k_\alpha \cdot u_y \tag{62}$$

where S_{nom} is the nominal strength, k_α is the quantile corresponding to probability α and u_y is the standard uncertainty.

The strength is often modelled in its logarithmic form:

$$\ln S_\alpha = \ln S_{nom} - k_\alpha \cdot u_y \tag{63}$$

giving

$$S_\alpha = S_{nom} \cdot \exp\left(-k_\alpha \cdot u_y\right) = S_{nom} \cdot \gamma_\alpha \tag{64}$$

where γ_α is called a partial coefficient. Several additional partial factors may be included to account for different effects, in order to obtain the design strength. The design load is defined in a similar manner as the design strength, on the same scale. In the partial factor method the design strength is then compared to the (factored) design load, see e.g. Eurocode (CEN/TC 250, 2002) and DNV-GL ("DNVGL-RP-C203," 2014; "DNVGL-OS-C101," 2016) for more details.

6.3.2 Reliability Index and Safety Factors

The reliability target is often formulated such that the target function should exceed some limit with a proper safety margin. Here, it is assumed that the target function is formulated as (or can be re-formulated as) a so-called limit state function, with values below zero representing failure. Thus, the target function should exceed zero with a proper safety margin. The Cornell reliability index, (Cornell, 1969), is first presented, and then a method for deriving safety factors is demonstrated. It should also be noted that there are more advanced methods for reliability indices, e.g. the Hasofer-Lind reliability index (Hasofer and Lind, 1974), which is based on normal distribution of the input variables, and has the advantage of being invariant to the formulation of the target function.

The Cornell reliability index represents a first-order, second-moment method, and thus fits well together with the VMEA method which is based on second-moment statistics. The result from the probabilistic VMEA can easily be transformed into the Cornell reliability index. For the general formulation using the limit state function $f(\cdot)$, the reliability index β is given by:

$$\beta = \frac{\delta}{\tau} \tag{65}$$

with:

$$\delta = E[f(X_1, X_2, X_3, \ldots)] \quad \text{and} \quad \tau = \sqrt{\mathrm{Var}[f(X_1, X_2, X_3, \ldots)]} \tag{66}$$

where δ is the mean value of the target function and τ is its standard deviation. The reliability index is sometimes denoted as safety index or distance from failure mode, since it can be interpreted as the number of standard deviations from the failure mode, see e.g. (O'Connor, 2002; Davis, 2006). The reliability index is useful for defining design targets, but also for comparing different design alternatives and to evaluate the effect improvement measures.

It is often convenient to formulate the target function in terms of load and strength, more generally denoted demand and capacity. In engineering, they are often modelled in logarithmic scale. For the case of load and strength, the limit state function is then formulated as:

$$f(X_1, X_2, X_3, \dots) = \ln\big(S(X_1, X_2, X_3, \dots)\big) - \ln\big(L(X_1, X_2, X_3, \dots)\big) \tag{67}$$

where $\ln(S)$ and $\ln(L)$, are the load and strength variables, respectively. The reliability index is given by:

$$\beta = \frac{\delta}{\tau} \quad \text{with} \quad \delta = \ln(S_{nom}) - \ln(L_{nom}) \tag{68}$$

where the numerator δ is the nominal (or mean) difference between the logarithmic values of scalar metrics of strength $\ln(S_{nom})$ and load $\ln(L_{nom})$, respectively, and the denominator τ is a measure of the uncertainty corresponding to the statistical standard deviation.

The reliability index is often used for comparing the determined index value with a predefined requirement, say $\beta > \beta_{req}$, giving the requirement of the safety margin, i.e., the separation between nominal strength and load values:

$$\ln(S_{nom}) - \ln(L_{nom}) > \beta_{req} \cdot \tau = \delta_{req} \tag{69}$$

For structural reliability, the Joint Committee on Structural Safety, (JCSS, 2001), gives some guidance on determining the required safety index, β_{req}.

Furthermore, it is possible to derive a safety factor from the reliability index when the load and strength variables are defined in logarithmic scale. The relation between the reliability index and a safety factor is just a mathematical transformation, namely:

$$SF_\beta = \exp(\beta_{req} \cdot \tau) \tag{70}$$

Finally, if it is assumed that the difference $\ln(S_{nom}) - \ln(L_{nom})$ is normally distributed, the reliability index can be converted to a probability of failure:

$$P_F = \Phi(-\beta) \tag{71}$$

where $\Phi(\cdot)$ is the cumulative distribution function of the standard normal distribution. However, such relations are highly doubtful, since the assumption of normality is only speculative for such low probabilities of failure that are the result of high requirements on β. Therefore, it is suggested to use the probabilities as notional values for defining design requirements of for comparing different design solutions, rather than trusting the calculated probability value, see e.g. (Kiureghian and Ditlevsen, 2009).

Part B: Applications to VALID User Cases

In this part, the uncertainty analyses performed on the VALID User Cases are explained. A qualitative assessment was performed during a series of workshops where the insights of various stakeholders were gathered and categorized using the framework of Basic VMEA. Individual sources of uncertainty were identified and ranked according to their expected impact as estimated by technical specialists in each of the test rigs targeted in the User Cases. After this screening exercise, the uncertainties were quantified and aggregated using the framework of Probabilistic VMEA.

This project has received funding from the European Union's Horizon 2020
research and innovation programme under grant agreement No 101006927.

7 User Case #1: CorPower

The CorPower WEC is of point absorber type, with a heaving buoy on the surface, absorbing energy from ocean waves, which is connected to the seabed using a tensioned mooring line. A composite buoy, interacting with this wave motion, drives a PTO, a powertrain located inside the buoy, that converts the mechanical energy into electricity. By means of novel and patented technologies, the CorPower WEC moves in resonance with incoming waves, making it move in and out of the water surface, whereas in a conventional point absorber, the buoy follows the motion of the waves. The CorPower WEC uses a combination of pretension and the WaveSpring technology to better leverage the motion of the waves by pushing the buoy into perfect timing with each wave. Consequently, the buoy motion increases due to resonance, and along with it, so does the power output. The main components of the CorPower WEC are shown in Figure 27, where the critical sealing components are the wave springs, the pre-tension cylinder and the ocean rods.

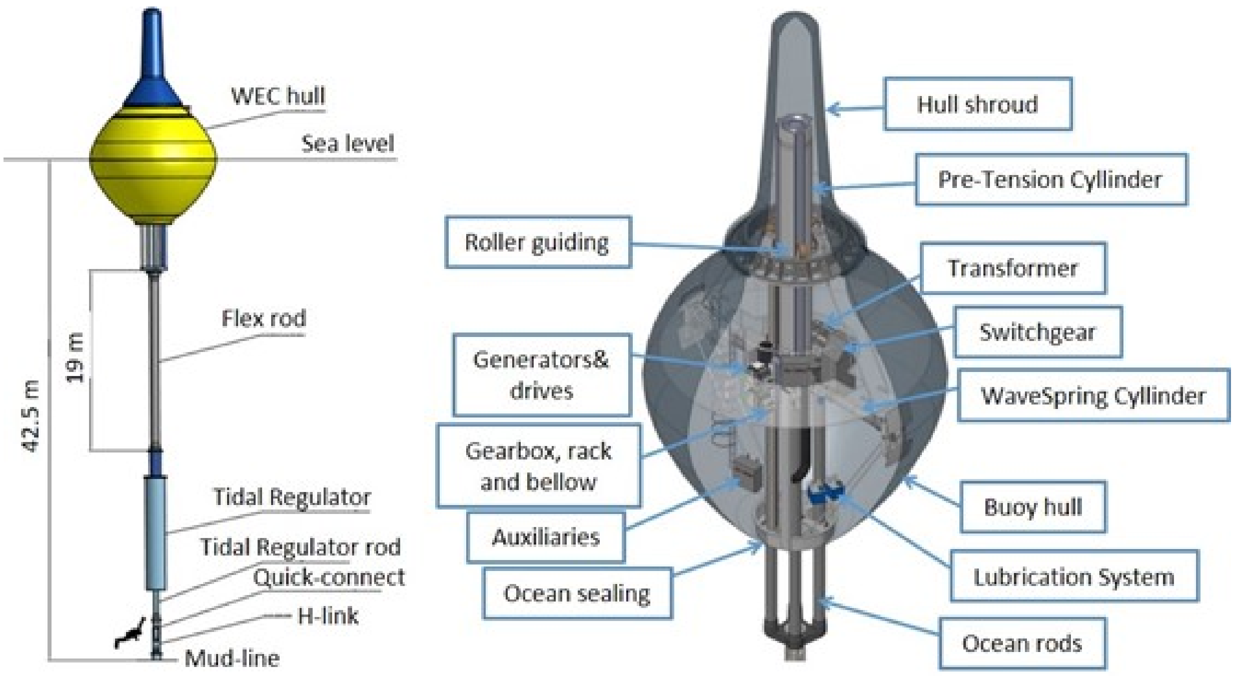

Figure 27: The CorPower WEC and subsystem overview.

7.1 Dynamic Seals

Seals between moving parts are called dynamic seals. Seals are used to separate two media, e.g., oil and water or air and seawater. Different kinds of seals are used depending on the kinds of media to be separated, as well as the operating conditions. Dynamic sealing systems can be exposed to severe conditions and subject to complex physical interactions between housings, sliding surfaces, sealing components, lubrication media and outside environment.

Figure 28 shows an annotated illustration of a typical piston chamber sealing system. Here you can see standard components such as the seals, O-rings, seal carrier, mating surface, and guide rings. The majority of CorPower's dynamic sealing systems consists of the seal itself, an O-ring to provide sufficient contact pressure of the seal against the mating surface, and the mating surface itself. Guide rings are occasionally used in situations where large side forces can arise. These are stiff components that are designed to guide the mating surface

This project has received funding from the European Union's Horizon 2020
research and innovation programme under grant agreement No 101006927.

within the seal gland, and avoid the seals having to react large transverse forces. Sealing systems often consist of several seals and/or guide rings in series.

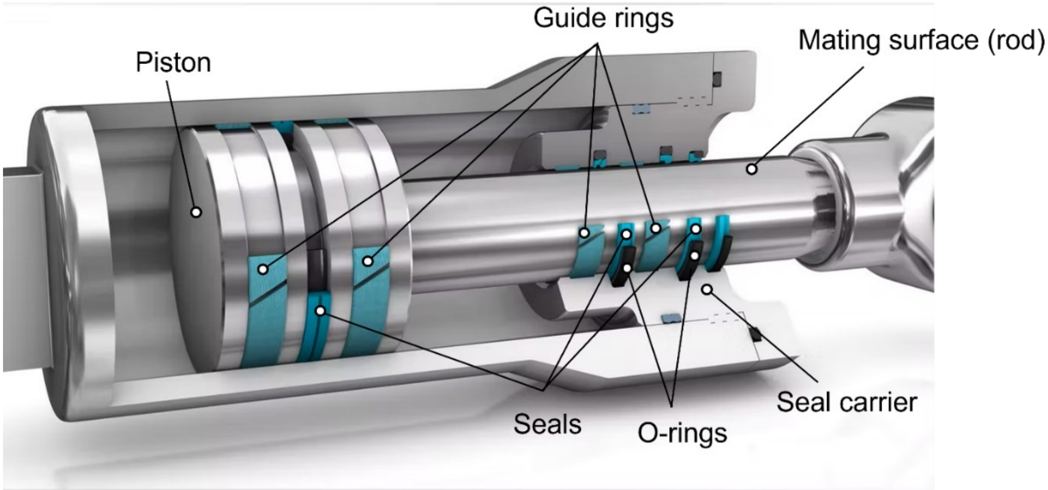

Figure 28: Illustration of a typical piston chamber sealing system.

7.2 Overview of the Test Rig

The key piece of equipment within the WP3 test campaign is the dynamic seal test rig. The seal rig is a customised piece of testing equipment specifically designed to test dynamic sealing systems, see Figure 29.

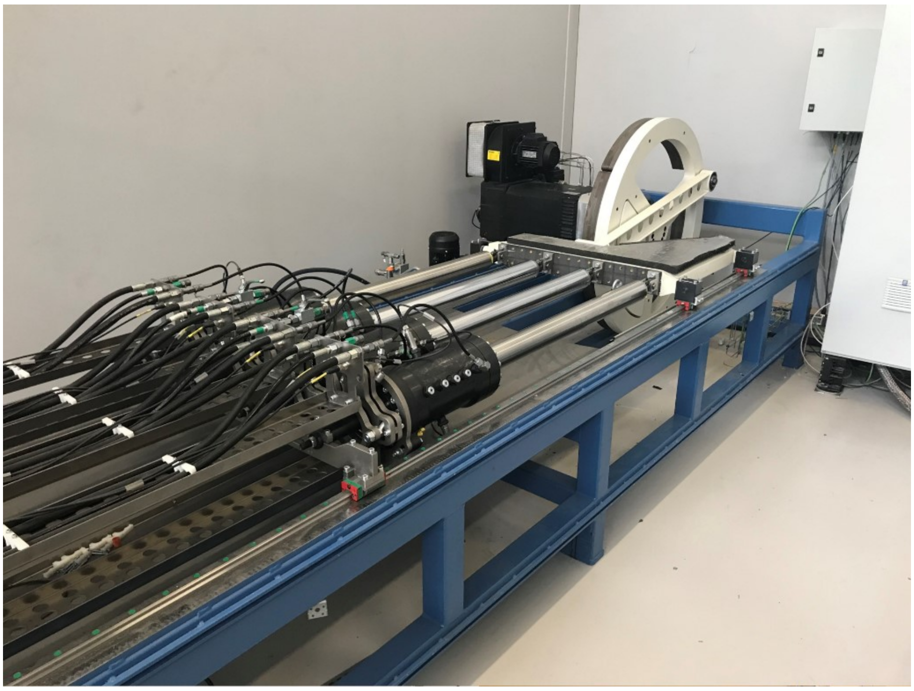

Figure 29: The CorPower dynamic seal test rig.

The aim of the component testing in WP3 is to fully characterise CorPower's sealing systems over a range of speeds and accelerations, with consideration for degradation mechanisms such as wear, fatigue at joints, corrosion, tribocorrosion, and biofouling. The results will be used to better quantify the reliability and survivability of the sealing systems, as well as to implement a component model of the seals within CorPower's Wave-2-Wire model. The seals test rig is used to evaluate friction, leakage and life. Parameters that can be controlled or measured are movement, forces, pressure, temperature and lubrication.

7.3 Basic VMEA

The information gathered during the first series of UQ workshops with CorPower using basic VMEA will be presented here, together with some reflections on their outcomes. The subsections reflect the main stages of the VMEA methodology.

7.3.1 Target Variable

The main goal here is to define the physical quantity measured in the test rig for which the measurement uncertainty is being quantified. There are two different types of dynamic sealing systems in the WEC, high pressure seals and ocean seals. This assessment will focus on the ocean seals that are exposed to sea water.

The material for the sealing system is:

- Seals: Polyethylene
- Rod: Metal

The design case considered is the Fatigue Limit State (FLS), i.e., we consider loads contributing to wear of seals. The load conditions for the ocean seals are:

- External loads: Ocean environment
- Component loads: Travelled distance of seal, speed, turning points, pressure, temperature, lubrication, etc.

The failure type considered is seal failure due to wear, where the consequence is leakage. Hence, the target variable is the life of seals due to the wear process.

Acceleration can be achieved by means of, for example, speed, pressure, temperature and lubrication quality. The test object has a diameter of d=80 mm, which corresponds to approximately 1:4 scale compared to full-scale WEC. The design life for sealing systems is typically 5 years, whereas the design life for the WEC system is 20 years.

More details on material, load cases, and acceleration, etc., are found in VALID D3.1, (Harnden et al., 2022).The bottom line is that the target variable is defined as "Life of ocean seals due to wear process".

7.3.2 Identification of Uncertainty Sources

The uncertainty sources identified during the workshops are summarized in Figure 30. The list of uncertainties originated from the discussion at the workshops but also from earlier analysis reported in other deliverables, e.g., FMECA, experience from other projects, and technical literature.

This project has received funding from the European Union's Horizon 2020 research and innovation programme under grant agreement No 101006927.

Figure 30: Identified uncertainty sources in basic VMEA for UC#1, CorPower.

In the screening exercise based on basic VMEA, we did not investigate in detail the uncertainties in the virtual part of the test rig. A more in-depth analysis of this aspect was reserved to a later stage, partly because the actual implementation of the virtual components of the test rig was not fully defined. The focus in the basic VMEA work was more on the design, manufacture and operation of the physical devices, as well as on the differences between the test and the marine environment.

7.3.3 Assessment of Uncertainties

In Table 11, the assessment of size and sensitivity, on a scale from 1 to 10, is presented for the various uncertainty sources identified during the workshops.

Table 11: Assessment of uncertainties in basic VMEA for UC#1, CorPower.

Input			Comments
Uncertainty components	Sensitivity c_i (1-10)	Uncertainty input σ_i (1-10)	The assessment of Sensitivity and Size are based on Workshop on 20th September 2022.
Environmental conditions			**Uncertainties due to assessment of Environmental conditions (Pre-processing stage)**
Waves climate (Hs, Tp)	6	3	Assessment of ocean wave climate
Wind (magnitude, direction)	4	3	Assessment of wind climate
Current (magnitude, direction)	4	4	Assessment of ocean current climate
Salinity	5	2	Assessment of salinity in environment
Level of oxygen	5	3	Assessment of oxygen level in environment
Sea water temperature	3	2	Assessment of oxygen level in environment
Bio fouling environment	6	5	Assessment of bio fouling environment
Corrosion environment	6	4	Assessment of suspended particles in environment
Total			
Physical test rig			**Uncertainties due to physical test rig environment (Processing stage)**
Total travelled distance (TTD)	6	2	Main local load variable
Motion (position, speed, acc)	6	2	Other effect (than TTD) due to position, speed and acceleration.
Pressure	6	2	Pressure measurements in test rig (vs. desired pressure)
Temperature	6	3	Temperature measurements in test rig
Force measurements	6	3	Force measurements in test rig
Side loads in test rig	3	2	Horizontal rod in test rig vs. Vertical rod in real environment. Effect?
Lubrication oil flow and quality	6	4	Need to be well controlled in lab environment
Diameter of seal and rod/piston	7	2	Need to be well controlled in lab environment
Rod roughness	7	4	Variation of rod roughness between test objects
Mounting error of seal	6	4	Need to be well controlled in lab environment
Total			
Numerical simulation - WEC model			**Uncertainty due to numerical modelling of External-to-Local loads (Processing stage)**
Errors in numerical simulation	6	7	Uncertainty due to numerical modelling of External-to-Local loads (mot
Total			
Life modelling			**Uncertainties due to models for life & wearout (Post-processing stage)**
Acceleration - TTD & Motion	5	3	Acceleration model error - TTD & Motion
Acceleration - Pressure	5	7	Acceleration model error - Pressure
Acceleration - Temperature	5	7	Acceleration model error - Temperature
Acceleration - Lubrication	5	7	Acceleration model error - Lubrication
Acceleration - Other effects	5	3	Acceleration model error - Other effects on seal wear models
Scaling - Rod diameter	5	7	Scaling model error - Rod diameter
Scaling - Stroke length	5	3	Scaling model error - Stroke length
Scaling - Other effects	5	2	Scaling model error - Other scaling effects
Marine growth effects	6	4	Model error - marine growth prediction
Corrosion effects	6	4	Model error - Corrosion prediction
Sea water exposure	5	4	Model error - Effect of sea water exposure other than marine growth an
Total			
Manufacturing of WEC			**Uncertainties due to Manufacturing (Post-processing stage)**
Surface finish of rod/piston	7	2	Manufacturing variation
Diameter of seals and piston	7	2	Manufacturing variation
Variation of material properties, rod	5	4	Manufacturing variation
Variation of material properties, seal	5	3	Manufacturing variation
Variation of seal housing	5	5	Manufacturing & assembly variation
Handling during mounting of seals	5	4	Assembly variation
Total			

7.3.4 Evaluation of Total Uncertainty

The total variation is calculated as the square sum of the resulting variation from the sources, resulting in the total VRPN. The relative contribution of the VRPN from the different uncertainty sources are of interest rather than the absolute value of the total VRPN. The Pareto chart in

This project has received funding from the European Union's Horizon 2020
research and innovation programme under grant agreement No 101006927.

Figure 31 shows the resulting ranking of the various uncertainty sources identified during the workshops, highlighting those which contribute most to the uncertainty of the target variable.

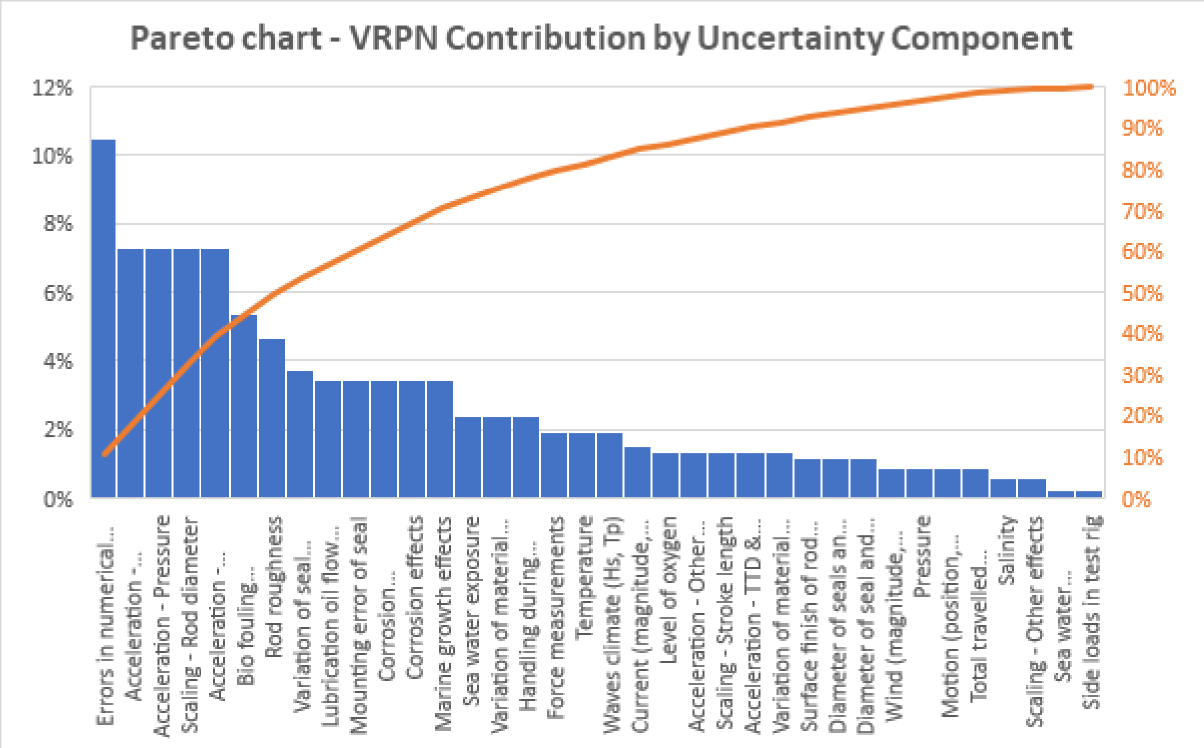

Figure 31: Pareto chart of uncertainties in basic VMEA for UC#1, CorPower.

7.3.5 Conclusions and Lessons Learned

The largest variation contributions are shown in Table 12, where the larges one is due to error in numerical simulation. However, note that all uncertainties due to numerical simulation are combined into a single source. This will be divided into several uncertainty sources in the detailed studies later.

Table 12: The largest uncertainties in basic VMEA for UC#1, CorPower.

Uncertainty components	Proportion
Errors in numerical simulation	10%
Acceleration - Pressure	7%
Acceleration - Temperature	7%
Acceleration - Lubrication	7%
Scaling - Rod diameter	7%
Bio fouling environment	5%
Rod roughness	5%

This project has received funding from the European Union's Horizon 2020 research and innovation programme under grant agreement No 101006927.

It can also be of interest to study the relative contribution of uncertainties between the five categories of uncertainties, see Figure 32. Here we can observe that "Life & wearout" group contributes to 50% of the total variation. The contributions mainly originate from lack of knowledge of wear models including material degradation in the different lubrication regimes, the impact of marine growth and acceleration effects. Hence, it points at the importance of studying the wear models, acceleration effects, and scaling models.

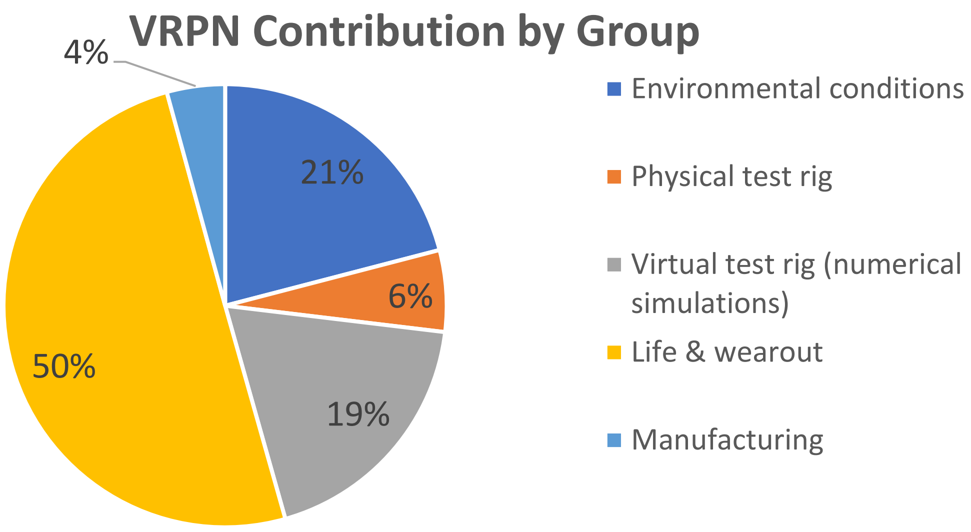

Figure 32: The variation contribution by group of uncertainties in basic VMEA for UC#1, CorPower

7.4 Probabilistic VMEA

The second series of workshops on the probabilistic VMEA was carried out about 9 months after the basic VMEA workshops. During that period of time, the upgrade of the CorPower test rig was completed, and some initial tests had been performed, allowing for more detailed information of the test rig and uncertainties. In the probabilistic VMEA each source of uncertainty is evaluated in physical units by means of its size and sensitivity with respect to the target variable uncertainty. The procedure for the probabilistic VMEA is the same as for the basic one. The information from the basic VMEA is used as a starting point and it is re-evaluated or refined when needed.

It was decided to limit the scope of the workshops to uncertainties directly connected to the hybrid testing, thus disregarding uncertainties related to environmental conditions and manufacturing (these can instead be evaluated later following the same process). The results from the second series of UQ workshops with CorPower using probabilistic VMEA are summarized below, together with some reflections on their outcomes. The subsections reflect the main stages of the VMEA methodology.

7.4.1 Target Variable

The target variable was confirmed to be the life of the dynamic ocean seals. The target variable was formulated in terms of the logarithmic life, namely , $Y = \ln N = f(X_1, X_2, \ldots)$, as suggested in section 3.4.1 and exemplified in section 3.4.6.

This project has received funding from the European Union's Horizon 2020
research and innovation programme under grant agreement No 101006927.

7.4.2 Uncertainty Sources

The list of uncertainty sources was reviewed and in that process some adjustments and refinements were made. The list of uncertainty sources is reflected in the resulting probabilistic VMEA table (see Table 15 below).

7.4.3 Assessment of Uncertainties

At this stage, limited information and data from the testing is available. Therefore, the probabilistic VMEA assessment is mainly based on engineering judgement together with information from literature. The uncertainties of input variables were assessed in logarithmic scale, which corresponds to percentage uncertainty. Thus, the sensitivity coefficients are evaluated with respect to the logarithmic variables, and the input uncertainties are assessed as relative uncertainties. The full detailed assessment will not be reported here, However, an overview and some examples of the assessment for selected uncertainty sources will be given. The resulting assessments are presented in Table 15 below.

Most of the uncertainties connected to the physical test rig were assessed based on informed guesses or measurement uncertainty specifications for the measurement equipment.

The numerical uncertainties originate from the numerical WEC simulation model. A more detailed assessment was performed compared to the basic VMEA, however, it was primarily based on engineering judgement. The errors in the four relevant output variables from wave-to-wire model were assessed in terms of maximum error according to Table 13. These maximum errors, $(\pm d)$, were then converted to a standard deviation assuming a uniform distribution, using:

$$u = \frac{d}{\sqrt{3}} \tag{72}$$

see Section 3.4.4.2 for details.

Table 13: Assessment of errors in the wave-to-wire model, UC#1 - CorPower.

Wave-2-Wire model	Judged error
Travelled distance	Max ±1% in life
Number of turning point	Max ±40% in life
Pressure	Max ±5% in pressure
Temperature	Max ±10 Kelvin temperature

The uncertainties connected to the life modelling includes acceleration, scaling, corrosion, and marine growth effects. The uncertainties associated to these effects were assessed based on engineering judgement where experience from previous testing and information from literature are incorporated. All these uncertainties were assessed in terms of maximum error with respect to life, as shown in Table 14, and transformed into a standard deviation using Eq. (72).

This project has received funding from the European Union's Horizon 2020
research and innovation programme under grant agreement No 101006927.

Table 14: Assessment of errors in life modelling for VMEA, UC#1 - CorPower.

Model parameter	Judged error
Acceleration model error - TTD (Total travelled distance)	Error in life at most ±10%
Acceleration model error - Number of turning points	Error in life at most ±25%
Acceleration model error - Pressure	Error in life at most ±5%
Acceleration model error - Temperature	Error in life at most ±10%
Scaling model error - Rod diameter	Error in life at most ±10%
Scaling model error - Stroke length	Error in life at most ±20%
Scaling model error - Reversal at same position	Error in life at most ±20%
Model error - Corrosion prediction	Error in life at most ±25%
Model error - marine growth prediction	Error in life at most ±40%

7.4.4 Evaluation of Total Uncertainty

The results of the probabilistic VMEA are summarized in the VMEA table presented in Table 15. The total uncertainty is calculated as the root sum of square of the resulting uncertainty from each source. We can observe that the total uncertainty is estimated to 60%, which represents the measurement uncertainty of the CorPower hybrid testing. The relative contribution, in terms of variance contribution, from the different uncertainty sources are presented in the last column in Table 15. The result is best illustrated by graphs, e.g., the Pareto chart in Figure 33 shows the resulting ranking of the various uncertainty sources identified during the workshops, highlighting those ones which contribute most to the uncertainty of the target variable.

This project has received funding from the European Union's Horizon 2020 research and innovation programme under grant agreement No 101006927.

Table 15: VMEA table for probabilistic VMEA, UC#1 - CorPower.

Input			Result	
Uncertainty components	Sensitivity c_i	Uncertainty input u_i	Uncertainty output $\tau_i = c_i \cdot u_i$	Variation contribution proportion
Physical test rig				
Total travelled distance (TTD)	1	0.1%	0.1%	0%
Pressure	1	5.8%	5.8%	1%
Temperature-measurement	15	0.1%	0.8%	0%
Temperature-deviance	15	1.8%	27.7%	21%
Force measurements	1	0.1%	0.1%	0%
Side loads in test rig	1	0.6%	0.6%	0%
Lubrication oil flow and quality	1	1.2%	1.2%	0%
Diameter of seal and rod/piston	1	1.2%	1.2%	0%
Rod roughness	1	1.2%	1.2%	0%
Mounting error of seal	1	2.9%	2.9%	0%
Scatter in life	1	14.4%	14.4%	6%
Total			**31.9%**	**28%**
Numerical simulation - WEC model				
Travelled distance (num.error)	1	0.6%	0.6%	0%
Number of turning points (num.error)	1	23.1%	23.1%	15%
Pressure (num.error)	1	2.9%	2.9%	0%
Temperature (num.error)	15	1.8%	27.7%	21%
Total			**36.2%**	**36%**
Life modelling				
Acceleration - TTD	1	5.8%	5.8%	1%
Acceleration - NO turning points	1	14.4%	14.4%	6%
Acceleration - Pressure	1	2.9%	2.9%	0%
Acceleration - Temperature	1	5.8%	5.8%	1%
Scaling - Rod diameter	1	5.8%	5.8%	1%
Scaling - Stroke length	1	11.5%	11.5%	4%
Scaling - Reversal position	1	11.5%	11.5%	4%
Corrosion effects	1	14.4%	14.4%	6%
Marine growth effects	1	23.1%	23.1%	15%
Total			**36.4%**	**36%**
Total uncertainty			**60.4%**	**100%**

This project has received funding from the European Union's Horizon 2020
research and innovation programme under grant agreement No 101006927.

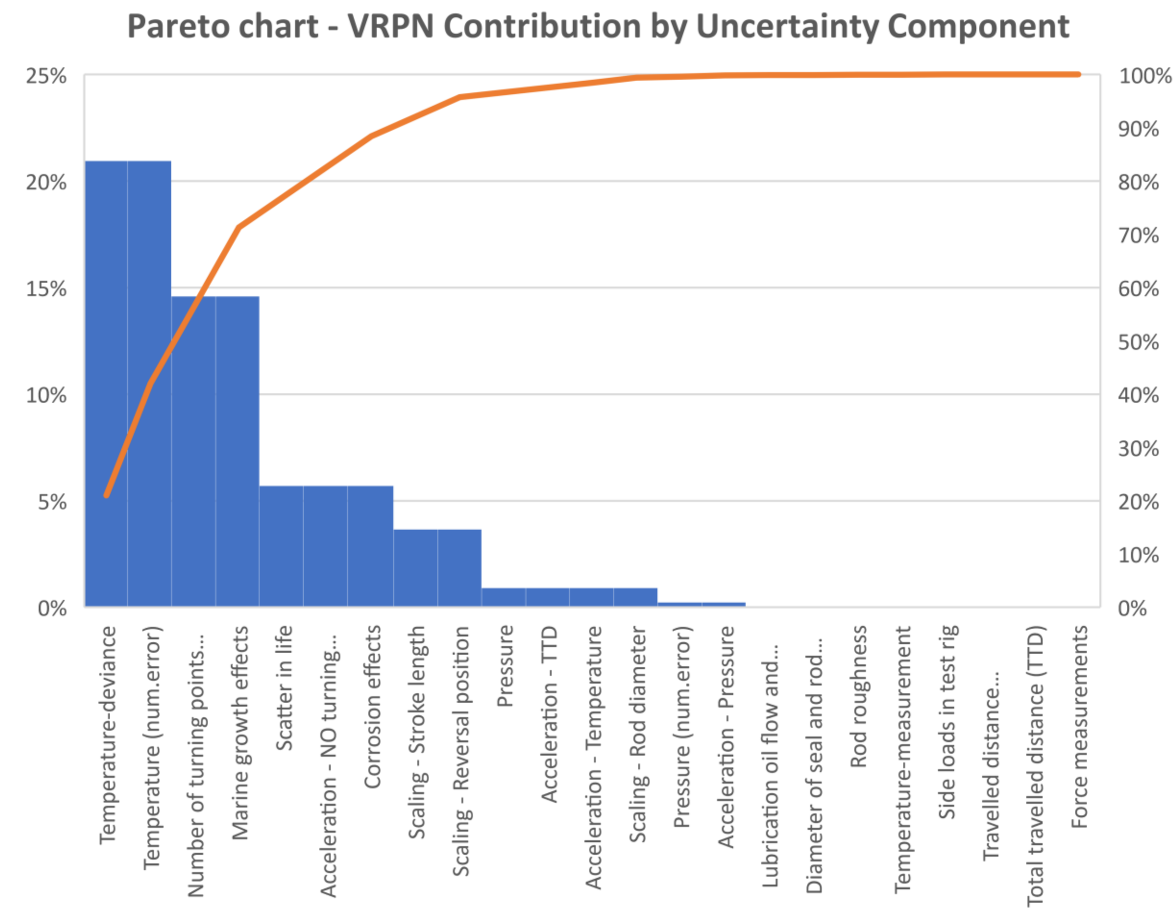

Figure 33: Pareto chart of uncertainties in probabilistic VMEA for UC#1, CorPower.

7.4.5 Conclusions and Lessons Learned

The probabilistic VMEA gives an estimate of the measurement uncertainty of the hybrid testing, but also gives input to the improvement work. The overall picture of the largest contributions to the total uncertainty is similar to the result from the basic VMEA. The largest variation contributions are shown in Figure 33. Note that the "Error in numerical simulation" in the basic VMEA has now been assessed in more detail and been split into four uncertainty sources. It should also be noted that the uncertainties connected to the temperature give the largest contributions. The reason behind this is the difficulty in both modeling and measuring the actual temperature of the seal, in combination with the large sensitivity to temperature.

There is potential for improving the uncertainty assessment. The result from the probabilistic VMEA serves as an initial estimate of the measurement uncertainty for the hybrid testing set-up. However, equally important, the VMEA workshops have also served as a platform for discussing the hybrid testing set-up, resulting in several new insights, which have helped the design and improvement work for the testing by highlighting the most significant sources of uncertainty.

8 User Case #2: IDOM

8.1 Overview of the Test Rig

User Case #2 is concerned with the wave energy converting technology developed by IDOM, which falls in the category of oscillating water column systems. In this case, the component identified as the most critical is the generator in the PTO system. As illustrated in the graphical wave-to-wire model of a generic WEC shown in Figure 34, the generator is part of the electrical PTO, which transforms mechanical power to electrical power. It interacts with the primary PTO (in this user case, an air turbine), with power electronics and the control system, in order to deliver electrical power to the grid.

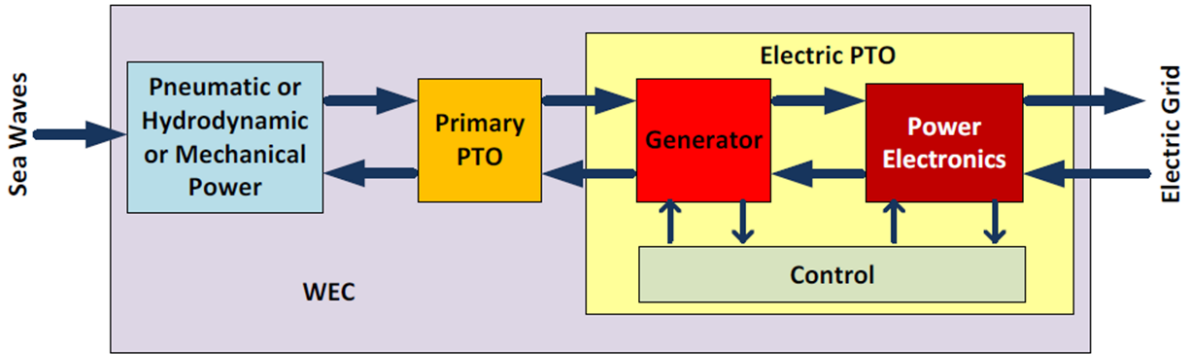

Figure 34: Wave-to-wire model of a generic WEC.

A set of physical design parameters characterises the generator. During the workshops carried out within T6.2 of the VALID project and documented in VALID D6.3, (Nava and Ruiz Minguela, 2023), IDOM has identified the following design parameters as the most influential for the most relevant evaluation areas:

- Cut-out sea state (Hs, Tp) [m, s]
- Rated power [kW]
- Efficiency curve at partial loads (P/P_{rated}) [-]
- Rated power [kW]
- Design life [year]
- Redundancy level (no. of generators) [-]
- Maximum to Nominal Voltage [-]
- Response time [s]
- Acceptable no of failed generators (k out of n)
- Replacement time [hour]
- Maintenance vessel cost [€/day]
- Maintenance strategy [-]
- Generator mass [kg]
- Unit cost of the generator[€/kW]

This project has received funding from the European Union's Horizon 2020 research and innovation programme under grant agreement No 101006927.

During the hybrid testing campaign, the following quantities will be directly measured, using the sensors described in VALID D4.2, (Lekube et al., 2023):

- Current [A]
- Rotational speed [rpm]
- Stator Resistance [Ohm]
- Temperature [ºC]
- Torque [Nm]
- Voltage [V]
- Frequency [Hz]

Some other quantities will be measured indirectly by postprocessing the direct measurements. The list of targeted indirect measurements includes, for example, the generator efficiency (which is evaluated by comparing the values of mechanical power at the shaft and electrical power output of the generator) and the motor current signature analysis (by analysing the electrical signals in the frequency domain).

8.2 Basic VMEA

As defined in Section 3.3, the basic VMEA aims to identify and roughly assess the main sources of uncertainty. Four sessions (April 27, May 13, June 14 and June 23, 2022) were held for carrying out the initial stages of the basic VMEA. After describing the methodology, the sessions were tailored in order to identity which are the most relevant uncertainties, their source (the virtual or physical environment) and potential strategies to be adopted for their reduction in the hybrid testing campaign for the electrical generator. Participants to the workshop were researchers from RISE as task leader and organiser of the event, TECNALIA as test rig manager, IDOM as User Case Leader, Y4C, AVL, BIMEP, and Delft University as contributors to the task. The outcome of the basic VMEA have been presented to VALID consortium during the VALID Technical Meeting on 29th September 2022.

The structure of the following subsections follows the main stages of the methodology.

8.2.1 Target Variable

The target variable is the thermal fatigue life of the generator, and particularly of the stator windings insulation, which is indeed the critical component investigated in UC#2.

The hybrid procedure developed in UC#2 is designed to test the performance of the electrical PTO under conditions that should realistically emulate significant sea scenarios for the insulation life in shorter time than it would take for a full-scale test in marine environment. Neither all the PTO components of the WEC nor environmental factors can be reproduced at laboratory scale. Figure 35 illustrates schematically the architecture of the test rig available at the premises of TECNALIA (the so-called "Electrical PTO lab"), clarifying which parts are physical devices representative of the actual components of the WEC (that is, generator, power electronics, and control system) and which ones are instead emulated by lab-scale equipment (that is, the electrical motor with dedicated inverter and control software which reproduce the mechanical loads produced by the air chamber and turbine in the actual WEC) or numerical models (that is, the sea states). Further details on the Electrical PTO lab and the test plan devised in UC#2 are reported in Deliverable 4.2.

With the configuration shown in Figure 35, the hybrid testing protocol developed in UC#2 can be categorized as a form of hardware-in-the Loop test methodology. As described in VALID

D4.2, (Lekube et al., 2023),the initial configuration of the test rig has been adapted and updated in order to accomplish the objectives of the hybrid testing campaign (see Figure 36).

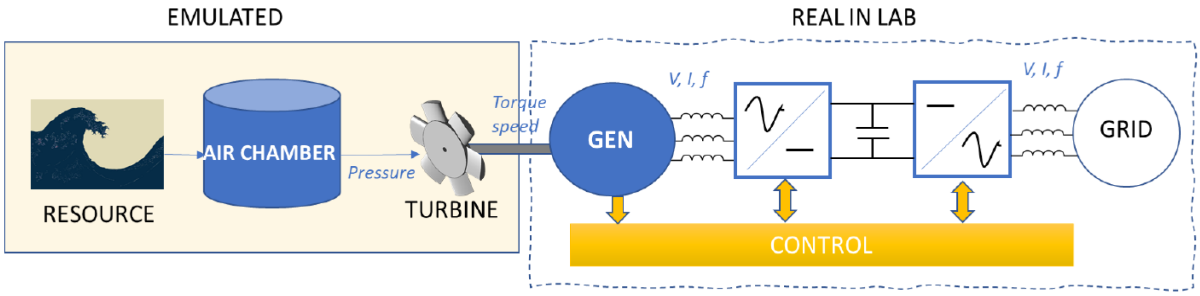

Figure 35: Schematic view of the emulated or virtual and "real" or physical components in the hybrid test rig Electrical PTO Lab at TECNALIA.

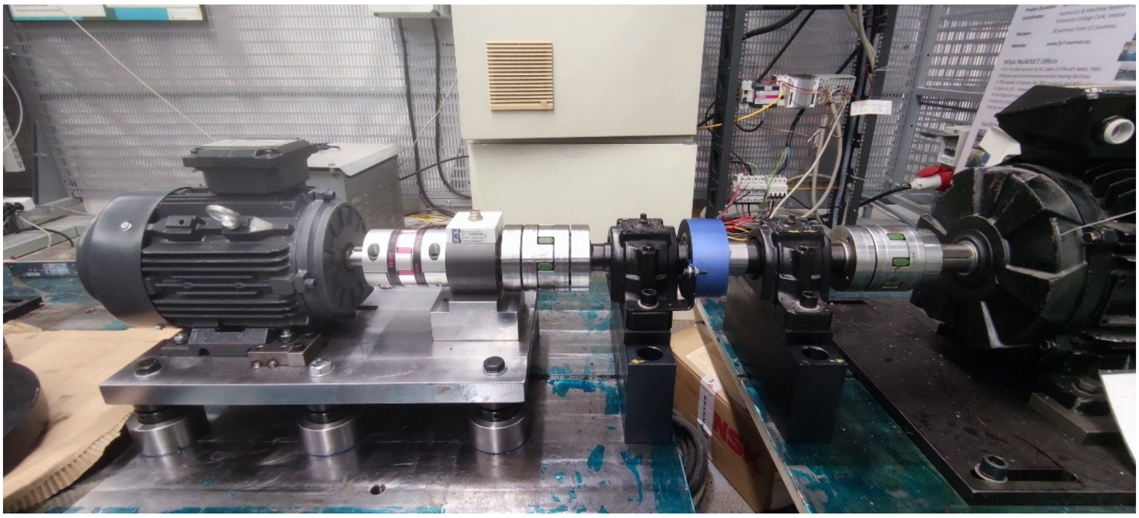

Figure 36: Final configuration of the test rig with the new generator installed.

As stated in VALID D4.2, (Lekube et al., 2023), the materials of the winding insulation are Nomex® Based Laminate Type NMN and Dupont Mylar Dacron. The generators purchased for this User Case have Class F insulation in accordance with IEC 60034-1, which translates into the following temperature limits:

- Maximum ambient temperature of 40°C
- Permissible temperature rise of 105°C
- Hotspot temperature margin of 10°C
- Maximum winding temperature of 155°C

In general, the target design life in such insulation class is up to 20,000 hours below the maximum rated temperature.

Since the objective of UC#2 is the assessment of the thermal fatigue life of the generator, the design load cases (which are defined in terms of both sea and machine states) included in the test plan should represent not only normal operational conditions (FLS), but also extreme conditions (ULS), which potentially could lead to unwanted peaks of temperature in the

This project has received funding from the European Union's Horizon 2020
research and innovation programme under grant agreement No 101006927.

generator. The test campaign devised in UC#2 aims at estimating the thermal fatigue life of the generator and at characterizing the accumulated damage at the end of its service life. The test procedure is articulated in several stages (for a preliminary full description, we refer to VALID D4.2, (Lekube et al., 2023)): after the calibration stage, during the characterisation phase, a series of voltage peaks of appropriate duration is going to be imposed to the generator, in order to represent the state of damage that is expected to be induced by the environmental conditions at BiMEP. Then, during the validation phase, the generator will be excited by mechanical loads of the same magnitude that the component would experience under in-service conditions (that is, sea states).

The main hypothesis is that the variation of temperature can lead to the failure of the critical component. For this reason, the test rig has been equipped with temperature sensors. Other factors, however, may affect the degradation of the stator windings, as humidity and salinity; however, the lack of an appropriate numerical model for these conditions and the impossibility of reproduce them appropriately in a dry test campaign introduce an element of uncertainty that is hard to quantify.

The test campaign will be conducted at reduced physical and power scale. Additionally, the thermal properties of generators of different nominal power have been characterised in order to transfer the lab results into full scale.

8.2.2 Identification of Uncertainty Sources

During the first two sessions of the workshop, the effort was devoted mostly in the identification and classification of the uncertainty sources. The results are summarised in Figure 37.

This project has received funding from the European Union's Horizon 2020 research and innovation programme under grant agreement No 101006927.

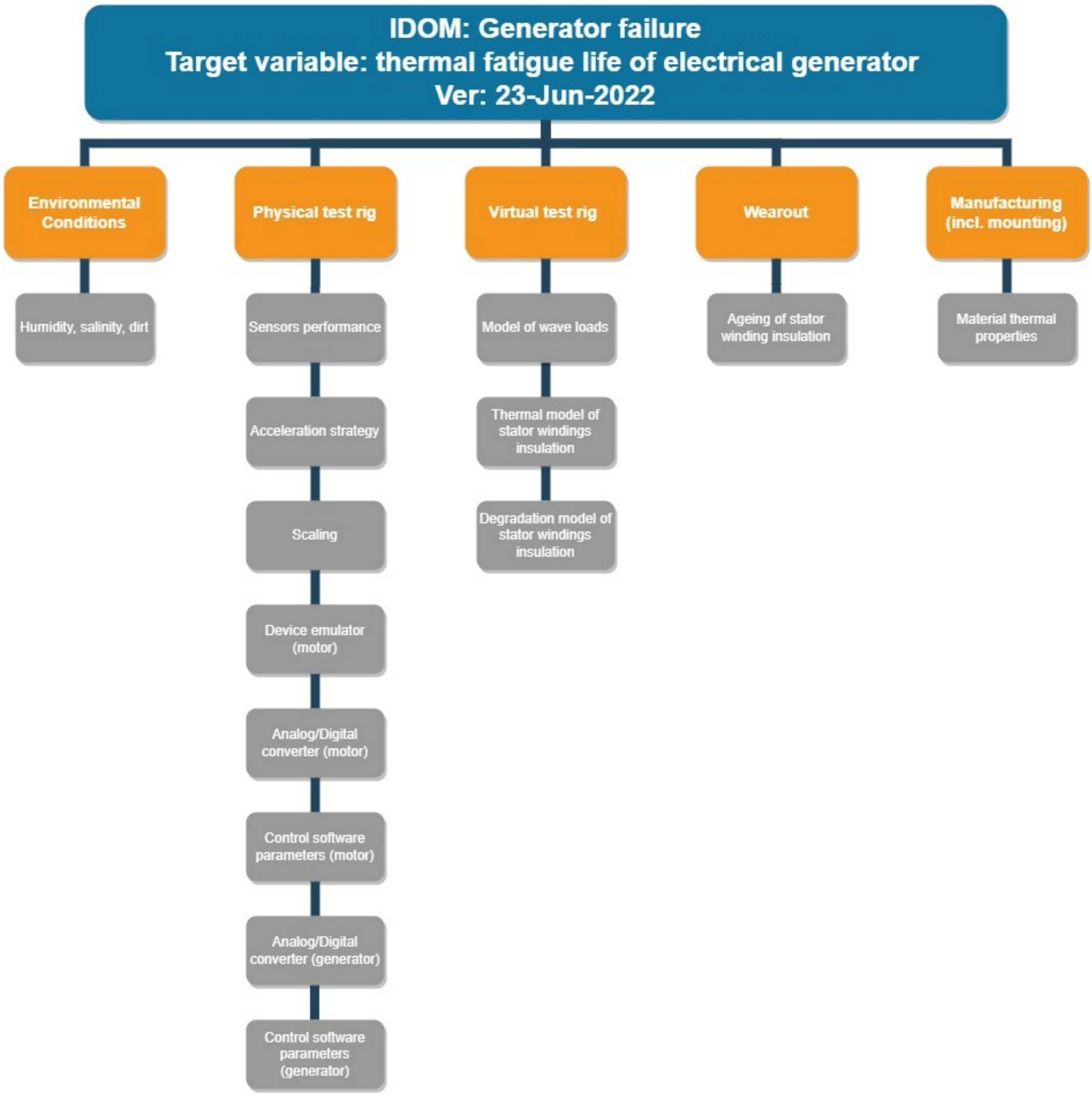

Figure 37: Classification of the uncertainty sources for UC#2.

The list of uncertainties originated from the discussion at the workshops but also from earlier analysis reported in other deliverables, e.g., FMECA, experience from other projects, and technical literature.

The uncertainties have been classified under five families:

- **Environmental conditions**: as mentioned in Section 8.2.1, it is difficult to reproduce in the experimental setup the specific harsh environment which the generator will be subject to. The presence of humidity and salinity as well other factors as dirt may affect the behaviour of the generator and it will not be modelled experimentally.
- **Virtual test rig**: the models behind the simulation of realistic sea states, as well as the thermal and degradation model of the stator windings are affected by some level of inaccuracy due to their approximation to the reality. This is somehow related to the complexity of the models adopted and the trade-off between computational burden, need of real time simulation and accuracy.

This project has received funding from the European Union's Horizon 2020
research and innovation programme under grant agreement No 101006927.

- **Physical test rig**: several uncertainties affect the physical asset of the hybrid testing platform. Sensor accuracy, scale effects, calibration of control software parameters, the acceleration strategies and the motor can introduce sources of uncertainty.
- **Wear-out**: the degradation due to ageing of the stator winding insulation is a potential source of uncertainty.
- **Manufacturing (including mounting)**: materials used for the insulation may introduce a source of uncertainty if the thermal characterisation is not accurate.

8.2.3 Assessment of Uncertainties

During the workshop, an analysis of the uncertainties has been carried out for UC#2.

Table 16: Basic VMEA table for UC#2 after the initial workshops.

Input	Sensitivity	Uncertainty input
Uncertainty components	c_i (1-10)	σ_i (1-10)
Environmental conditions		
Humidity, salinity, dirt	4	8
Physical test rig		
Sensors performance	7	3
Acceleration strategy	5	5
Scaling	5	1
Device emulator (motor)	5	1
Analog/Digital converter (motor)	5	1
Control software parameters (motor)	5	1
Analog/Digital converter (generator)	5	1
Control software parameters (generator)	5	1
Virtual test rig		
Model of wave loads	6	3
Thermal model of stator windings insulation	6	7
Degradation model of stator windings insulation	6	7
Wear-out		
Ageing of stator windings insulation	0	0
Manufacturing		
Material thermal properties	7	7

Each of the uncertainty sources were evaluated, following the procedure described in Section 3, in terms of sensitivity (i.e. a quantification of the propagation of uncertainty from inputs to outputs) as well as in terms of uncertainty input (i.e. a measure on the dimension of the uncertainty) both in a range from 1 to 10.

The uncertainty sources were grouped into five categories:

a. **Environmental conditions**: this category includes all the sources of uncertainty that are difficult to reproduce in a controlled environment or to accurately model numerically. Essentially, they refer to humidity, salinity, and dirt, which are present in the marine environment, but not in the test rig. Environmental factors represent chemical agents that accelerate the degradation of the stator winding insulation, a known effect which is hardly quantifiable In the hybrid testing platform of UC#2, environmental factors are characterised by significant uncertainty, but secondary impact on the life of the generator.

b. **Physical test rig**: there are several uncertainty sources in the physical part of the hybrid platform, namely the sensors performance, the acceleration strategy, the scaling, the device emulator (motor), the analog/digital converter (motor), the control software parameters (motor), the analog/digital converter (generator) and the control software parameters (generator). Most of the categories are characterised by a medium value of sensitivity and low uncertainty, due to fact that the peaks of tension to be generated are fast but they can be emulated in a well-controlled manner. The sensor performance, however, is characterised by a higher sensitivity and a medium-to-low uncertainty, while the acceleration strategy is affected by a medium value of uncertainty.

c. **Virtual test rig**: this category includes the epistemic uncertainty related to the model of wave loads, the thermal model of stator windings insulation as well as the degradation model of stator windings insulation. For all of them, it is given a high sensitivity (equal to 6); however, the wave load modelling has a reduced uncertainty, while the thermal and degradation models are seen as more uncertain (up to 7).

d. **Wear-out**: the ageing of stator windings insulation is considered not to induce any uncertainty, due to fact that a new generator is used for the hybrid testing.

e. **Manufacturing**: in this category, all the issues pertinent to the thermal properties of the materials are included. They are considered to be highly important to account for, so a high sensitivity and uncertainty are assigned.

8.2.4 Evaluation of Total Uncertainty

The assessment results and their representation in terms of VRPN are reported in Figure 38 and Table 17. In Figure 39, the VRPN contribution per group is reported.

This project has received funding from the European Union's Horizon 2020
research and innovation programme under grant agreement No 101006927.

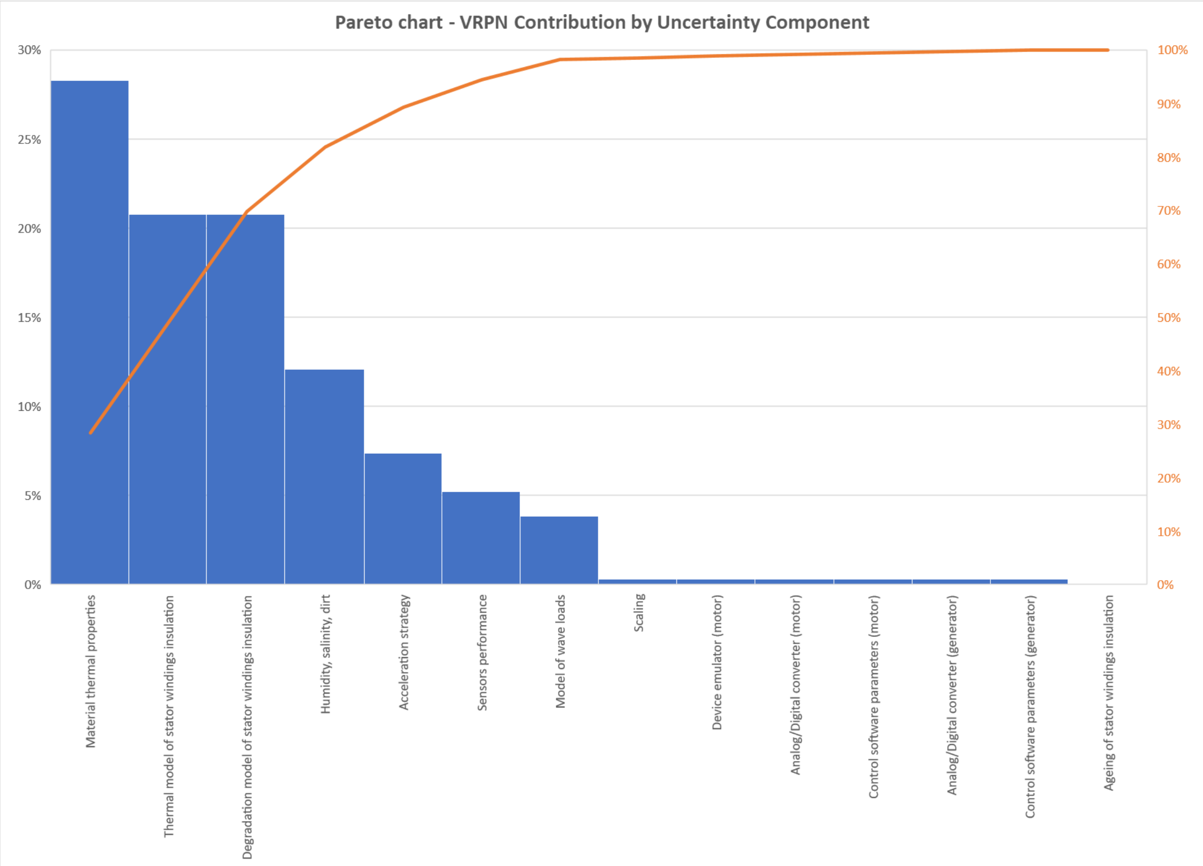

Figure 38: VRPN of the source of uncertainties in UC#2.

Table 17: VRPN of the source of uncertainties in UC#2.

Uncertainty components	Proportion
Material thermal properties	28%
Thermal model of stator windings insulation	21%
Degradation model of stator windings insulation	21%
Humidity, salinity, dirt	12%
Acceleration strategy	7%
Sensors' performance	5%
Model of wave loads	4%

This project has received funding from the European Union's Horizon 2020 research and innovation programme under grant agreement No 101006927.

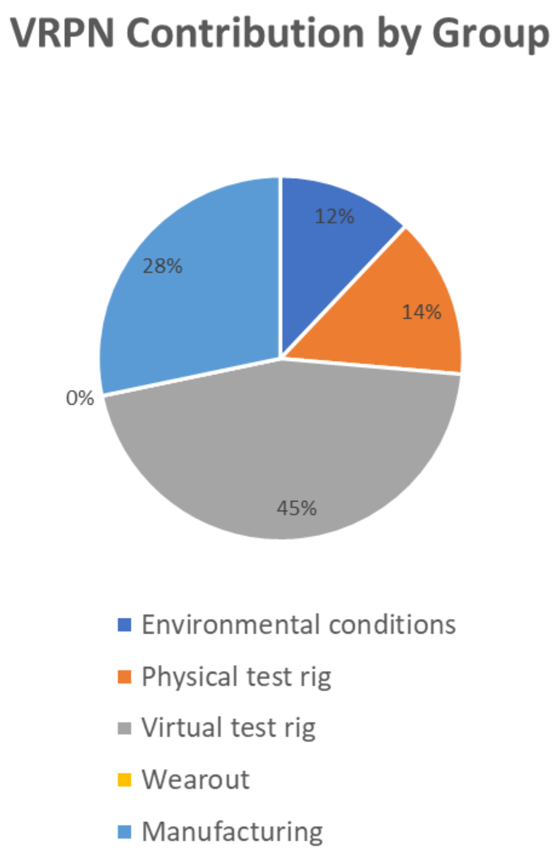

Figure 39: VRPN of the uncertainty sources per group for UC#2.

8.2.5 Conclusions and Lessons Learned

The uncertainties are not well balanced among sources. Only seven sources of uncertainty contribute to the 100% of the total risk. In particular, the uncertainties due to the characterisation of the physical test rig is about 14% of the total risk. Similarly, the characterisation of the environmental condition represents about 12% of the total risk. It seems that the virtual test rig and the manufacturing can lead to higher uncertainties, because they are highly affected by the thermal properties of the materials (manufacturing) and by the degradation model. However, some of the uncertainties identified during the workshops still should be investigated, and require further analysis, especially in their quantification (e.g., the ageing of the insulation materials)

8.3 Probabilistic VMEA

The outcomes of the basic VMEA workshops were further elaborated in a follow-up series of workshops that addressed the quantification of the identified uncertainties using probabilistic VMEA. Four online sessions were arranged on these dates: 13th March, 24th March, 3 April, 20 April. Participants to the workshop were researchers from RISE as task leader and organiser of the event, TECNALIA as test rig manager, IDOM as user case leader, Y4C, AVL, BIMEP, and Delft University as contributors to the task. After describing the methodology, the sessions were tailored to illustrate possible approaches to the quantification of relevant variables for the user case, considering that several elements of the test procedure were still under development.

The structure of the following subsections follows the main stages of the methodology.

This project has received funding from the European Union's Horizon 2020 research and innovation programme under grant agreement No 101006927.

8.3.1 Target Variable

As in the basic VMEA, the target variable was the life of the winding insulation, under the assumption that thermal stress was the dominant degradation factor. The difference with respect to the basic VMEA is that a specific life model was selected here, in order to illustrate the quantification procedure.

The life model considered in the probabilistic VMEA workshops was based on the analytical approach described in (Tshiloz et al., 2016) and it is mathematically described by the following expression:

$$\ln(L) = C_1 + \frac{C_2(T)}{T} \equiv Y, \quad (73)$$

where L is the life of the generator, T is the windings temperature and, at any given T, C_1, $C_2(T)$ are phenomenological parameters to be determined experimentally.

While the details of the derivation of Eq. (73) are not reported here (they can be straightforwardly reconstructed from (Tshiloz et al., 2016)), it is worth mentioning the two main physical assumptions on which the model relies upon: 1) thermal stress is the dominant degradation mechanism for the windings insulation; 2) the rate of degradation $k$depends exponentially on temperature according to the Arrhenius' model: $k = A\exp(-E_a/T)$, where A, E_a are phenomenological costants and T the absolute temperature.

The two parameters C_1, $C_2(T)$ in equation (73) are determined by imposing the empirically observed constraint denoted as "10 degrees rule", which states that every 10 degrees increase in temperature halves the life of the generator.

Every generator is designed to perform its intended function at a given temperature for minimum life span, depending on the class of the insulation material. For example, a generator in class F should work at least 20 000 hours at 155 °C. The expected life at given operating temperature is the criterion adopted to characterize the generator thermal "strength" (or endurance) in most of the industrial classification schemes, for example NEMA-G1 (see Figure 40). The degradation process never stops, but it is significantly accelerated if the winding temperature rises above the operating temperature of the thermal class that characterises the generator.

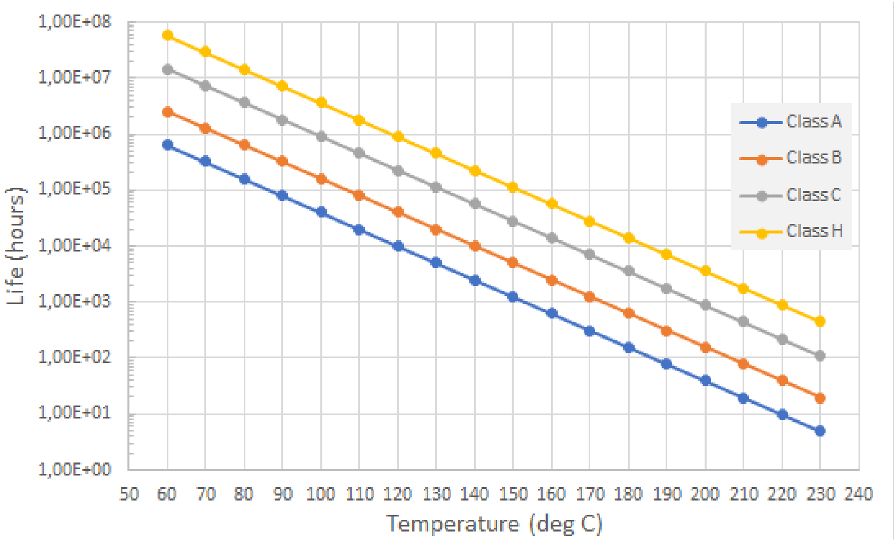

Figure 40: Thermal endurance curves (life vs temperature) for classification of generators in the NEMA-G1 scheme.

This project has received funding from the European Union's Horizon 2020 research and innovation programme under grant agreement No 101006927.

8.3.2 Uncertainty Sources

The sources of uncertainty considered in the analysis were the three input variables of the life model: T, C_1, and $C_2(T)$.

8.3.3 Assessment of Uncertainties

The coefficients C_1, C_2 can be estimated from experimental data according to standardized procedures, such as those described in the standard EN 60034-18-21.

In case to run dedicated characterization tests on the generator is not an option, one can still estimate C_1, C_2 and the associated uncertainty starting from the nominal values derived from the generator thermal classification (which should be known anyway from the manufacturer).

For each class (e.g., A, B, F, H in NEMA-G1), nominal values for $C_1, C_2(T)$ can be derived. They might not well represent the actual state of the generator, especially if it has been in service already some time. Detailed information on the past history of the device might not be available. Actually only C_1 discriminates between the different classes, C_2 being the same (but dependent on temperature).

Using a wrong C_1 might entail to overestimate the resistance of the generator against thermal stress. For example, a class H generator might actually be closer to class F or B, which means significantly smaller thermal endurance than expected (hence, shorter expected life at given temperature). Table 18 shows the relative differences in C_1 among the various NEMA-G1 classes.

Table 18: The relative differences in parameter C_1 among the various NEMA-G1 classes.

C_1	A	B	F	H
A	0%	8%	19%	27%
B	8%	0%	10%	17%
F	16%	9%	0%	7%
H	21%	15%	6%	0%

In contrast to the coefficients C_1, C_2, in the approach pursued in UC#2, the temperature is estimated numerically, using the analytical model presented in VALID D4.2, (Lekube et al., 2023), which is reported below for reference with a slight change of notation ($\theta \rightarrow T$):

$$T(t) = T_{SS}\left(1 - e^{-\frac{t}{\tau}}\right) + T_1 e^{-\frac{t}{\tau}}, \tag{74}$$

where T_{SS} is the steady state temperature, T_1 the initial temperature, and τ the characteristic response time of the winding temperature to thermal loads.

The sensitivity coefficients can be evaluated analytically at any given temperature T^*:

$$\left(\frac{\partial Y}{\partial C_1}\right)_* = 1, \left(\frac{\partial Y}{\partial C_2}\right)_* = \frac{1}{T^*}, \left(\frac{\partial Y}{\partial T}\right)_* = -\frac{C_2^*}{T^{*2}}. \tag{75}$$

This project has received funding from the European Union's Horizon 2020
research and innovation programme under grant agreement No 101006927.

8.3.4 Evaluation of Total Uncertainty

For illustration purpose, suppose we have a generator of class F and that the thermal model returns a temperature in the insulation of T^* =200 °C. Nominal values of C_1, C_2 for class F at that temperature are $C_1^* = 19.96$, $C_2^* = -2633.96$ °C.

These values were corroborated by characterization tests which supported the belief that the generator can be actually considered as class F, in spite of having been already several years in service. The uncertainty in the estimated values for C_1, C_2 was quantified in 1%, based on the quality and quantity of available data and fitting procedure. Alternatively, the expected values of C_1, C_2 could have been corroborated – or not – by engineering judgment based on past experience with similar machines, perhaps allowing for a somewhat larger margin of error. The temperature value was estimated to be correct within a ±2 °C interval.

The expected life of the generator is $L^* = \exp\left(C_1^* + \frac{C_2^*(T^*)}{T^*}\right)$ = 884 hours.

Plugging these input data into the probabilistic VMEA formula for the uncertainty on the target variable, we get:

$$u_Y = \sqrt{(1)_*^2 u_{C_1}^2 + \left(\frac{1}{T^*}\right)_*^2 u_{C_2}^2 + \left(-\frac{C_2^*}{T^{*2}}\right)_*^2 u_T^2} = 0.27. \quad (76)$$

The variance of the target function can be decomposed in its components to evaluate the contributions of each input variable:

$$u_{lnL}^2 = \tau_{C_1}^2 + \tau_{C_2}^2 + \tau_T^2 \quad (77)$$

where $\tau_X \equiv (\partial Y/\partial X)_* u_X$, see also Figure 41.

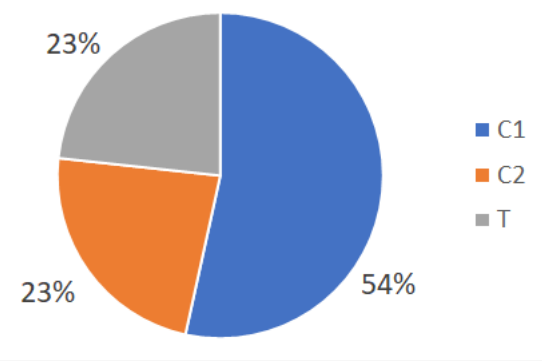

Figure 41: Decomposition of the total variance of $ln\ (life)$ into contributions from the three uncertain variables in the thermal model used to estimate the winding temperature.

It can be readily shown that the absolute uncertainty in the logarithmic life equals the fractional uncertainty (that is, percentage) in life, that is:

$$u_{lnL} \cong \frac{u_L}{L^*} \to u_L \cong L^* u_{lnt} = 241 \text{ hours} \quad (78)$$

The result of the test can therefore be expressed as:

$$L = L^* \pm u_L = 884 \pm 241 \text{ hours}. \quad (79)$$

This project has received funding from the European Union's Horizon 2020
research and innovation programme under grant agreement No 101006927.

8.3.5 Conclusions and Lessons Learned

The method highlights the importance of the modular approach to uncertainty analysis. It is recommended to start from the target variable and go backwards to map the interdependencies among all variables considered in the test procedure, each evaluated via numerical modelling or experiment. Moreover, the representation of the test method in terms of functional blocks is useful to understand how the uncertainty propagates from basic variables that are directly measured or computed to the overall target variable, that is component life, see Figure 42.

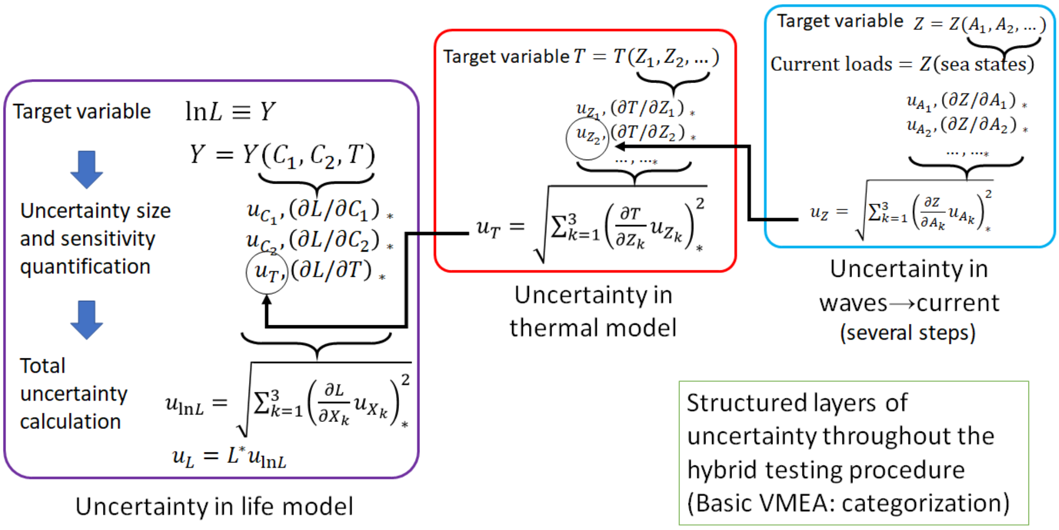

Figure 42: The representation of the test method in terms of functional blocks, UC#2.

This project has received funding from the European Union's Horizon 2020
research and innovation programme under grant agreement No 101006927.

9 User Case #3: Wavepiston

9.1 Overview of the Test Rig

Wavepiston is a multi-body floating oscillating wave surge converter constructed by surging plates connected through beams. Each plate is attached to a wagon, that is connected to two telescopic hydraulic pumps. A unit of plate, wagon, support beam and pumps is called energy collector and is illustrated in Figure 43. The hydraulic pump pushes seawater through a transport pipe to a turbine. The wear of the hydraulic seals has been identified as a critical factor for the Wavepiston WEC.

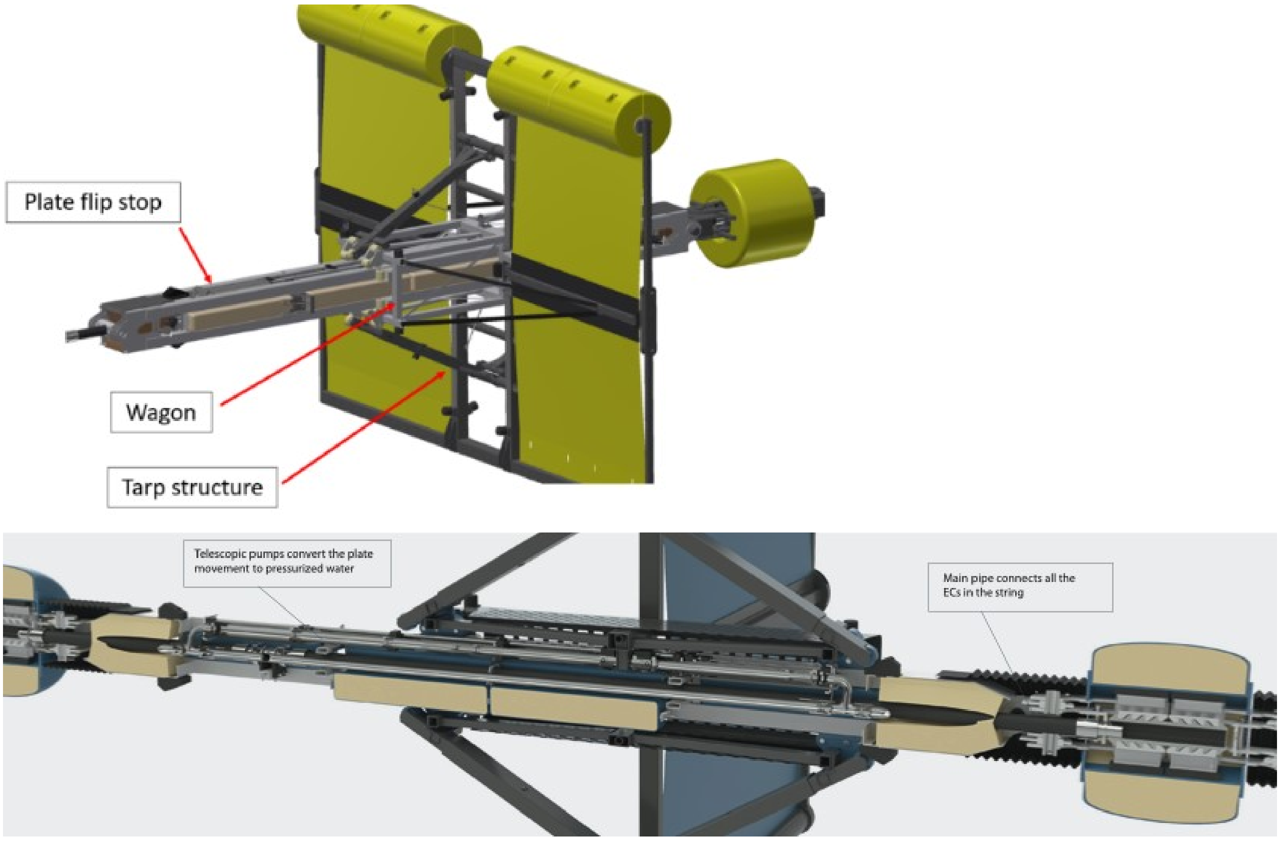

Figure 43: Overview of one Wavepiston energy collector and the seawater hydraulic pump.

The hydraulic pump seal test rig is used to assess the wear on the seals and the wear on the rods of the hydraulic rams of the Wavepiston system. It mimics the translation in one degree of freedom motion of the primary PTO, which in turn is caused by the wave motion. An overview of the Wavepiston test rig is shown in Figure 44. The pump displacement actuation is controlled as hardware-in-the-loop by a 'wave-to-wire' simulation software that is modelling the wave and sea state and incorporating a hydrodynamic model to calculate the interaction between the waves and the energy collector.

This project has received funding from the European Union's Horizon 2020 research and innovation programme under grant agreement No 101006927.

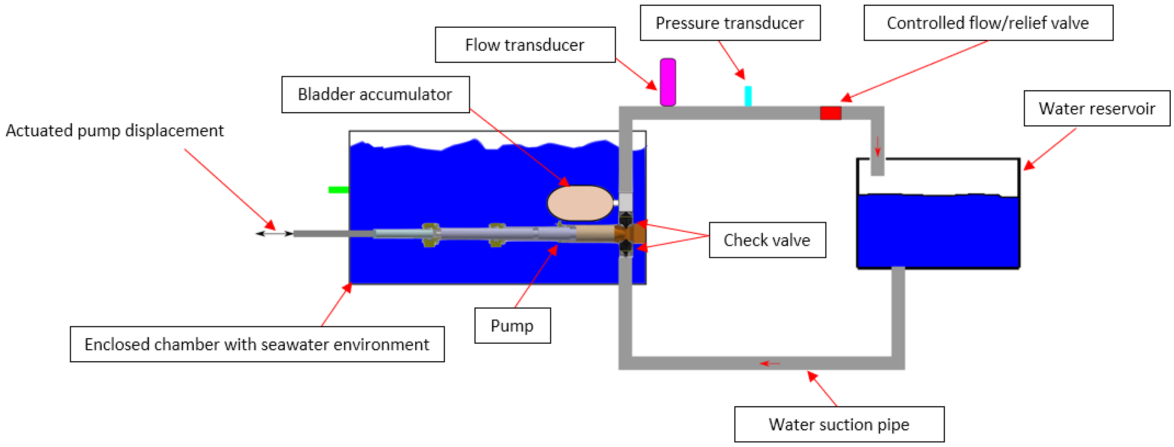

Figure 44: Wavepiston test rig.

9.2 Basic VMEA

Three workshops were held in the spring of 2022 to perform basic VMEA analysis of the Wavepiston hybrid test method.

9.2.1 Target Variable

The target variable is the hydraulic seal life, as the wear of the seal is considered a critical factor for the WEC. The design life for the pump unit and seals is 7 years. External loads that have impact on this target variable are wave sea states, salinity, oxygen levels, temperature, marine growth and suspended particles. Internally, the displacement of the piston is important and in particular the motion reversion.

9.2.2 Identification of Uncertainty Sources

The identified sources of uncertainty are illustrated in Figure 45. They were divided into five different categories: environmental loads, physical test rig, numerical simulation, life & wearout and manufacturing.

This project has received funding from the European Union's Horizon 2020
research and innovation programme under grant agreement No 101006927.

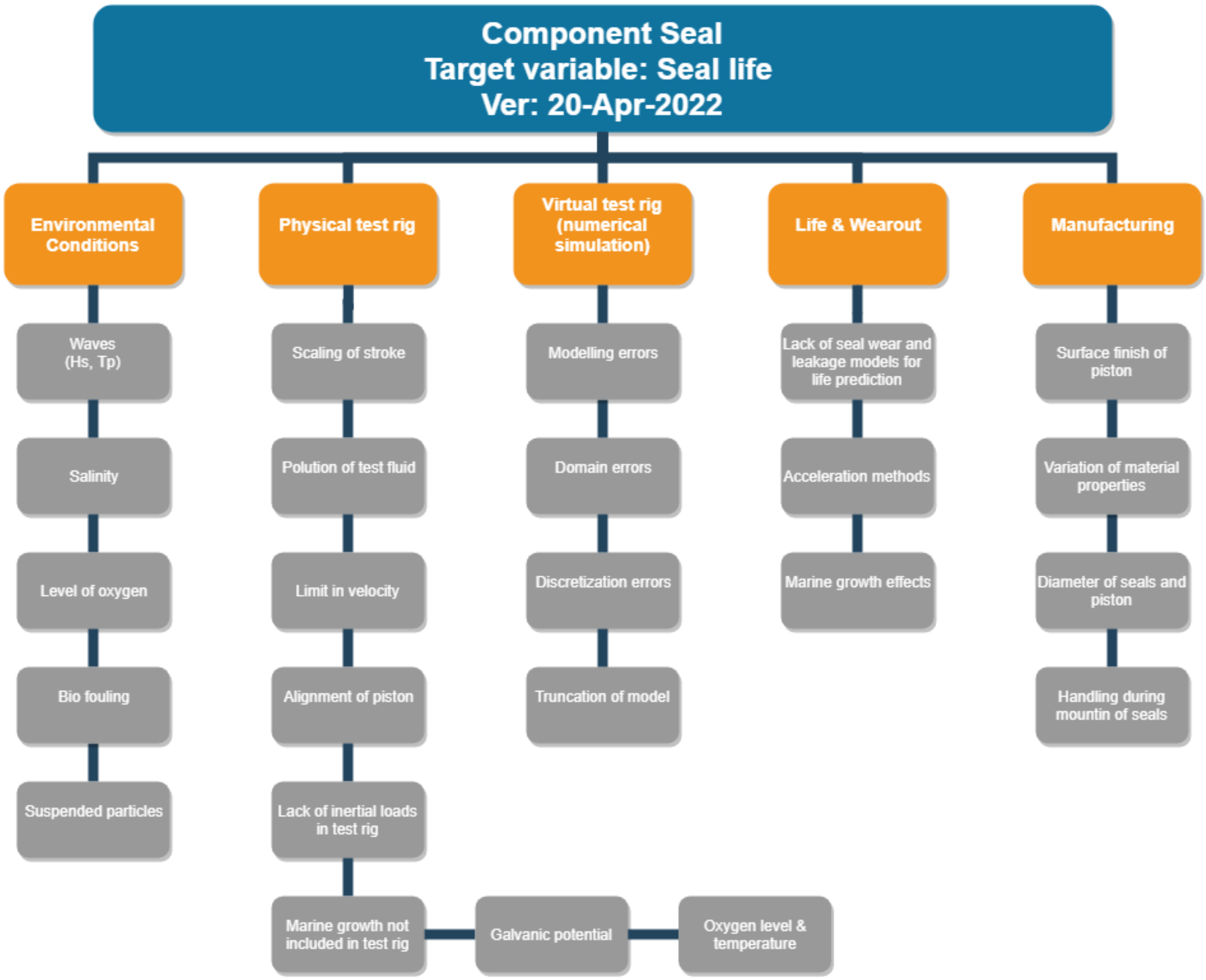

Figure 45: Identified sources of uncertainty in measured seal life for UC#3, Wavepiston.

9.2.3 Assessment of Uncertainties

During the second Basic VMEA workshop, an assessment of the uncertainties in terms of sensitivity and uncertainty size was carried out. For the basic VMEA, the assessment of size and sensitivity is made on a scale from 1 to 10, and the result is found in Table 19.

As the physical test rig does not include the marine growth impact, a post-processing model for seal life correction is needed. This correction introduces the marine growth uncertainty in the life & wearout category and, consequently, the identified uncertainty 'Marine growth not included in test rig' in the physical test rig category was set to zero.

Table 19: Uncertainty analysis in basic VMEA for UC#3, Wavepiston.

Input			**Result**		
	Sensitivity	**Uncertainty input**	**Uncertainty output**	**Variation contribution**	
				VRPN	**VRPN**
Uncertainty components	c_i **(1-10)**	σ_i **(1-10)**	$\tau_i = c_i \cdot \sigma_i$	τ_i^2	**proportion**
Environmental conditions					
Waves (Hs, Tp)	5	5	25.0	625	4%
Salinity	3	1	3.0	9	0%
Level of oxygen	2	3	6.0	36	0%
Bio fouling	7	6	42.0	1764	12%
Suspended particles	6	4	24.0	576	4%
Total			**54.9**	**3010**	**21%**
Physical test rig					
Scaling of stroke	3	3	9.0	81	1%
Polution of test fluid	8	2	16.0	256	2%
Limit in velocity	3	3	9.0	81	1%
Alignment of piston	6	2	12.0	144	1%
Lack of inertial loads in test rig	2	2	4.0	16	0%
Marine growth not included in test rig	7	0	0.0	0	0%
Galvanic potential	9	1	9.0	81	1%
Oxygen level & temerature	7	2	14.0	196	1%
Total			**29.2**	**855**	**6%**
Virtual test rig (numerical simulations)					
Modelling errors	6	6	36.0	1296	9%
Domain errors	3	3	9.0	81	1%
Discretization errors	2	2	4.0	16	0%
Truncation of model	6	6	36.0	1296	9%
Total			**51.9**	**2689**	**19%**
Life & wearout					
Lack of seal wear and leakage models	7	7	49.0	2401	17%
Acceleration methods	7	7	49.0	2401	17%
Marine growth effects	7	7	49.0	2401	17%
Total			**84.9**	**7203**	**50%**
Manufacturing					
Surface finish of piston	6	2	12.0	144	1%
Variation of material properties	3	5	15.0	225	2%
Diameter of seals and piston	2	2	4.0	16	0%
Handling during mounting of seals	3	5	15.0	225	2%
Total			**24.7**	**610**	**4%**
Total uncertainty			**119.9**	**14367**	**100%**

9.2.4 Evaluation of Total Uncertainty

The total variation is calculated as the square sum of the resulting variation from the sources, resulting in the total VRPN. The relative contribution of the VRPN from the different uncertainty sources are of interest rather than the absolute value of the total VRPN. The Pareto chart in Figure 46 shows the resulting ranking of the various uncertainty sources identified during the workshops, highlighting those ones which contribute most to the uncertainty of the target variable.

This project has received funding from the European Union's Horizon 2020
research and innovation programme under grant agreement No 101006927.

It can also be of interest to study the relative contribution of uncertainties between the five categories of uncertainties, as shown in Figure 47. Here we can observe that "Life & wearout" group contributes to 50% of the total variation.

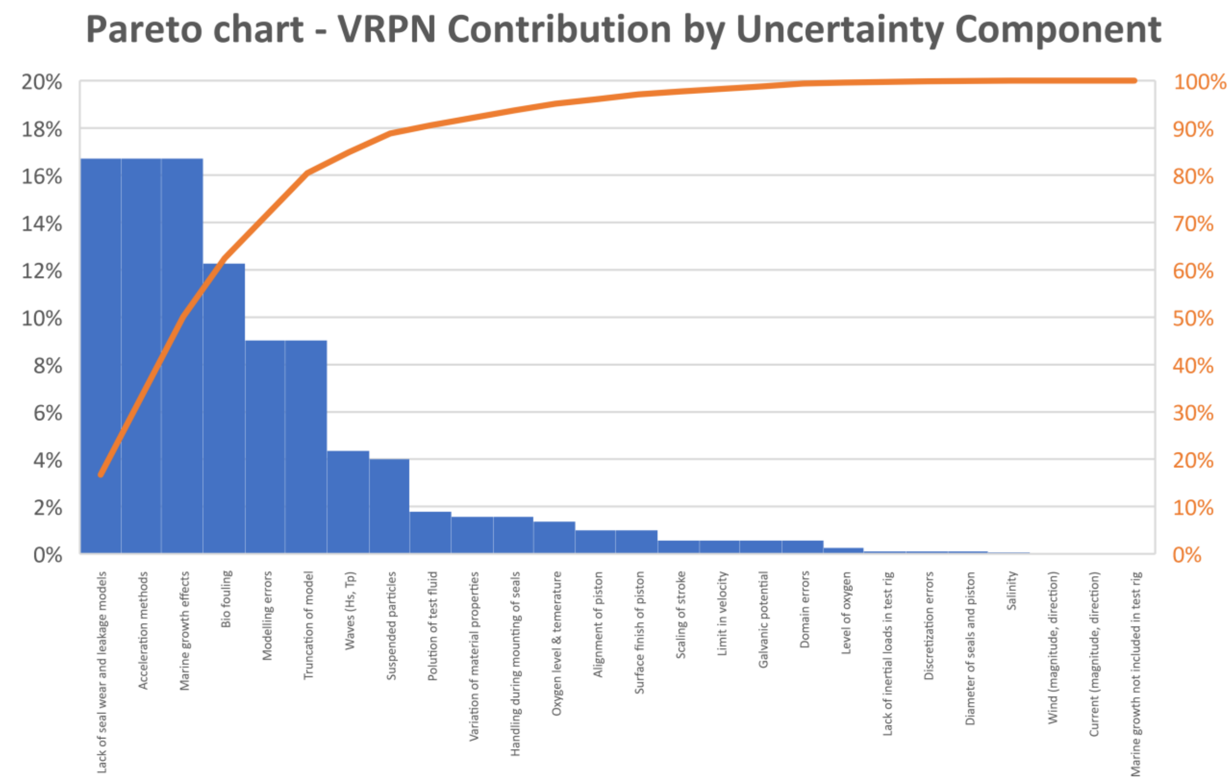

Figure 46: Pareto chart of uncertainties in basic VMEA for UC#3, Wavepiston.

This project has received funding from the European Union's Horizon 2020 research and innovation programme under grant agreement No 101006927.

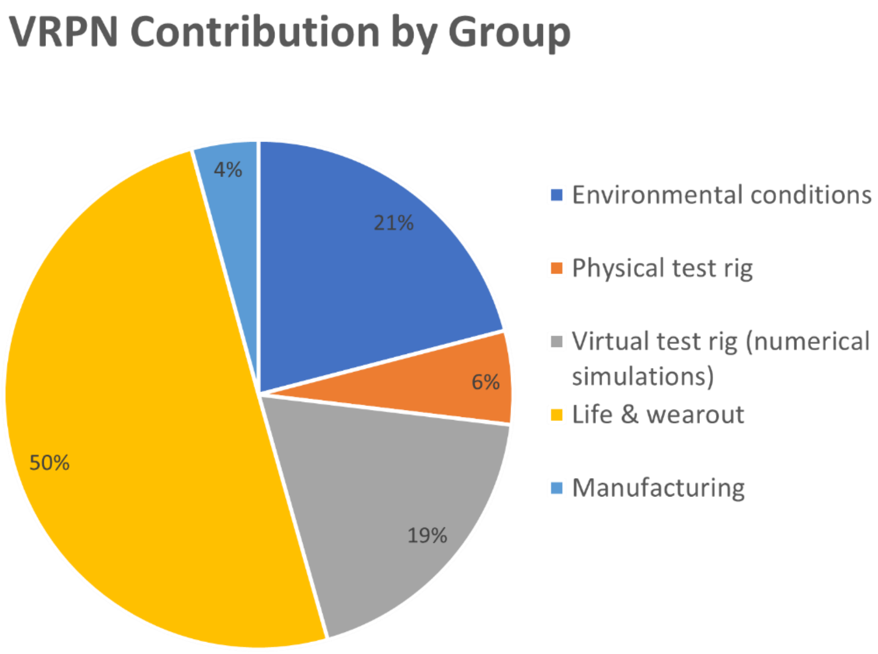

Figure 47: The contribution by group of uncertainties in basic VMEA for UC#3, Wavepiston.

9.2.5 Conclusions and Lessons Learned

The largest contributions to the total seal life uncertainty indicate which uncertainty sources are most important to focus on when trying to reduce uncertainty. Candidates are:

- Lack of seal wear and leakage models (17%)
- Acceleration methods (17%)
- Marine growth effects (17%)
- Bio fouling assessment (12%)
- Modelling errors (9%)
- Truncation of model (9%)

9.3 Probabilistic VMEA

Four workshops were held in the spring of 2023 to perform the probabilistic VMEA analysis of the Wavepiston hybrid test method. After confirmation or update of the target variable definition and its sources for measurement uncertainty, from the basic VMEA workshop, each source uncertainty was this time estimated in physical units together with its impact on the target variable uncertainty, i.e., the sensitivity coefficient.

It was decided to focus on the three uncertainty source categories that are directly involved in the hybrid testing execution, as the scope for the workshop. Uncertainties related to environmental conditions and manufacturing can instead be evaluated later following the same process.

This project has received funding from the European Union's Horizon 2020 research and innovation programme under grant agreement No 101006927.

9.3.1 Target Variable

The target variable was confirmed to be the hydraulic seal life. Actually, when quantifying its variation due to uncertainty sources, the target variable was set to the logarithm of the seal life, $Y = \ln N = f(X_1, X_2, \dots)$, as suggested in section 3.4.1. and exemplified in section 3.4.6.

9.3.2 Uncertainty Sources

The set of sources of uncertainty identified during the basic VMEA was confirmed without any adjustment, see Figure 45.

9.3.3 Assessment of Uncertainties

An estimate of standard deviation was used to quantify the uncertainty of each uncertainty source. Almost all sources have uncertainty type B, because of lack of data from experiments. Experience and intuition were used in discussions to establish rough estimates during the workshop. It turned out to be easier to estimate contribution to the target variable uncertainty directly, without losing accuracy, instead of estimating the uncertainty in the source and its sensitivity coefficient. The source variation could also be difficult to measure, as for the rig water pollution as an example. This means that an uncertainty source was evaluated by giving an interval, typically, of the resulting seal life variation caused by the source variation. The sensitivity was set to 1 so that the source uncertainty measure was the same as the seal life uncertainty estimate.

With the logarithm of life as target variable, it was favourable to use the approximation for percentage uncertainty as described in section 3.4.4. Hence, if the standard uncertainty is 10% in seal life, then the standard deviation of $Y = \ln N$ is approximately 0.1. The result from the uncertainty evaluation is shown in Table 20. The largest contributions to the seal life uncertainty are now the marine growth effects and the pollution of the test rig fluid. As an example, the latter uncertainty source was evaluated as follows. First, it was stated that the pollution needs to be well controlled in the rig. Even so, the uncertainty was estimated to have an impact on the seal life of at most ±25%. A uniform probability distribution was assumed within the interval of [-25%, +25%] of the expected life, which means that the standard deviation is $25\%/\sqrt{3} = 14\%$, using Eq. (15).

One of the largest uncertainties from the basic VMEA, 'Lack of seal wear and leakage models' in the Life & wearout category, was set to zero in this evaluation, because it does not relate to the hybrid test method.

This project has received funding from the European Union's Horizon 2020 research and innovation programme under grant agreement No 101006927.

Table 20: Uncertainty analysis in probabilistic VMEA for UC#3, Wavepiston. Marine growth effects are included in the life & wearout category, not in the physical rig.

Input			**Result**		
	Sensitivity	**Uncertainty input**	**Uncertainty output**	**Variation contribution**	
Uncertainty components	c_i	u_i	$\tau_i = c_i \cdot \sigma_i$	**VRPN** τ_i^2	**VRPN proportion**
Physical test rig					
Scaling of stroke	1	2%	2,0%	0,0004	**1%**
Polution of test fluid	1	14%	14,4%	0,0208	**27%**
Limit in velocity	1	6%	5,8%	0,0033	**4%**
Alignment of piston	1	1%	1,0%	0,0001	**0%**
Lack of inertial loads in test rig	1	0%	0,0%	0	**0%**
Marine growth not included in test rig	1	0%	0,0%	0	**0%**
Galvanic potential	1	1%	1,0%	0,0001	**0%**
Oxygen level	1	1%	1,0%	0,0001	**0%**
Temperature	1	2%	2,0%	0,0004	**1%**
Virtual test rig (numerical simulations)					
Modelling errors	0,2	20%	4%	0,0016	**2%**
Domain errors	0,2	1%	0%	4E-06	**0%**
Discretization errors	0,2	10%	2%	0,0004	**1%**
Truncation of model	0,2	1%	0%	4E-06	**0%**
Life & wearout					
Lack of seal wear and leakage models			0%	0	**0%**
Acceleration methods	1	5%	5%	0,0025	**3%**
Marine growth effects	1	22%	22%	0,0484	**62%**
Total			**28%**	**0,0782**	**100%**

9.3.4 Evaluation of Total Uncertainty

The total uncertainty is calculated as the root sum of square of the resulting uncertainty from each source. The relative contribution, in terms of variance contribution, from the different uncertainty sources are presented in the last column in Table 20. The result is best illustrated by graphs. A Pareto chart in Figure 48 shows the resulting ranking of the various uncertainty sources identified during the workshops, highlighting those ones which contribute most to the uncertainty of the target variable.

This project has received funding from the European Union's Horizon 2020 research and innovation programme under grant agreement No 101006927.

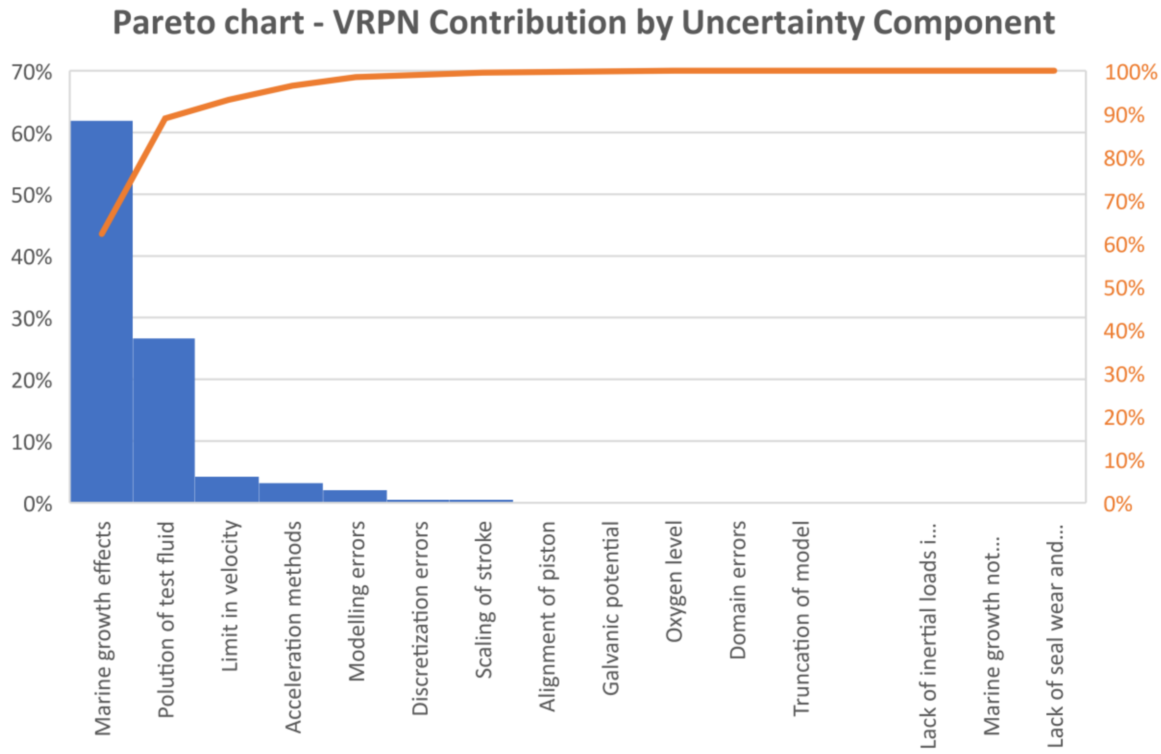

Figure 48: Pareto chart of uncertainties in probabilistic VMEA for UC#3, Wavepiston.

9.3.5 Conclusions and Lessons Learned

With the focus on three of the uncertainty categories, in the probabilistic VMEA, which are related to the hybrid testing results, the largest contributions to the total seal life uncertainty are:

- Marine growth effects (62%)
- Pollution of test fluid (27%)

Note that the marine growth effects are not possible to model in the current physical test rig. The marine growth impact is instead modelled by a correction factor in life. The large uncertainty in the marine growth effects is reflected by the lack of knowledge about this correction factor.

Part C: Nomenclature and References

This project has received funding from the European Union's Horizon 2020 research and innovation programme under grant agreement No 101006927.

10 Nomenclature

Abbreviations

AEP	Annual Energy Production
EMRP	European Metrology Research Programme
FMEA	Failure Mode and Effect Analysis
FMECA	Failure Mode, Effect and Criticality Analysis
CAE	Computer Aided Engineering
CFD	Computational Fluid Dynamics
DoE	Design of Experiments
FLS	Fatigue Limit State
GUM	Guide to the Expression of Uncertainty in Measurement
HALT	Highly Accelerated Life Test
MSA	Measurement System Analysis
NAFEMS	National Agency for Finite Element Methods and Standards
PCE	Polynomial Chaos Expansion
PTO	Power Take Off
RANSE	Reynolds-Avergaed Navier Stokes
SA	Sensitivity Analysis
UQ	Uncertainty Quantification
ULS	Ultimate Limit State
V&V	Verification and Validation
VIM	Vocabulaire international de métrologie (International Vocabulary of Metrology)
VMEA	Variation Mode and Effect Analysis
VRPN	Variation Risk Priority Number
WEC	Wave Energy Converter

11 References

AAIA, 1998. Guide for the Verification and Validation of Computational Fluid Dynamics Simulations (No. AIAA G-077-1998).

Adams, B.M., Bohnhoff, W.J., Dalbey, K.R., Ebeida, M.S., Eddy, J.P., Elred, M.S., Hooper, R.W., Hough, P.D., Hu, K.T., Jakeman, J.D., Khalil, M., Maupin, K.A., Momschke, J.A., Ridgeway, E.M., Rushdi, A.A., Seidl, D.T., Stephens, J.A., Swiler, L.P., Winkour, J.G., 2021. Dakota, A Multilevel Parallel Object-Oriented Framework for Design Optimization, Parameter Estimation, Uncertainty Quantification, and Sensitivity Analysis: Version 6.11 User's Manual (No. Sandia Technical Report SAND2014-4633). Sandia.

Allard, A., Bär, M., Barton, E., Bunde Kondrup, J., Demeyer, S., Fiebach, A., Fischer, N., Gross, H., Heidenreich, S., Henn, M.-A., Kok, G., Model, R., Partridge, D., Pelevic, N., Rasmussen, K., Schmelter, S., Wright, L., 2015. Best practice guide to uncertainty evaluation for computationally expensive models (Deliverable of EMRP project NEW04 "Novel mathematical and statistical approaches to uncertainty evaluation" No. D 2.5.1).

Ambühl, S., 2015. Reliability of Wave Energy Converters: revised version.

Andersen, J., Eskilsson, C., 2023. Detached-Eddy Simulation of Normal Flow past Flat Plates: The Influence from Corner Curvature, in: Proceedings of the 33rd International Ocean and Polar Engineering Conference. Ottawa, Canada.

Arnold, D.N., 2009. The sinking of the Sleipner A offshore platform [WWW Document]. URL https://www-users.cse.umn.edu/~arnold/disasters/sleipner.html (accessed 1.26.23).

ASME, 2023. Codes & Standards in Verification & Validation, and Uncertainty Quantification in Computational Modeling and Simulation [WWW Document]. URL https://cstools.asme.org/csconnect/CommitteePages.cfm?Committee=100003367 (accessed 1.13.23).

ASME, 2009. Standard for Verification and Validation in Computational Fluid Dynamics and Heat Transfer (No. ASME-V&V 20-2009).

Atcheson, M., Cruz, J., Martins, T., 2019. Quantification of load uncertainties in the design process of a WEC, in: 13th European Wave and Tidal Energy Conference. Napoli, Italy.

Bargiacchi, D., Roccatagliata, F., Roncallo, F., Xhani, I., Barra, M., Johannesson, P., Cruz, J., Robles Sestafe, E., 2021. VALID Deliverable 1.1: Accelerated Testing Requirements.

Baudin, M., Dutfoy, A., Iooss, B., Popelin, A.-L., 2015. OpenTURNS: An Industrial Software for Uncertainty Quantification in Simulation, in: Ghanem, R., Higdon, D., Owhadi, H. (Eds.), Handbook of Uncertainty Quantification. Springer International Publishing, Cham, pp. 1–38. https://doi.org/10.1007/978-3-319-11259-6_64-1

Bergman, B. (Ed.), 2009. Robust design methodology for reliability: exploring the effects of variation and uncertainty. Wiley, Chichester, U.K.

Borgonovo, E., Plischke, E., 2016. Sensitivity analysis: A review of recent advances. European Journal of Operational Research 248, 869–887. https://doi.org/10.1016/j.ejor.2015.06.032

Brown, S.A., Ransley, E.J., Greaves, D.M., 2021. Assessing focused wave impacts on floating wave energy converters using OpenFOAM. Proceedings of the Institution of Civil Engineers - Engineering and Computational Mechanics 174, 4–18. https://doi.org/10.1680/jencm.19.00036

CEN/TC 250, 2002. BS EN 1990:2002+A1:2005 Eurocode - Basis of structural design. CEN, Brussels.

Chakhunashvili, A., Barone, S., Johansson, P., Bergman, B., 2009. Robust Product Development Using Variation Mode and Effect Analysis, in: Bergman, B., de Mar, J., Lorn, S., Svensson, T. (Eds.), Robust Design Methodology for Reliability. John Wiley & Sons, Ltd, Chichester, UK, pp. 57–70. https://doi.org/10.1002/9780470748794.ch5

This project has received funding from the European Union's Horizon 2020
research and innovation programme under grant agreement No 101006927.

Chakhunashvili, A., Johansson, P.M., Bergman, B.L.S., 2004. Variation mode and effect analysis, in: Annual Symposium Reliability and Maintainability, 2004 - RAMS. Presented at the Annual Symposium Reliability and Maintainability, 2004 - RAMS, IEEE, Los Angeles, CA, USA, pp. 364–369. https://doi.org/10.1109/RAMS.2004.1285476

Coe, R.G., Michelen, C., Eckert-Gallup, A., Sallaberry, C., 2018. Full long-term design response analysis of a wave energy converter. Renewable Energy 116, 356–366. https://doi.org/10.1016/j.renene.2017.09.056

Coleman, H.W., Steele, W.G., 2009. Experimentation, Validation, and Uncertainty Analysis for Engineers. John Wiley & Sons, Inc., Hoboken, NJ, USA. https://doi.org/10.1002/9780470485682

Cornell, C.A., 1969. A Probability Based Structural Code. ACI-Journal 66, 974–985.

Council, N.R., 2012. Assessing the Reliability of Complex Models: Mathematical and Statistical Foundations of Verification, Validation, and Uncertainty Quantification. The National Academies Press, Washington, DC. https://doi.org/10.17226/13395

C/S2ESC, 2018. P1012 Standard for System, Software, and Hardware Verification and Validation. IEEE Computer Society.

Davis, T.P., 2006. Science, engineering, and statistics. Appl. Stochastic Models Bus. Ind. 22, 401–430. https://doi.org/10.1002/asmb.643

Ditlevsen, O., Madsen, H.O., 2007. Structural Reliability Methods. Technical University of Denmark.

DNVGL-OS-C101 Design of offshore steel structures, general - LRFD method, 2016. . DNV GL.

DNVGL-RP-C203: Fatigue design of offshore steel structures, 2014. . DNV GL.

Downing, S., Socie, D., 1982. Simple rainflow counting algorithms. International Journal of Fatigue 4, 31–40. https://doi.org/10.1016/0142-1123(82)90018-4

Eça, L., Hoekstra, M., 2014. A procedure for the estimation of the numerical uncertainty of CFD calculations based on grid refinement studies. Journal of Computational Physics 262, 104–130. https://doi.org/10.1016/j.jcp.2014.01.006

Eça, L., Hoekstra, M., 2009. Evaluation of numerical error estimation based on grid refinement studies with the method of the manufactured solutions. Computers & Fluids 38, 1580–1591. https://doi.org/10.1016/j.compfluid.2009.01.003

Eça, L., Vaz, G., Hoekstra, M., 2010. A VERIFICATION AND VALIDATION EXERCISE FOR THE FLOW OVER A BACKWARD FACING STEP, in: V European Conference on Computational Fluid Dynamics. Presented at the ECCOMAS CFD 2010, Lisbon.

Elster, C., Klauenberg, K., Walzel, M., Wübbeler, G., Harris, S., Cox, M., Matthews, C., Smith, I., Wright, L., Allard, A., Fischer, N., Cowen, S., Ellison, S., Wilson, P., Pennecchi, F., Kok, G., van derr Veen, A., Pendrill, L., 2015. A guide to Bayesian inference for regression problems (Deliverable of EMRP project NEW04 "Novel mathematical and statistical approaches to uncertainty evaluation").

Eskilsson, C., Palm, J., Johannesson, P., Paredes, G.M., 2022. Sensitivity analysis of extreme loads acting on a point-absorbing wave energy converter. Int. J. Mar. Ene. 5, 91–101. https://doi.org/10.36688/imej.5.91-101

Faltinsen, O.M., 1990. Sea loads on ships and offshore structures, Cambridge ocean technology series. Cambridge University Press, Cambridge ; New York.

Freitas, C.J., 2020. Standards and Methods for Verification, Validation, and Uncertainty Assessments in Modeling and Simulation. Journal of Verification, Validation and Uncertainty Quantification 5. https://doi.org/10.1115/1.4047274

Ghanem, R., Higdon, D., Owhadi, H. (Eds.), 2017. Handbook of Uncertainty Quantification. Springer International Publishing, Cham. https://doi.org/10.1007/978-3-319-12385-1

Harnden, R., Bonel, A., Lindén, J., Johannesson, P., Sandström, J., 2022. VALID Deliverable 3.1: User case and methodology report for User Case 1.

Haselsteiner, A.F., Coe, R.G., Manuel, L., Chai, W., Leira, B., Clarindo, G., Soares, C.G., Hannesdóttir, Á., Dimitrov, N., Sander, A., Ohlendorf, J.-H., Thoben, K.-D., Hauteclocque, G. de, Mackay, E., Jonathan, P., Qiao, C., Myers, A., Rode, A., Hildebrandt, A., Schmidt, B., Vanem, E., Huseby, A.B., 2021. A benchmarking exercise for environmental contours. Ocean Engineering 236, 109504. https://doi.org/10.1016/j.oceaneng.2021.109504

Haselsteiner, A.F., Frieling, M., Mackay, E., Sander, A., Thoben, K.-D., 2022. Long-term extreme response of an offshore turbine: How accurate are contour-based estimates? Renewable Energy 181, 945–965. https://doi.org/10.1016/j.renene.2021.09.077

Hasofer, A.M., Lind, N.C., 1974. An Exact and Invariant First Order Reliability Format. Journal of Engineering Mechanics. Div. Proc. ASCE 100(EMI), 111–121.

Hodges, J., Henderson, J., Ruedy, L., Soede, M., Weber, J., Ruiz-Miguela, P., Jeffrey, H., Bannon, E., Holland, M., Maciver, R., Hume, D., Villate, J., Ramsey, T., 2021. An International Evaluation and Guidance Framework for Ocean Energy Technology. IEA-OES.

Hu, Z., Mahadevan, S., 2017. Uncertainty quantification in prediction of material properties during additive manufacturing. Scripta Materialia 135, 135–140. https://doi.org/10.1016/j.scriptamat.2016.10.014

IEC TS 62600-103, 2018. IEC TS 62600-103: Marine energy - Wave, tidal and other water current converters - Part 103: Guidelines for the early stage development of wave energy converters - Best practices and recommended procedures for the testing of pre-prototype devices.

ISO/TMBG, 2008. ISO/IEC Guide 98-3:2008 Uncertainty of measurement - Part 3: Guide to the expression of uncertainty in measurement (GUM:1995). International Organization for Standardization.

ISO/TMBG, 2007. ISO/IEC Guide 99:2007 International vocabulary of metrology - Basic and general concepts and associated terms (VIM). International Organization for Standardization.

ITTC, 2017. Uncertainty analysis in CFD Validation and Verification Methodologies and Procedures (No. 7.5-03-01–01), ITTC Recommended Procedures and Guidelines.

James C. Hoffman, Robin R. Murphy, 1993. Comparison of Bayesian and Dempster-Shafer theory for sensing: a practitioner's approach. Presented at the Proc.SPIE, pp. 266–279. https://doi.org/10.1117/12.162045

JCSS, 2001. JCSS Probabilistic Model Code. Joint Committee on Structural Safety (JCSS).

Jia, C., Ng, C., Johannesson, P., Svensson, T., Buck, E., Shanks, A., 2017. Improving the reliability in a sea of risk. Presented at the European Wave and Tidal Energy Conference (EXTEC), Cork, Ireland.

Johannesson, P., Bergman, B., Svensson, T., Arvidsson, M., Lönnqvist, Å., Barone, S., de Maré, J., 2013. A Robustness Approach to Reliability. Qual. Reliab. Engng. Int. 29, 17–32. https://doi.org/10.1002/qre.1294

Johannesson, P., Lang, X., Johnson, E., Ringsberg, J.W., 2022. Mechanical Reliability Analysis of Flexible Power Cables for Marine Energy. JMSE 10, 716. https://doi.org/10.3390/jmse10060716

Johannesson, P., Speckert, M. (Eds.), 2013. Guide to load analysis for durability in vehicle engineering, First edition. ed, Automotive series. Wiley, Chichester, West Sussex.

Johannesson, P., Svensson, T., Gaviglio, H., 2019. Reliability evaluation using variation mode and effect analysis: Application to CorPower's mooring pre-tension cylinder. Presented at the 13th European Wave and Tidal Energy Conference, Naples, Italy.

Johannesson, P., Svensson, T., Samuelsson, L., Bergman, B., de Maré, J., 2009. Variation mode and effect analysis: an application to fatigue life prediction. Quality and Reliability Engineering International 25, 167–179. https://doi.org/10.1002/qre.960

Johannesson, P., Thomas, S., Fabio, S., Chong, N., Chunjiang, J., Elaine, B., Andy, S., 2016. Reliability Guidance for Marine Energy Converters.

Johansson, P., Chakhunashvili, A., Barone, S., Bergman, B., 2006. Variation Mode and Effect Analysis: a Practical Tool for Quality Improvement. Qual. Reliab. Engng. Int. 22, 865–876. https://doi.org/10.1002/qre.773

Kiureghian, A.D., Ditlevsen, O., 2009. Aleatory or Epistemic? Does it matter? Structural Safety 31, 105–112.

This project has received funding from the European Union's Horizon 2020 research and innovation programme under grant agreement No 101006927.

Lekube, J., Zubiate, L., Robles, E., Ruiz Minguela, P., López, J., Etxaniz, P., Lee, J., 2023. VALID Deliverable 4.2: Definition of generator thermal fatigue testing.

Marelli, S., Sudret, B., 2014. UQLab: A Framework for Uncertainty Quantification in Matlab, in: Vulnerability, Uncertainty, and Risk. Presented at the Second International Conference on Vulnerability and Risk Analysis and Management (ICVRAM) and the Sixth International Symposium on Uncertainty, Modeling, and Analysis (ISUMA), American Society of Civil Engineers, Liverpool, UK, pp. 2554–2563. https://doi.org/10.1061/9780784413609.257

Mckay, M.D., Beckman, R.J., Conover, W.J., 2000. A Comparison of Three Methods for Selecting Values of Input Variables in the Analysis of Output From a Computer Code. Technometrics 42, 55–61. https://doi.org/10.1080/00401706.2000.10485979

Melchers, R.E., Beck, A.T., 2018. Structural reliability analysis and prediction, Third edition. ed. Wiley, Hoboken, NJ.

Morris, M.D., 1991. Factorial Sampling Plans for Preliminary Computational Experiments. Technometrics 33, 161–174. https://doi.org/10.1080/00401706.1991.10484804

Moura Paredes, G., Eskilsson, C., P. Engsig-Karup, A., 2020. Uncertainty Quantification in Mooring Cable Dynamics Using Polynomial Chaos Expansions. JMSE 8, 162. https://doi.org/10.3390/jmse8030162

NAFEMS, S.W.G., 2018. NAFEMS - What is Uncertainty Quantification (UQ)? [WWW Document]. URL https://www.nafems.org/publications/resource_center/wt08/ (accessed 11.3.21).

Nava, V., Ruiz Minguela, P., 2023. VALID Deliverable 6.3: Metrics and targets for stage-gate assessment of ocean energy technologies.

Nguyen, P.T.T., Manuel, L., Coe, R.G., 2019. On the Development of an Efficient Surrogate Model for Predicting Long-Term Extreme Loads on a Wave Energy Converter. Journal of Offshore Mechanics and Arctic Engineering 141. https://doi.org/10.1115/1.4042944

Nispel, A., Ekwaro-Osire, S., Dias, J.P., Cunha, A., 2021. Uncertainty Quantification for Fatigue Life of Offshore Wind Turbine Structure. ASCE-ASME J Risk and Uncert in Engrg Sys Part B Mech Engrg 7, 040901. https://doi.org/10.1115/1.4051162

Oberkampf, W., Helton, J., Sentz, K., 2001. Mathematical representation of uncertainty, in: 19th AIAA Applied Aerodynamics Conference. Presented at the 19th AIAA Applied Aerodynamics Conference, American Institute of Aeronautics and Astronautics, Anaheim,CA,U.S.A. https://doi.org/10.2514/6.2001-1645

Oberkampf, W.L., Imbert, J.-F., 2018. Simulation Governance Across the Product Lifecycle.

Oberkampf, W.L., Roy, C.J., 2010. Verification and validation in scientific computing. Cambridge University Press, New York.

O'Connor, P., Kleyner, A., 2012. Practical Reliability Engineering, 5th Edition, 5th ed, Wiley series in quality and reliability engineering. Wiley.

Owen, A., Zhou, Y., 2000. Safe and Effective Importance Sampling. Journal of the American Statistical Association 95, 135–143. https://doi.org/10.1080/01621459.2000.10473909

Pasanisi, A., Dutfoy, A., 2012. An Industrial Viewpoint on Uncertainty Quantification in Simulation: Stakes, Methods, Tools, Examples, in: Dienstfrey, A.M., Boisvert, R.F. (Eds.), Uncertainty Quantification in Scientific Computing, IFIP Advances in Information and Communication Technology. Springer Berlin Heidelberg, Berlin, Heidelberg, pp. 27–45. https://doi.org/10.1007/978-3-642-32677-6_3

Ragan, P., Manuel, L., 2007. Comparing Estimates of Wind Turbine Fatigue Loads Using Time-Domain and Spectral Methods. Wind Engineering 31, 83–99. https://doi.org/10.1260/030952407781494494

Reed, Patrick M., Hadjimichael, Antonia, Malek, Keyvan, Karimi, Tina, Vernon, Chris R., Srikrishnan, Vivek, Gupta, Rohini S., Gold, David F., Lee, Ben, Keller, Klaus, Thurber, Travis B., Rice, Jennie S., 2023. Addressing Uncertainty in Multisector Dynamics Research. https://doi.org/10.5281/ZENODO.6110623

Richter, P., Wolters, J., Frank, M., 2022. Uncertainty quantification of offshore wind farms using Monte Carlo and sparse grid. Energy Sources, Part B: Economics, Planning, and Policy 17, 2000520. https://doi.org/10.1080/15567249.2021.2000520

This project has received funding from the European Union's Horizon 2020 research and innovation programme under grant agreement No 101006927.

Roache, P.J., 1998. Verification and Validation in Computational Science and Engineering. Hermosa Publishers.

Ruiz-Minguela, P., Robles, E., Lopez-Mendia, J., Touzon, I., Cruz, J., Martini, M., Guadalupe Rangel Ramirez, J., Eskilsson, C., Sandström, J., Lavidas, G., Lang, G., Lekube, J., 2021. VALID Deliverable 1.2: Critical Components and Modelling Limitations.

Saltelli, A., Aleksankina, K., Becker, W., Fennell, P., Ferretti, F., Holst, N., Li, S., Wu, Q., 2019. Why so many published sensitivity analyses are false: A systematic review of sensitivity analysis practices. Environmental Modelling & Software 114, 29–39. https://doi.org/10.1016/j.envsoft.2019.01.012

Saltelli, A., Ratto, M., Andres, T., Campolongo, F., Cariboni, J., Gatelli, D., Saisana, M., Tarantola, S., 2007. Global Sensitivity Analysis. The Primer, 1st ed. Wiley. https://doi.org/10.1002/9780470725184

Sanchez-Sardi, H., Sankararaman, S., Escobet, T., Puig, V., Frost, S., Goebel, K., 2016. Analysis of two modeling approaches for fatigue estimation and remaining useful life predictions of wind turbine blades.

Schenkendorf, R., 2014. A General Framework for Uncertainty Propagation Based on Point Estimate Methods. https://doi.org/10.13140/2.1.2646.8489

Shahroozi, Z., Göteman, M., Nilsson, E., Engström, J., 2022. Environmental design load for the line force of a point-absorber wave energy converter. Applied Ocean Research 128, 103305. https://doi.org/10.1016/j.apor.2022.103305

Smith, J., 2021. Engineering Simulation Quality Management System.

Sobol, I.M., 1993. Sensitivity Estimates for Nonlinear Mathematical Models. Mathematical Modelling and Computational Experiments 4, 407–414.

Soize, C., 2017. Uncertainty Quantification: An Accelerated Course with Advanced Applications in Computational Engineering, Interdisciplinary Applied Mathematics. Springer International Publishing, Cham. https://doi.org/10.1007/978-3-319-54339-0

Stamatis, D.H., 2003. Failure mode and effect analysis: FMEA from theory to execution, 2nd ed., rev.expanded. ed. ASQ Quality Press, Milwaukee, Wisc.

Stern, F., Wilson, R.V., Coleman, H.W., Paterson, E.G., 2001. Comprehensive Approach to Verification and Validation of CFD Simulations—Part 1: Methodology and Procedures. Journal of Fluids Engineering 123, 793–802. https://doi.org/10.1115/1.1412235

Sudret, B., 2008. Global sensitivity analysis using polynomial chaos expansions. Reliability Engineering & System Safety 93, 964–979. https://doi.org/10.1016/j.ress.2007.04.002

Svensson, T., de Maré, J., 2008. On the choice of difference quotients for evaluating prediction intervals. Measurement 41, 755–762.

Svensson, T., de Maré, J., Johannesson, P., 2009. Predictive Safety Index for Variable Amplitude Fatigue Life, in: Bergman, B., de Maré, J., Lorén, S., Svensson, T. (Eds.), Robust Design Methodology for Reliability. John Wiley & Sons, Ltd, Chichester, UK, pp. 85–96. https://doi.org/10.1002/9780470748794.ch7

Svensson, T., Johannesson, P., 2013. Reliable Fatigue Design, by Rigid Rules, by Magic or by Enlightened Engineering. Procedia Engineering 66, 12–25. https://doi.org/10.1016/j.proeng.2013.12.058

Syam, W., 2021. Five reasons why measurement uncertainty is important [WWW Document]. Wasy Research. URL https://www.wasyresearch.com/five-reasons-why-measurement-uncertainty-is-important/ (accessed 1.24.23).

Szabó, B., Actis, R., 2012. Simulation governance: Technical requirements for mechanical design. Computer Methods in Applied Mechanics and Engineering 249–252, 158–168. https://doi.org/10.1016/j.cma.2012.02.008

Tshiloz, K., Smith, A.C., Mohammed, A., Djurovic, S., Feehally, T., 2016. Real-time insulation lifetime monitoring for motor windings, in: 2016 XXII International Conference on Electrical Machines (ICEM). Presented at the 2016 XXII International Conference on Electrical Machines (ICEM), IEEE, Lausanne, Switzerland, pp. 2335–2340. https://doi.org/10.1109/ICELMACH.2016.7732847

Walters, R.W., Huyse, L., 2002. Uncertainty analysis for Fluid Mechanics with Applications (No. NASA/CR-2002-211449 ICASE Report No. 2002-1).

Wang, W., Wu, M., Palm, J., Eskilsson, C., 2018. Estimation of numerical uncertainty in computational fluid dynamics simulations of a passively controlled wave energy converter. Proceedings of the IMechE 232, 71–84. https://doi.org/10.1177/1475090217726884

Wang, Y., McDowell, D.L., 2020. 1 - Uncertainty quantification in materials modeling, in: Wang, Y., McDowell, D.L. (Eds.), Uncertainty Quantification in Multiscale Materials Modeling. Woodhead Publishing, pp. 1–40. https://doi.org/10.1016/B978-0-08-102941-1.00001-8

Wiener, N., 1938. The Homogeneous Chaos. American Journal of Mathematics 60, 897. https://doi.org/10.2307/2371268